UILU-ENG-77-2011

CIVIL ENGINEERING STUDIES
Structural Research Series No. 441

SEISMIC SHEARS AND OVERTURNING MOMENTS IN BUILDINGS

by
R. SMILOWITZ
and
N. M. NEWMARK

A Technical Report of
Research Sponsored by the
NATIONAL SCIENCE FOUNDATION (RANN)
under Grant No. AEN 75-08456

DEPARTMENT OF CIVIL ENGINEERING
UNIVERSITY OF ILLINOIS
AT URBANA-CHAMPAIGN
URBANA, ILLINOIS
JULY 1977

BIBLIOGRAPHIC DATA SHEET	1. Report No. UILU-ENG-77-2011	2.	3. Recipient's Accession No.

4. Title and Subtitle	
Seismic Shears and Overturning Moments in Buildings	5. Report Date July 1977
	6.
7. Author(s) R. Smilowitz and N. M. Newmark	8. Performing Organization Rept. No. SRS 441
9. Performing Organization Name and Address University of Illinois at Urbana-Champaign Urbana, Illinois 61801	10. Project/Task/Work Unit No. AEN 75-08456
	11. Contract/Grant No.
12. Sponsoring Organization Name and Address National Science Foundation (RANN) Washington, D.C. 20550	13. Type of Report & Period Covered
	14.

15. Supplementary Notes

16. Abstracts

Seismic force distributions for simplified computation of shears and overturning moment for preliminary design of buildings have been generated. A parameter study of the significant variables has been made to determine the applicability of the proposed distributions. These distributions are intended to give greater accuracy than do existing procedures.

17. Key Words and Document Analysis. 17a. Descriptors

Seismic design, Seismic shears, Overturning moments,
High-rise buildings
Earthquake resistant design

17b. Identifiers/Open-Ended Terms

17c. COSATI Field/Group 13 13

18. Availability Statement	19. Security Class (This Report) UNCLASSIFIED	21. No. of Pages 137
Release Unlimited	20. Security Class (This Page UNCLASSIFIED	22. Price

ACKNOWLEDGMENT

This report was prepared as a doctoral dissertation by Mr. Robert Smilowitz and was submitted to the graduate college of the University of Illinois at Urbana-Champaign in partial fulfillment of the requirements for the degree of Doctor of Philosophy in Civil Engineering. The thesis was done under the supervision of Dr. N. M. Newmark, Professor of Civil Engineering and in the Center for Advanced Study Emeritus.

The investigation was part of a research program on the Design for Protection-Natural Hazards sponsored by the National Science Foundation (RANN), grant number AEN 75-08456.

The numerical results were obtained with the use of the IBM 360/75 computer system of the Computing Services Offices of the University of Illinois at Urbana-Champaign. The text was prepared and edited on the Civil Engineering Department's B6700 computer system. The authors wish to thank Dr. Leonard A. Lopez and F. Stephen McCollum for their generous assistance.

TABLE OF CONTENTS

LIST OF TABLES

LIST OF FIGURES

CHAPTER 1. INTRODUCTION

Seismic force distributions for simplified computation of shears and overturning moments for preliminary design of buildings have been generated and a parameter study of the significant variables has been made to determine the applicability of the proposed distributions. These distributions are intended to give greater accuracy than do existing procedures, which are based on more empirical concepts.

1.1 Motivation

The design of structures to resist seismic forces is an iterative process. Preliminary distributions of forces and overturning moments need to be determined in a consistent fashion so that member sizes can be initially proportioned. Further cycles of analysis and design converge to the proportions likely to behave best when subjected to a strong ground motion. The purpose of this thesis is to determine that set of shears and overturning moments which would permit this process to converge in the least number of cycles with a minimal effort.

More rigorous analyses are undesirable for preliminary proportioning as they are time consuming and they require information that may not be available at that stage of analysis. Furthermore, some of the more rigorous methods presuppose an actual earthquake to determine the structural response, as is the case for time history analyses, and unless the next strong ground motion closely resembles the one designed against, the structure may suffer excessive damage. Stochastic methods have often been used to construct a probable ground motion and to analyze the structural response to these spectra. However, much effort is required at too early a stage in design to warrant their use. Structures proportioned initially with the proposed distributions may be reanalyzed in later cycles of the design-analysis iteration by more rigorous approaches if greater accuracy is desired.

1.2 Scope

The purpose of this thesis is to look at realistic response spectra and determine the distributions of shears and overturning moments over a range of significant parameters. The parameters studied involve the type of building, whether shear wall or shear beam or a combination of the two (see Fig. 1), the uniformity of the structure along its height (see Fig. 2), the spacing of the lower modal frequencies, the fundamental frequency relative to the intersection of the constant velocity and constant acceleration branches of the response spectrum (see Fig. 3), the slenderness of the structure and the shear wave velocity of the soil on which it is founded. The distributions should be applicable to the majority of structures of either frame, shear wall or combination of the two lateral resisting structural systems. This study represents a more inclusive continuation of a previous investigation presented in Ref. [4] and discussed in Ref. [21].

Damping is accounted for in a relative sense and the overall effective damping of the structure is incorporated in the determining of the fundamental mode spectral acceleration as is currently the case (see Fig. 4).

Structural behavior was assumed to be linear and although this is never quite the case for strong motion responses, nor is it desirable for the structure to resist the seismic induced forces in the elastic range, this provides an upper bound for structural proportioning. Nonlinearities due to secondary effects, excessive deformations beyond the elastic limit and progressive damage of structural components cause a redistribution of stresses as the earthquake progresses and an accurate determination of the response would require extensive analysis. Furthermore, several analyses for several time histories of select recorded earthquakes would be required for an accurate appraisal of the redistributions. A well proportioned structure analyzed in the elastic range will generally exhibit superior structural behavior as it exceeds its elastic limits.

The response studied in this thesis is for motion in one principal direction only; twisting moments arising from ground motions not coincident with the principal directions of the structure as well as masses and stiffness eccentricities within the structure were not investigated in this study. Account of these twisting moments must be made by either considering a modal analysis with the torsional ground motion response spectra or in an equivalent static manner by proportioning the effective moment induced by intentional, in addition to accidental, eccentricities.

Soil structure interaction was investigated to assess its effect on the response of the structures in this study. The soil structure interaction investigated should not be confused with the amplification or attenuation of the ground motion as it is filtered through the founding soil. By varying the slenderness ratio of the structure and the shear wave velocity of the soil on which it is founded, the foundation flexibility's effect on reducing the structure's apparent natural frequency and its dynamic response can be assessed. The interaction model considered is that of a disk attached to an infinite elastic or visco-elastic halfspace. Results of previous studies, in Refs. [15],[19],[24],[26],[29],[30],[31],[32] and [33], on the effect of soil structure interaction have been incorporated into this study.

1.3 Organization

The results of this study along with the explanation of the methods by which they were obtained are presented in the following chapters. The theory on which the study was based is presented in chapter 2. The mathematical models adopted in order to apply these theories to this investigation are discussed in chapter 3. Chapter 4 lists and explains the variables investigated to effect the parameter study. Chapter 5 explains the means by which the response data was normalized enabling the data to be reduced in the desired fashion. Chapter 6 discusses the resulting design distributions and base values for the several parametric variations. The conclusions and recommendations for further study are the subject of chapter 7.

1.4 Notation

a_o	dimensionless frequency parameter
A	area of cross section
A_c	acceleration distribution along the height
AF_a	spectral acceleration amplification factor
AF_v	spectral velocity amplification factor
A_m	transform matrix from story forces to overturning moments
A_s	transformation matrix fromstory forces to story shears
B	polynomial acceleration distribution coefficients
C	damping matrix
C_s	effective seismic velocity
E	modulus of elasticity
f	story forces
F	forcing function
g	gravity acceleration
G	shear stiffness
h	story height
H	height of structure
I	moment of inertia of cross section
i, j, k, λ	dummy indices
K	stiffness matrix

L	element length
M	mass matrix
n	mode number
N	total number of story levels and degrees of freedom
P	load
Q	load factor
r	radius of gyration
R	radius of foundation
S	story shear
S_a	spectral acceleration
S_d	spectral displacement
S_f	portion of base shear resisted by frame
t	time
T	period
u	displacement (subscripts correspond to the direction or mode of deformation); direction of transverse displacement
U	strain energy
v	direction of axial displacement
V	convolution integral
x	direction of base translation
X	position along the unit height of the structure
y_n	normal mode displacement
Y	polynomial distribution along the height of the structure
Z	distribution coefficient as a function of position and height of setback
α	dimensionless frequency dependent coefficient for calculating dynamic stiffness of halfspace

β	percent of critical damping
γ	percent of strain energy due to shear deformation
Δ	story drift
δ_{st}	static displacement
ε	index of correlation
θ	direction of end rotation
κ	shear area shape factor
M	overturning moment
ν	Poisson's ratio
ρ	mass density ratio
σ	dimensionless wave parameter
ϕ	eigenvectors
χ	regression coefficient as a function of position and height of setback
ψ	direction of base rotation
ω	circular frequency

CHAPTER 2. THEORY

In the course of this study it was necessary to establish the equations of motion for various types of structures. These structural types were expressed in terms of the percent of total strain energy due to shear deformation. A variety of these equations of motion were solved for structures ranging from shear beams to flexural beams. In order to determine the structure's response to strong ground motion a modal anlysis was performed and the eigenvalues and eigenvectors were calculated. The secondary effects of P-Δ and soil structure interaction were included in the modal analysis and distributions of story shears and overturning moments were determined. A polynomial regression analysis was then performed on the distributions resulting in base coefficients and design acceleration distributions for a class of structural types and founding media.

This chapter explains the theory behind the operations performed in this investigation. The formulation and description of the various equations and terms is presented in the following sections.

2.1 Equations of Motion

Simplified force equilibrium equations can be expressed for structures subjected to ground motions similarly to structures subjected to static forces. In the dynamic problem inertial and damping forces, actions proportional to accelerations and velocities respectively, must be included to transform the time dependent problem into a series of static cases. A more detailed discussion is available in Refs. [2],[12] and[[20].

The interstory shear term,[K]{u}, is the product of the shear stiffnesses and the interstory displacements. The interstory damping term, [C]{u}, is the product of the equivalent viscus damping and the interstory velocities. The inertial term, [M]{u}, is the product of the interstory accelerations and the lumped story masses. These force terms are summed equal to the lumped story masses times the ground acceleration, $[M]\{1\}u_g(t)$, at the level in question.

$$[M]\{\ddot{u}\} + [C]\{\dot{u}\} + [K]\{u\} = - [M]\{1\}\ \ddot{u}_g(t) \qquad (1)$$

This can be transformed into normal coordinates which effectively decouple the equations to represent a series of independent single degree of freedom systems

$$\{\phi_n\}^T[M]\{\phi_n\}\ddot{y}_n + \{\phi_n\}^T[C]\{\phi_n\}\dot{y}_n + \{\phi_n\}^T[K]\{\phi_n\}y_n = - \{\phi_n\}^T[M]\{1\}\ddot{u}_g(t) \qquad (2)$$

This equation can be solved for undamped free vibration without significant loss of accuracy. The normal mode displacements can be found equal to :

$$y_n = \left(\frac{\{\phi_n\}^T [M] \{1\}}{\{\phi_n\}^T [M] \{\phi_n\}} \right) \frac{V_n(t)}{\omega_n} \tag{3}$$

where

$$V_n(t) = \int_o^t \ddot{u}_g(t)\, e^{-\beta_n \omega_n (t-\tau)} \sin(t-\tau)\, d\tau \tag{4}$$

The relative displacement of the ith node in the nth mode is obtained upon transforming back to our original system.

$$\{u_n(t)\} = \{\phi_n\}\, y_n \tag{5}$$

Elastic story forces corresponding to the displacements are obtained by premultiplying the displacements by the stiffness matrix:

$$\{f_n(t)\} = [K]\{u_n(t)\} \tag{6}$$

or equivalently:

$$\{f_n(t)\} = [M]\{u_n(t)\}\, \omega_n^2 \tag{7}$$

Elastic interstory shears are found by summing the story forces from the top down to the story of interest. Story shears for each mode are calculated separately.

$$\{S_n(t)\} = [A_s]\{f_n(t)\} \tag{8}$$

where $[A_s]$ is a unit upper triangle matrix which produces the story shears when postmultiplied by the story forces. The matrix $[A_s]$ for a five story structure is:

$$[A_s] = \begin{bmatrix} 1 & 1 & 1 & 1 & 1 \\ 0 & 1 & 1 & 1 & 1 \\ 0 & 0 & 1 & 1 & 1 \\ 0 & 0 & 0 & 1 & 1 \\ 0 & 0 & 0 & 0 & 1 \end{bmatrix} \tag{9}$$

The inverse of $[A_s]$ is the matrix which produces the story forces when postmultiplied by the story shears.

$$[A_s]^{-1} = \begin{bmatrix} 1 & -1 & 0 & 0 & 0 \\ 0 & 1 & -1 & 0 & 0 \\ 0 & 0 & 1 & -1 & 0 \\ 0 & 0 & 0 & 1 & -1 \\ 0 & 0 & 0 & 0 & 1 \end{bmatrix} \tag{10}$$

Overturning moments are calculated by summing the first moment of the story forces from the top down to the story of interest.

$$\{M_n(t)\} = [A_m]\{f_n(t)\} \tag{11}$$

where $[A_m]$ is an upper triangle matrix of the cumulative story heights. When $[A_m]$ is postmultiplied by the story forces the resulting values are the overturning moments. A five story structure with constant story heights produces the following matrix for $[A_m]$:

$$[A_m] = \begin{bmatrix} 1 & 2 & 3 & 4 & 5 \\ 0 & 1 & 2 & 3 & 4 \\ 0 & 0 & 1 & 2 & 3 \\ 0 & 0 & 0 & 1 & 2 \\ 0 & 0 & 0 & 0 & 1 \end{bmatrix} (h) \tag{12}$$

Similarly, the inverse of $[A_m]$ is the matrix which produces the story forces when postmultiplied by the overturning moments. For the five story structure with uniform story heights:

$$[A_m]^{-1} = \begin{bmatrix} 1 & -2 & 1 & 0 & 0 \\ 0 & 1 & -2 & 1 & 0 \\ 0 & 0 & 1 & -2 & 1 \\ 0 & 0 & 0 & 1 & -2 \\ 0 & 0 & 0 & 0 & 1 \end{bmatrix} \left(\frac{1}{h}\right) \tag{13}$$

The maximum response of each mode of vibration can be read directly from a response spectrum and these maximum modal responses can be combined to give a total response.

$$\{u_n\}_{max} = \{\phi_n\} \left[\frac{\{\phi_n\}^T [M]\{1\}}{\{\phi_n\}^T [M]\{\phi_n\}}\right] S_d(\beta_n, T_n) \quad (14)$$

$$\{f_n\}_{max} = [M]\{\phi_n\} \left[\frac{\{\phi_n\}^T [M]\{1\}}{\{\phi_n\}^T [M]\{\phi_n\}}\right] S_a(\beta_n, T_n) \quad (15)$$

We note that the damping term had been ignored in computing the normal coordinate displacements. This is only a minor error since the contribution of damping to the force equilibrium equation is small. The damping is accounted for in the response spectral values of maximum displacement and acceleration.

2.1.1 Stiffness Matrix

The structural idealization of the building frames analyzed for this parameter study was carried out by means of the direct stiffness approach. An energy expression for the beam and column elements was used to calculate the total potential energy of an elastic frame in terms of the displacements and rotations of the joints. Using the slope deflection equations, relating the end actions of a beam element to its deflected shape, the energy expression was then arranged in a quadratic form. The expression was differentiated with respect to the generalized coordinates and expressed in matrix notation.

$$U = \frac{2EI}{L}\left[u_{\theta i}^2 + u_{\theta i}u_{\theta j} + u_{\theta j}^2 - 3\left(\frac{u_{uj} - u_{ui}}{L}\right)(u_{\theta i} + u_{\theta j}) + 3\left(\frac{u_{\theta j} - u_{\theta i}}{L}\right)^2\right] + \frac{EA}{2L}(u_{vj} - u_{vi})^2 + \text{constant} \qquad (16)$$

Where u_θ, u_u and u_v are the rotational, transverse and axial displacements at the i and j nodes. The stiffness matrix generated in this fashion contains no rigid body motions and is not singular. Furthermore, it is important to note that the matrix is necessarily positive definite since the energy function is positive definite. A more detailed discussion is available in Ref. [17].

Shear walls, behaving as cantilever deep beams containing both flexural and shear modes of deformation, were treated separately. Flexibility coefficients, expressing the displacements of the wall due to a unit load at any one floor level, were generated by means of the unit dummy load method.

$$u = \frac{\partial U}{\partial P} = \int\left(\frac{Mm}{EI} + \frac{\kappa\, Ss}{GA}\right) dx \qquad (17)$$

Where $M = mP$, $S = sP$ and κ is the shear area shape factor. The applied moments and shears, M and S, are linear homogeneous functions of the external load P whereas the dummy moments and shears, m and s, are due to a unit load acting alone. The displacement at any level i due to a load at level j is therefore calculated as:

$$u = \sum_{k=1}^{k^*} \left[X_i X_j X_k - \frac{1}{2} \left(X_i + X_j \right) X_k^2 + \frac{1}{3} X_k^3 + \frac{30}{13} \kappa r^2 X_k \right] \frac{(EI)_{k+1} - (EI)_k}{(EI)_{k+1} \cdot (EI)_k} \qquad (18)$$

where k^* is equal to the smaller of i and j. For a rectangular wall the product of κ and r^2 equals one tenth of the square of the width of the wall.

Once the flexibity matrix is determined it is easily inverted by Gaussian elimination techniques to obtain the lateral stiffness matrix. This matrix, expressing the cantilever beam's loading required to effect a unit displacement at a specific level with no displacements elsewhere, is in a convenient form for calculating the natural frequencies associated with the lateral degrees of freedom.

2.1.2 Condensation

The structural stiffness coefficients, as derived from the potential energy of the elastic system, may contain degrees of freedom corresponding to which the inertial, damping and forcing functions may have no components. These degrees of freedom may be condensed out to preserve their effects without explicitly expressing them. Vertical joint displacements and joint rotations may be expressed in terms of the horizontal displacements and, by means of back substitution, their effects can be preserved.

This process is easiest done by partitioning the stiffness matrix into nine submatrices setting P_θ and P_V equal to zero.

$$\begin{Bmatrix} P_u \\ P_\theta \\ P_v \end{Bmatrix} = \left[\begin{array}{c|c|c} K_{uu} & K_{u\theta} & \cancelto{0}{K_{uv}} \\ \hline K_{\theta u} & K_{\theta\theta} & K_{\theta v} \\ \hline \cancelto{0}{K_{vu}} & K_{v\theta} & K_{vv} \end{array}\right] \begin{Bmatrix} u_u \\ u_\theta \\ u_v \end{Bmatrix} \tag{19}$$

The bottom row of partitioned matrices may be expanded to a self-equilibrating equation and $\{u_v\}$ may be solved in terms of $\{u_\theta\}$.

$$[\cancelto{0}{k_{vu}}]\{u_u\} + [K_{v\theta}]\{u_\theta\} + [K_{vv}]\{u_v\} = 0 \tag{20}$$

$$\{u_v\} = -[K_{vv}]^{-1}[K_{v\theta}]\{u_\theta\} \tag{21}$$

Similarly, the next row of matrices can be expanded, the vector $\{u_v\}$ can be replaced by its equivalent and $\{u_\theta\}$ may be solved in terms of $\{u_u\}$

$$[K_{\theta u}]\{u_u\} + [K_{\theta\theta}]\{u_\theta\} + [K_{\theta v}]\{u_v\} = 0 \tag{22}$$

$$[K_{\theta u}]\{u_u\} + \Big[[K_{\theta\theta}] - [K_{\theta v}][K_{vv}]^{-1}[K_{v\theta}]\Big]\{u_\theta\} \tag{23}$$

$$\{u_\theta\} = -\Big[[K_{\theta\theta}] - [K_{\theta v}][K_{vv}]^{-1}[K_{v\theta}]\Big]^{-1}[K_{\theta u}]\{u_u\} \tag{24}$$

Finally, we may substitute for $\{u_\theta\}$ and $\{u_v\}$ into the top row of the equilibrium equation and express the stiffness coefficients solely in terms of the lateral displacements.

$$\{P_u\} = [K_{uu}]\{u_u\} + [K_{u\theta}]\{u_\theta\} + [\cancelto{0}{K_{uv}}]\{u_v\} \tag{25}$$

$$\{P_u\} = \Big[[K_{uu}] - [K_{u\theta}]\Big[[K_{\theta\theta}] - [K_{\theta v}][K_{vv}]^{-1}[K_{v\theta}]\Big]^{-1}[K_{\theta u}]\Big]\{u_u\} \tag{26}$$

The equations of motion may be written using the condensed stiffness coefficients so the terms are all of the same order and the degrees of freedom are consistent in all their derivatives. These equations will be decoupled by transforming them into normal coordinates.

2.1.3 Mass Matrix

A consistent mass matrix may be derived from the kinetic energy of the system just as the stiffness coefficients were obtained from the potential energy. The element velocity distributions were related to the nodal values via the same functions which related element displacement distributions to the nodal values. The first derivative of the kinetic energy relation with respect to the nodal velocity gives the desired mass coefficients.

The lumped mass approximation follows the same theory except the element velocites are assumed to be zero everywhere but at the nodes. Only diagonal terms representing the mass associated with translational degrees of freedom are retained. The mass of each floor is considered to be concentrated at a node and it is understood that an acceleration at any node produces inertia forces at that node only. Rotational degrees of freedom are assigned no rotary inertia and no mass is assigned to them. The lumped mass representation greatly simplifies the calculations by introducing no mass coupling.

The consistent mass matrix may be condensed, in a fashion similar to the stiffness matrix condensation, to reduce the degrees of freedom while preserving their effects. Such a condensation would produce an upper bound to the correct frequencies, however, the benefits do not justify the computational effort required. A detailed description of mass matrix condensation is available in Ref. [23].

2.1.4 Damping

Structural damping is the mechanism to which energy dissipation in elastic analysis is attributed. This damping is due to the hysteretic nature of structural systems and the energy loss per cycle is equal to the area within the hysteretic force-displacement plot. This energy loss per cycle must also equal the work done by the external forces. Although the energy loss is proportional to the square of the amplitude of the structure's response, for a harmonic excitation this can be equated to an equivalent viscous damping which is proportional to the response velocity, though opposite to its direction. The magnitude of equivalent viscous damping for each mode of vibration is the subject for considerable debate. For computational convenience proportional damping is assumed to permit the equation of motion to uncouple when transformed into normal coordinates. A convenient form for the damping matrix, to assure its uncoupling, is to assign its coefficients values proportional to a linear combination of the mass and stiffness matrices. Two factors of proportionality can then be assigned to assure two modes to be damped to the desired degree. In general, however, the damping matrix can be constructed from the stiffness and mass matrices to guarantee its uncoupling specifying as many modes of damping as degrees of freedom. The remaining values of modal damping will result from the process of enforcing the specified values. Computationally, this procedure gets cumbersome beyond specifying the first two modes. A thorough discussion of these procedures is available in Refs. [2] and [12].

Although the form of the damping matrix is essential for dynamic analyses involving numerical integration of a specified time history input, it will be shown that this is not the case for response spectrum techniques. The magnitude of relative fixed base modal damping is essential and in this study the ratios were assumed equal in the first few significant modes of vibration. Studies conducted elsewhere and discussed in Ref. [21] support this assumption.

2.1.5 Forcing Function

The forcing function, for the case of a horizontal ground acceleration base input, is simply the negative of the product of the story masses and the ground acceleration. A unit vector is used to represent each degree of freedom's uniform translation due to a unit base motion. Obviously, were the masses not all collinear and perpendicular to the assumed base motion the unit vector would be replaced by the appropriate relation.

If the forcing function were subtracted from both sides of the equation of motion and combined, on the left side, with the inertia force term, we would then have the product of the mass matrix and the total acceleration the masses are subjected to. The right hand side of the equation would be zero and the equation would be reduced to:

$$[M]\{\ddot{u}_t\} + [C]\{\dot{u}\} + [K]\{u\} = 0 \tag{27}$$

where

$$u_t = u + u_g \tag{28}$$

2.2 Eigenvalues

Having generated the stiffness coefficients and mass matrix, these can now be combined into the dynamical matrix for the purpose of calculating the natural frequencies and mode shapes of the vibrating structure. The equilibrium equation can be written relating the spring force, inertial force and damping force. The damping force however, is much smaller than the other two and may be safely ignored. The resulting equilibrium equation may be expressed in symmetric form for computational facility.

$$[M]\{\ddot{u}\} + [K]\{u\} = 0 \tag{29}$$

$$\{u\} = \{\phi\} \sin \omega t \tag{30}$$

$$-\omega^2 [M]\{\phi\} + [K]\{\phi\} = 0 \tag{31}$$

$$\left([K] - \omega^2 [M]\right)\{\phi\} = 0 \tag{32}$$

$$[M]^{T^{-1/2}} [K] (M]^{-1/2} - \omega^2 \; [I] \; = 0 \tag{33}$$

The EISPAC subroutine was used to solve the eigenvalue problem for the symmetric, positive definite, dynamical matrix and the values were back substituted to obtain the associated vectors. The EISPAC system employs the method of bisection applied to the Sturm sequence for smaller systems of equations and the rational Q R method with Newtonian corrections for larger systems in which only a few solutions are desired. A complete writeup of the EISPAC system is available in Ref. [6].

The vectors obtained from the EISPAC routine were orthogonally normalized so that the result of postmultiplying and premultiplying the mass matrix by the scaled vectors and their transposes resulted in the identity matrix.

$$[\phi]^T [M] [\phi] = [I] \tag{34}$$

The eigenvectors established for the linear system represent independent motions in a normal coordinate system and they may be combined by the principal of superposition.

2.3 Modal Analysis

The eigenvalues and the scaled eigenvectors are the squared circular frequencies and the orthonormalized mode shapes which define the dynamic response for the fixed base structure. The maximum response and displacements can be obtained from a response spectrum which charts the maximum responses of a damped single degree of freedom system of varying natural frequency to a given strong ground motion. Each mode may be considered a single degree of freedom system with a percent of the total mass considered effective and the desired response can be calculated, whether it be displacement, force, story shear, overturning moment, etc. independent of the other modes. The responses of all the modes can be combined in a suitable manner to indicate the most probable response of the system.

The percent of the total mass considered effective may be derived from the forcing function as expressed in the right hand side of the equilibrium equation of ground motion.

$$F_n(t) = \{\phi_n\}^T [M]\{1\}\ \ddot{u}_g(t) \tag{35}$$

Since the mode shapes are orthonormalized the total components of base acceleration each mass is subjected to is identically equal to the ratio of mass effective in a mode of vibration.

$$M_n = \frac{\{\phi_n\}^T [M]\{1\}}{\{\phi_n\}^T [M]\{\phi_n\}} = \{\phi_n\}^T [M]\{1\} \tag{36}$$

The modal elastic displacements result from the product of the normalized mode shapes, the ratio of effective mass and spectral displacements for the frequency and percent of critical damping corresponding to the mode.

$$\{u_n\} = M_n \; S_d(\beta_n, T_n)\{\phi_n\} \tag{37}$$

The modal elastic forces result from the product of the normalized mode shapes, the mass matrix, the ratio of effective mass and the spectral acceleratrions.

$$\{f_n\} = M_n \; S_a(\beta_n, T_n)\{\phi_n\} \tag{38}$$

The modal shears and moments may be calculated from the elastic forces as in a conventional static analysis.

2.4 P-Δ Effects

Secondary effects due to the additional moments the structure's weight produces when deflected from its stationary vertical configuration may be sizable for tall, flexible buildings. These additional moments result in amplified story shears and amplified story drifts which, in turn, result in yet additional overturning moments. An iterative scheme is required until a stable and equilibrated deflected configuration is reached.

$$S^* = S + \frac{P\Delta^*}{h} \tag{39}$$

$$S^* = S + \frac{P\Delta^* S^*}{S^* \; h} \tag{40}$$

$$S^* = (1 - \frac{P\Delta^*}{S^*h})\ S^* \tag{41}$$

$$S^* = \frac{S}{(1 - \frac{P\Delta^*}{S^*h})} \tag{42}$$

For linearly elastic structures the story stiffness, the slope of the story shear vs story drift curve, is constant so

$$K = \frac{S}{\Delta} = \frac{S^*}{\Delta^*} \tag{43}$$

and

$$S^* = \frac{S}{(1 - \frac{P\Delta}{Sh})} \tag{44}$$

These effective story shears correspond to the equilibrated displaced shape of the structure and may be used to calculate the overturning moments. The effective shears take into account the eccentricity of the story weight in its deflected configuration in addition to the inertial force of the story masses due to the strong ground motion. Each modal shear and overturning moment distribution, assumed to be independent of the others, is amplified to account for the P-Δ effects.

A similar amplification procedure may be applied to the interstory displacements which, when summed from the ground up, yield the equilibrated displaced configuration.

$$\Delta^* = \frac{\Delta}{(1 - \frac{P\Delta}{Sh})} \tag{45}$$

Alternatively, since the system is assumed to behave elastically, the additional displacement due to the P-Δ effects may be calculated from the effective increase in story forces corresponding to V*.

$$\{f^*\} - \{f\} = [A_s]^{-1}(\{S^*\} - \{S\}) \quad (46)$$

$$\{\Delta^*\} - \{\Delta\} = [K]^{-1} (\{S^*\} - \{S\}) \quad (47)$$

These procedures are explained in greater detail in Refs. [5],[24],[27],[34].

2.5 Soil Structure Interaction

The effect of a compliant foundation on the dynamic behavior of the superstructure is to lengthen the fundamental periods and increase the amount of energy dissipated through radiation of waves into the supporting soil. The principal effects may be represented by two additional springs and dampers at the base of the structure, one pair representing the foundation's rotational degree of freedom, the other representing the foundation's translational degree of freedom. The development and discussion of the soil structure interaction equations is presented in Refs. [7],[15],[21] and [26]. These studies have shown that the coupling between the horizontal and rotational motions may be, for multistory structures, neglected with little loss of accuracy. Neglecting the coupling permits the representation of the motion by normal coordinates and a solution by modal analysis techniques.

The equations of motion for the compliant foundation differ from the fixed base in that there are two additional degrees of freedom and two additional equations.

$$[M]\{\ddot{u}_t\} + [C]\{\dot{u}\} + [K]\{u\} = 0 \qquad (48)$$

$$\{1\}[M]\{\ddot{u}_t\} + m_b(\ddot{u}_g + \ddot{u}_x) = -S_b(t) \qquad (49)$$

$$\{h\}[M]\{\ddot{u}_t\} + I_t(\ddot{u}_\psi) = -M_b(t) \qquad (50)$$

The impedance relations for the elastic half space are

$$\begin{Bmatrix} S_b(t) \\ M_b(t) \end{Bmatrix} = \begin{bmatrix} C_x & 0 \\ 0 & C_\psi \end{bmatrix} \begin{Bmatrix} \dot{u}_x \\ \dot{u}_\psi \end{Bmatrix} + \begin{bmatrix} K_x & 0 \\ 0 & K_\psi \end{bmatrix} \begin{Bmatrix} u_x \\ u_\psi \end{Bmatrix} \qquad (51)$$

Where $S_b(t)$ and $M_b(t)$ are the base shear and overturning moments at the structure-foundation interface.

$$\{u_t\} = u_g\{1\} + u_x\{1\} + u_\psi\{h\} + \{u\} \qquad (52)$$

Rearranging the terms results in the following three equations

$$[M]\{\ddot{u}\} + \ddot{u}_x[M]\{1\} + \ddot{u}_\psi[M]\{h\} + [C]\{\dot{u}\} + [K]\{u\} = -\ddot{u}_g[M]\{1\} \qquad (53)$$

$$\{1\}^T[M]\{\ddot{u}\} + \ddot{u}_x\{1\}^T[M]\{1\} + \ddot{u}_\psi\{1\}^T[M]\{h\} + m_b\ddot{u}_x + C_x u_x + K_x u_x = - \ddot{u}_g(\{1\}^T[M]\{1\} + m_b) \qquad (54)$$

$$\{h\}^T[M]\{\ddot{u}\} + \ddot{u}_x\{h\}[M]\{1\} + \ddot{u}_\psi\{h\}^T[M]\{h\} + I_t\ddot{u}_\psi + C_\psi\dot{u}_\psi + K_\psi u_\psi = - \ddot{u}_g\{h\}^T[M]\{1\} \tag{55}$$

Combining into a single expression

$$[M']\{\ddot{u}'\} + [C']\{\dot{u}'\} + [K']\{u'\} = \{F'\} \tag{56}$$

$$[M'] = \left[\begin{array}{c|c|c} [M] & [M]\{1\} & [M]\{h\} \\ \hline \{1\}^T[M] & \{1\}^T[M]\{1\} & \{1\}^T[M]\{h\} \\ \hline \{h\}^T[M] & \{h\}^T[M]\{1\} & \{h\}^T[M]\{h\} \end{array}\right] \tag{57}$$

$$[C'] = \left[\begin{array}{c|c|c} [C] & 0 & 0 \\ \hline 0 & C_x & 0 \\ \hline 0 & 0 & C_\psi \end{array}\right] \tag{58}$$

$$[K'] = \left[\begin{array}{c|c|c} [K] & 0 & 0 \\ \hline 0 & K_x & 0 \\ \hline 0 & 0 & K_\psi \end{array}\right] \tag{59}$$

$$\{u'\} = \left\{\begin{array}{c} \{u\} \\ u_x \\ u_\psi \end{array}\right\} \tag{60}$$

$$\{F'\} = -\ddot{u}_g \left\{\begin{array}{l} [M]\{1\} \\ m_b + \{1\}^T[M]\{1\} \\ \{h\}^T[M]\{1\} \end{array}\right\} \tag{61}$$

The equations may be uncoupled to perform a modal analysis by meas of Foss' method,described in Refs. [12] and [15]. The (N+2) degree of freedom system is first transformed into a 2(N+2) degree of freedom system of lower order.

$$\begin{bmatrix} 0 & [M'] \\ [M'] & [C'] \end{bmatrix} \begin{Bmatrix} \ddot{u}' \\ \dot{u}' \end{Bmatrix} + \begin{bmatrix} -[M'] & 0 \\ 0 & [C'] \end{bmatrix} \begin{Bmatrix} \dot{u}' \\ u' \end{Bmatrix} = \begin{Bmatrix} 0 \\ \{F'\} \end{Bmatrix} \qquad (62)$$

This form of the equation yields (N+2) complex eigen values and (N+2) complex conjugates. An iterative procedure must be used to account for the frequency dependent impedance functions. Alternatively, the equations may be solved in the frequency domain using fast fourier transform techniques.

Simplifications arising from parametric studies of the solutions of these equations, presented in Refs. [19],[29],[30],[31] and [32], may obviate the need of a rigorous solution. Good correlation between exact and simplified approaches allow for the use of the fixed base mode shapes with the modified frequencies and dampings.

2.6 Combination of Modes

The story displacements, shears and overturning moments calculated for each mode of interest, amplified for P-Δ effects and modified to account for soil structure interaction are combined to represent the most probable response. Most structures' natural frequencies are well enough separated that their responses to strong ground motion are considered independent of each other. For such separated systems the most probable combined response is the square root of the sum of the squares of the individual modal responses. An upper bound to the structural response is the sum of the absolute values of the individual modal responses. It is highly unlikely for the maximum responses of all the modes due to a strong ground motion to occur simultaneously. The sum of absolute maximum responses is highly overconservative for multidegree of freedom systems.

2.7 Energy Relations

The elastic strain energy of a structural system is a function of the loads acting on the system and the resulting deformations. Two systems with different load resisting properties subjected to identical loads would generate different amounts of strain energy depending solely on the difference in deflected shapes. A prescribed load applied statically along a cantilever shear beam generates a different deflected shape than does a cantilever flexure beam. In a system in which the lateral resisting elements exhibit combinations of shear and flexural deformations, the ratio of energy due to either action divided by the total energy ought to provide a measure for the influence of either component.

For the discretized systems the strain energies of the several structural components may be determined for the most probable deflected shape of the system. The percent of shear strain enengy for a system composed of any number, N*, of lateral load resisting systems may be calculated from the stiffness matrices which describe the linear system and the deflected shape. The subscripts s and f refer to the shear and flexure modes of deformation respectively and the subscript t indicates a total value, whether it be stiffness, strain energy or deformation.

$$[K_i] = ([K_{is}]^{-1} + [K_{if}]^{-1})^{-1} \tag{63}$$

$$[K_t] = \sum_{i=1}^{N^*} [K_i] \tag{64}$$

$$\{u_t\} = \{u_{if}\} + \{u_{is}\} \tag{65}$$

$$\{P_i\} = [K_{if}]\{u_{if}\} = [K_{is}]\{u_{is}\} \tag{66}$$

$$\{u_{if}\} = [K_{if}]^{-1}[K_{is}]\{u_{is}\} \tag{67}$$

$$\{u_t\} = \left([I] + [K_{if}]^{-1}[K_{is}]\right)\{u_{is}\} \tag{68}$$

$$\{u_{is}\} = \left([I] + [K_{if}]^{-1}[K_{is}]\right)^{-1}\{u_t\} \tag{69}$$

$$\{u_{is}\} = \left([I] + \left([K_i]^{-1} - [K_{is}]^{-1}\right)[K_{is}]\right)^{-1}\{u_t\} \tag{70}$$

$$\{u_{is}\} = [K_{is}]^{-1}[K_i]\{u_t\} \tag{71}$$

$$U_{is} = \frac{1}{2}\{u_{is}\}^T[K_{is}]\{u_{is}\} \tag{72}$$

$$U_s = \sum_{i=1}^{N^*} U_{is} \tag{73}$$

$$U_s = 1/2\ \{u_t\}^T \left(\sum_{i=1}^{N^*} [K_i][K_{is}]^{-1}[K_i] \right) \{u_t\} \tag{74}$$

$$U_t = 1/2\ \{u_t\}^T \left(\sum_{i=1}^{N^*} [K_i] \right) \{u_t\} \tag{75}$$

$$\gamma' = 100\ \frac{U_s}{U_t} \tag{76}$$

2.8 Regression Analysis

The story accelerations distributions may be expressed as cubic polynomial equations.

$$A_c(X) = B_1^* X^3 + B_2^* X^2 + B_3^* X + B_4^* \tag{77}$$

The several variations in structural discontinuities and soil structure interaction for each height of structure and percent of shear deformation may be combined by the method of least squares to produce a generalized design distribution. Story shears and overturning moments need first be normalized to produce a unit base shear assuming unit story masses at each level. This has the effect of normalizing the story accelerations, allowing the story shears and overturning moment distributions to be compared directly regardless of the actual story masses. The least squares regression therefore minimizes the variation in the fourth and fifth order polynomial response distributions with respect to the cubic polynomial acceleration distributions' coefficients. To minimize the variation between the modal response distributions and the expressions to fit this data, the following four simultaneous equations must be solved.

$$\sum_{i=1}^{N'} \frac{\partial}{\partial B_1^*} (Y_i - Y_i^*)^2 = 0 \qquad (78a)$$

$$\sum_{i=1}^{N'} \frac{\partial}{\partial B_2^*} (Y_i - Y_i^*)^2 = 0 \qquad (78b)$$

$$\sum_{i=1}^{N'} \frac{\partial}{\partial B_3^*} (Y_i - Y_i^*)^2 = 0 \qquad (78c)$$

$$\sum_{i=1}^{N'} \frac{\partial}{\partial B_4^*} (Y_i - Y_i^*)^2 = 0 \qquad (78d)$$

The Y_i are the values obtained from the modal analysis, whether they be story shears or overturning moments, the Y_i^* are the polynomial expressions for the respective response distributions in terms of B_1^*, B_2^*, B_3^* and B_4^*, and N' is the total number of distribution points included in the regression analysis. The acceleration distributions for calculating the most probable shears and overturning moments for a particular structure will not necessarily be the same. Two distinct distributions must therefore be determined for each structural idealization.

Assuming the story accelerations to be of the cubic polynomial form

$$(A_c)^*_i = B^*_1 \left(\frac{i}{N}\right)^3 + B^*_2 \left(\frac{i}{N}\right)^2 + B^*_3 \left(\frac{i}{N}\right) + B^*_4 \qquad (79)$$

$$f_i = m_i\left(B^*_1 \left(\frac{i}{N}\right)^3 + B^*_2 \left(\frac{i}{N}\right)^2 + B^*_3 \left(\frac{i}{N}\right) + B^*_4\right) \qquad (80)$$

$$S_j = \sum_{i=j}^{N} f_i = \sum_{i=1}^{N} f_i - \sum_{i=1}^{j-1} f_i \qquad (81)$$

$$S_j = \sum_{\lambda=0}^{3} \frac{B^*_{(4-\lambda)}}{N^\lambda} \left[\sum_{i=1}^{N} (m_i)(i)^\lambda - \sum_{i=1}^{j-1} (m_i)(i)^\lambda\right] \qquad (82)$$

If we were to assume all base masses to be equal to unity and all setback masses to be equal to m, the equation for story shears at level j becomes:

$$S_j = \sum_{\lambda=0}^{3} \frac{B^*_{(4-\lambda)}}{N^\lambda} \left[\sum_{i=1}^{N} m(i)^\lambda + \sum_{i=1}^{N}(1-m)(i)^\lambda - \sum_{i=1}^{j-1} m(i)^\lambda - \sum_{i=1}^{k^*} (1-m)(i)^\lambda\right] \qquad (83)$$

Where k is the story at which the setback occurs,

And $k^*=k$ but not greater than $(j-1)$

The sum of constants, integers, their squares, cubes and quartics from one to N has been calculated in Ref. [16] to be

$$\sum_{i=1}^{N} (1) = N \qquad (84a)$$

$$\sum_{i=1}^{N} (i) = \frac{1}{2} N(N+1) \qquad (84b)$$

$$\sum_{i=1}^{N} (i)^2 = \frac{1}{6} (N)(N+1)(2N+1) \tag{84c}$$

$$\sum_{i=1}^{N} (i)^3 = \frac{1}{4} (N)^2 (N+1)^2 \tag{84d}$$

$$\sum_{i=1}^{N} (i)^4 = \frac{1}{30} (N)(N+1)(2N+1)(3N^2 + 3N-1) \tag{84e}$$

Substituting into the expression for story shears at a level and regrouping, we obtain the following equation.

$$S_j = \frac{B_1^*}{N^3}\left(\frac{Z_4}{4} + \frac{Z_3}{3} + \frac{Z_2}{2}\right) + \frac{B_2^*}{N^2}\left(\frac{Z_3}{3} + \frac{Z_2}{2} + \frac{Z_1}{6}\right) + \frac{B_3^*}{N}\left(\frac{Z_2}{2} + \frac{Z_1}{2}\right) + B_4^*(Z_1) \tag{85}$$

Where

$$Z_\lambda = m[N^\lambda - k^\lambda - (j-1)^\lambda + k^{*\lambda}] + k^\lambda - k^{*\lambda} \tag{86}$$

An expression for overturning moments at any story in terms of the acceleration coefficients B_1^*, B_2^*, B_3^* and B_4^* and functions Z_1, Z_2, Z_3 and Z_4 may be derived as follows:

$$M_j = \sum_{i=j}^{N} (i - j + 1)\ f_i \tag{87}$$

$$M_j = \sum_{i=1}^{N} (i - j + 1)\ f_i - \sum_{i=1}^{j-1} (i - j + 1)\ f_i \tag{88}$$

$$M_j = \sum_{\lambda=0}^{3} \frac{B^*_{(4-\lambda)}}{N^\lambda}\left(\sum_{i=1}^{N}\left[m_i(1-j)(i)^\lambda + m_i(i)^{\lambda+1}\right] - \sum_{i=1}^{j-1}\left[m_i(1-j)(i)^\lambda + m_i(i)^{\lambda+1}\right]\right) \tag{89}$$

If, as before, we assume all base masses to be equal to unity and all setback masses to be equal to m, the equation becomes:

$$M_j = \sum_{\lambda=0}^{3} \frac{B^*_{(4-\lambda)}}{N^\lambda} \left(\sum_{i=1}^{N} m(1-j)(i)^\lambda + \sum_{i=1}^{N} m(i)^{\lambda+1} + \sum_{i=1}^{k} (1-m)(1-j)(i)^\lambda + \sum_{i=1}^{k} (1-m)(i)^{\lambda+1} \right.$$
$$\left. - \sum_{i=1}^{j-1} m(1-j)(i)^\lambda - \sum_{i=1}^{j-1} m(i)^{\lambda+1} - \sum_{i=1}^{k^*} (1-m)(1-j)(i)^\lambda - \sum_{i=1}^{k^*} (1-m)(i)^{\lambda+1} \right) \quad (90)$$

After substituting the expressions for the summations and rearranging, the equations for overturning moments becomes:

$$\begin{aligned} M_j = {} & \frac{B_1^*}{N^3}\left[(1-j)\left(\frac{Z_4}{4} + \frac{Z_3}{2} + \frac{Z_2}{4}\right) + \left(\frac{Z_5}{5} + \frac{Z_4}{2} + \frac{Z_3}{3} - \frac{Z_1}{30}\right)\right] + \\ & \frac{B_2^*}{N^2}\left[(1-j)\left(\frac{Z_3}{3} + \frac{Z_2}{2} + \frac{Z_1}{6}\right) + \left(\frac{Z_4}{4} + \frac{Z_3}{2} + \frac{Z_2}{4}\right)\right] + \\ & \frac{B_3^*}{N}\left[(1-j)\left(\frac{Z_2}{2} + \frac{Z_1}{2}\right) + \left(\frac{Z_3}{3} + \frac{Z_2}{2} + \frac{Z_1}{6}\right)\right] + \\ & \frac{B_4^*}{N}\left[(1-j)(Z_1) + \left(\frac{Z_2}{2} + \frac{Z_1}{2}\right)\right] \end{aligned} \quad (91)$$

For both shear and overturning moment distributions, the polynomial regression equations take the same form and the acceleration distribution coefficients are solved in the same fashion.

$$Y_i^* = B_1^* \chi_{1i} + B_2^* \chi_{2i} + B_3^* \chi_{3i} + B_4^* \chi_{4i} \quad (92)$$

$$\left\{ \sum_{i=1}^{N^*} Y_i \chi_{ji} \right\} = \left[\sum_{i=1}^{N^*} \chi_{ji} \chi_{ki} \right] \{B_k^*\} \quad (93)$$

Solving for the coefficients

$$\{B_k^*\} = \left[\sum_{i=1}^{N^*} \chi_{ji} \chi_{ki} \right]^{-1} \left\{ \sum_{i=1}^{N^*} Y_i \chi_{ji} \right\} \quad (94)$$

If the acceleration distributions are constrained to be zero at the base of the structure, the coefficient B_4^* is set equal to zero. This allows the equations to be condensed and reduced from fourth order to third.

An index of correlation was calculated to measure the goodness of fit of the cubic regression equations to the derived distributions of shears and overturning moments. The index was defined as:

$$\varepsilon = \left\{ 1 - \frac{(N'-4) \sum_{i=1}^{N'} (Y_i - Y_i^*)^2}{(N'-1) \sum_{i=1}^{N'} (Y_i - \overline{Y}_i)^2} \right\}^{1/2} \qquad (95)$$

which is, for large values of N', a function of the unbiased conditional dispersion about the regression equation and the variance of the distribution about its mean value.

A more detailed discussion of polynomial regression analysis is presented in Refs. [1] and [3].

CHAPTER 3. MODELS

This chapter is a description of the models used to adapt the material in Chapter 2 to this study.

3.1 Type of Structure

Structures acting as multidegree of freedom oscillators responding to a strong ground motion, may be represented by spring-mass models (see Fig. 5a). The springs interconnecting the masses are of two basic types representing shear and flexural behavior. Buildings exhibit a combination of the two depending on the lateral force resisting systems. Although the relative proportions of shear and flexural behavior vary along the height of most buildings, the representative springs in the spring mass models may be combined to match the actual behavior.

Slender shear walls behave essentially as flexural beams with shear effects increasing along with the wall depth. Conversely, moment resisting frames behave essentially as shear beams with flexural effects increasing with beam flexibility and axial column deformation. Since beam to column stiffnesses vary along the height of the structure, as do the axial column stiffnesses, the rotational (flexural) effects vary as well. Frames with infinitely rigid beams and inextensible columns behave as pure shear beams and may be modeled as such. All other structural systems exhibit a combination of the two actions. Fig. 1 illustrates the deformation modes of frame-wall structures.

The model used to represent shear wall elements is a discrete spring mass representation of the Timoshenko Beam. In this model the shear and flexural stiffnesses are combined in series, indicating additional flexibility due to the inclusion of both actions. For combinations of walls, with different proportions of flexure and shear, or for the combination of walls and frames, the shear and flexural stiffnesses need to be combined in parallel. In this instance the combination of lateral resisting actions result in a stiffer system.

The Timoshenko Beam is comprised of both flexural and shear components of stiffness connected in series. The inclusion of the shear component softens the system and augments the deflected shape of the beam.

$$EI \frac{\partial^4 u}{\partial X^4} + m \frac{\partial^2 u}{\partial t^2} - \frac{m\kappa EI}{AG} \frac{\partial^4 u}{\partial X^2 \partial t^2} = 0 \qquad (96)$$

$$u = \phi(X) \sin \omega t \qquad (97)$$

$$EI \frac{\partial^4 \phi(X)}{\partial X^4} - m\omega^2 \phi(X) + \frac{m\kappa EI\omega^2}{AG} \frac{\partial^2 \phi(X)}{\partial X^2} = 0 \qquad (98)$$

The Heidebrecht and Smith beam contains both modes of deformation; however, the two are connected in parallel and the inclusion of the shear component stiffens the system, reducing the deflected shape of the beam.

$$EI \frac{\partial^4 u}{\partial X^4} + m \frac{\partial^2 u}{\partial t^2} - \frac{GA}{\kappa} \frac{\partial^2 u}{\partial X^2} \tag{99}$$

$$u = \phi(X) \sin \omega t \tag{97}$$

$$EI \frac{\partial^4 \phi(X)}{\partial X^4} - m\omega^2 \phi(X) - \frac{GA}{\kappa} \frac{\partial^2 \phi(X)}{\partial X^2} \tag{100}$$

The differential equations for the continuous cantilever beam representation of the two models are derived and discussed in Refs. [2],[10],[11],[13],[14],[17] and [28].

3.1.1 Stiffness Matrix

The discretized representation of the lateral structural stiffness matrix is accomplished by summing the condensed lateral frame stiffness coefficients and the lateral wall stiffness coefficients. The wall stiffness matrix is generated as the inverse of the sum of the component flexure and shear flexibility matrices. This procedure preserves the effects of beam flexibilities, column elongations and shear flexibilities maintaining only the lateral degrees of freedom. The assumption involved is that all the walls and frames are constrained to displace an equal amount at each floor level due to a floor slab infinitely rigid in its plane. Furthermore, simplifications in the frame stiffness formulation were obtained by assuming all joint rotations at a floor were equal. This assumption was tested against an exact formulation in Ref. [12] and was found to be quite adequate.

The wall stiffness factors were expressed as the sum of the EI/L for all walls at a story. The frame stiffnesses factors were expressed as the ratio of the sum of the column stiffnesses to the sum of the wall stiffnesses at a story. The beam stiffnesses were expressed as the ratio of the sum of the beam stiffnesses to the sum of the column stiffnesses for the floor below. The column shortening factors were expressed as the ratio of the sum of the column areas to the sum of the column stiffnesses.

The story stiffness distributions were assumed both uniform over the height of the structure and uniform to an intermediate level and uniform, though reduced, for the remaining height of the structure. The first uniform distribution represents a regular structure whereas the second discontinuous distribution represents a setback structure.

In this study the actual values of story stiffness are not as important as the relative values of story stiffness. The resulting lateral stiffness matrix may be scaled to yield the stiffness coefficients corresponding to a desired fundamental frequency. Furthermore, considerable computational economies may be achieved by working with fewer degrees of freedom than floor levels. This may be accomplished, preserving the relative influence of secondary effects, notably the P-Δ interactions, by multiplying the stiffness and dividing the masses by the ratio of reduced degrees of freedom to the number of stories in the structure. To preserve the P-Δ influence the story heights must also be factored when considering the ratio of PΔ/HV and H/R slenderness factor.

3.1.2 Mass Matrix

The masses were assumed to be concentrated at the joints and the resulting matrix representation is of diagonal form. Story masses were assumed to vary in the same relative distribution as story stiffnesses to represent uniform or setback structures.

The story weights used to calculate second order P-Δ effects were a multiple of the mass matrix. These weights were taken to be twenty five percent greater than the corresponding values used in the dynamic analysis. This twenty five percent increase was intended to account for live loads at the time of the strong ground motion.

3.2 Response Spectrum

The response spectrum used in this study is bilinear, representing a constant acceleration branch and a constant velocity branch. The intersection of these lines forms the knee in the spectrum and serves as a point of refrence in scaling the response. A unit constant acceleration was assumed and the frequency at which the knee occurs was assigned the value of 2.5 Hz. (see Fig. 3). This effectively fixes the value of the second branch at 24.6 in/sec. Both the value of the constant acceleration branch and the frequency at which the knee occurs may be varied to match the response of a strong ground motion. For modal analyses which do not include the secondary effects of soil structure and P-Δ interactions, the natural frequencies may be allowed to slide along the frequency axis to simulate the effect of varying fundamental frequencies with respect to the knee. It should be noted that either the structural stiffness matrix or the mass matrix may be multiplied by a constant factor to vary the fundamental frequency relative to the kneee. For this type of primary modal analysis it is only the relative spacing of the natural frequencies which are of interest. A family of responses for different heights of structures, masses or stiffness factors or strong ground motions may be easily generated for any particular relative stiffness and mass distribution.

When the secondary effects of soil-structure and P-Δ interactions are included in the modal analysis, the relative value of fundamental frequency to the knee is no longer sufficient and depending on the value of the fundamental frequency the secondary effects will be amplified or diminished.

3.3 Soil Structure Interaction

A replacement oscillator approximation to the actual structure-foundation system was used to account for foundation compliance in the modal analysis (see Fig. 5b). In this approach, developed and reported in Refs. [19],[29],[30] and [31], each mode of vibration, taken to be a single degree of freedom oscillatior of equivalent mass and height, was presumed to be attached to a pair of springs and dampers at the base. The foundation stiffnesses and dampings were calculated for a rigid circular disk on an elastic halfspace. These impedance functions were derived assuming the disk to be continuously connected to the halfspace, hence no uplifting, and no instabilities representing large foundation settlements.

The dynamic properties of the replacement oscillator were chosen such that the resonant shears of the modified system equalled the resonant shears of the actual system when subjected to the same base motion. For such an equality to exist, the component of structural displacement multiplied by the fixed base structural stiffness must equal the total displacement multiplied by the modified stiffness. Equating the two shears and dividing both sides by the mass we find the two displacements related by the following expression:

$$u = \left(\frac{T}{\tilde{T}}\right)^2 \tilde{u} \qquad (101)$$

However, to this structural displacement the effects of rigid body rotation must be added to give the total displacement of the story mass. The modified period of the replacement oscillator may be calculated from the static displacement it undergoes due to a force equal to the weight of its mass. Similarly, the period of the fixed base system may be approximated from the static displacement it undergoes due to the same force acting on it. The periods are proportional to the square roots of the respective elatic displacements. The ratio of modified to fixed base periods therefore equals the ratio of the square rooted displacements.

$$\tilde{\delta}_{st} = \left[1 + \frac{K}{K_x}\left(1 + \frac{K_x}{K_\psi}(H)^2\right)\right]\frac{mg}{K} \tag{102}$$

$$\delta_{st} = \frac{mg}{K} \tag{103}$$

$$\frac{\tilde{T}}{T} = \left\{1 + \frac{K}{K_x}\left(1 + \frac{K_x}{K_\psi}(H)^2\right)\right\}^{1/2} \tag{104}$$

The equivalent damper for the modified system may be considered to be the sum of the equivalent radiation damping and effective interfloor structural damping. The structural damping may no longer be considered as large as in the fixed base structure and must be reduced to account for the shift in resonant frequencies. By equating the resonant magnitudes of pseudo acceleration ratios due to the equivalent and original systems we obtain the following relation which has been derived in Ref. [19].

$$\left(\frac{u}{T^2 \ddot{u}_g}\right)_{max} = \frac{1}{2\beta} \left(\frac{\tilde{T}}{T}\right)^3 = \frac{1}{2\tilde{\beta}} \qquad (105)$$

$$\tilde{\beta} = \left(\frac{T}{\tilde{T}}\right)^3 \beta \qquad (106)$$

The total modal damping of the system is therefore the sum of the radiation damping due to the foundation flexibility and the modified fixed base structural damping. It is possible that the total damping of the interactive system may be calculated to be less than the assumed damping of the fixed base structure; however, the lower limit of the total interactive damping is set at its fixed base value. Since the percent of critical damping for the structure was based on observations which do not distinguish between foundation and structural components, the composite value is assumed never to be less than the estimated value of β.

The frequency dependent values of spring stiffnesses used to model the foundation flexibility result from the following equations:

$$K_x = \frac{8\alpha_x}{2-\nu} GR \qquad (107)$$

$$K_\psi = \frac{8\alpha_\psi}{3(1-\nu)} GR^3 \qquad (108)$$

Where α_x and α_ψ are the frequency dependent coefficients and were determined in previous studies. It was found that the coefficient for translation is, for all practical purposes, constant and equal to unity while the coefficient for rotation diminished with diminishing slenderness and and diminishing wave parameter. These relationships are illustrated in Fig. 6. The wave parameter describes the relative stiffness of the half space and structure and is equal to:

$$\sigma = \frac{C_s T}{H} \tag{109}$$

Other parameters affecting the degree of soil structure interaction are the relative density of the structure to the halfspace material and the Poisson's ratio for the halfspace. These parameters may be substituted into the relation for the modified period of the replacement oscillator to yield the following equation:

$$\frac{\tilde{T}}{T} = \left\{1 + \frac{2-\nu}{2} \frac{\pi^3}{\alpha_x} \frac{\rho}{\sigma^2} \left(\frac{R}{H}\right) \left[1 + \frac{3(1-\nu)}{(2-\nu)} \frac{\alpha_x}{\alpha_\psi} \left(\frac{H}{R}\right)^2\right]\right\}^{1/2} \tag{110}$$

3.4 Damping

The effects of structural damping on the response spectra may be included in relative terms with amplification or reduction factors applied to the bilinear response values. The factors will differ for the two branches and the frequency at which the knee occurs will diminish as the damping increases.

Statistical studies of earthquake spectra, presented in Ref. [8] , have provided plots of the amplification factors for the two branches of response for various percentiles (see Fig. 4). These factors are applicable up to twenty percent of critical damping. This limitation does not, for the majority of the models investigated, affect this study. Equations fitting the plots for mean values are as follows:

$$AF_a = \frac{4.389 - 0.994 \ln \beta'}{4.389 - 0.994 \ln \beta} \tag{111}$$

$$AF_v = \frac{3.119 - 0.677 \ln \beta'}{3.119 - 0.677 \ln \beta} \tag{112}$$

β' is the structural damping for the mode in question and β is the structural damping assumed for the bilinear representation.

The overall damping for a given mode of the soil structure system is a composite of the energy dissipated by the structure and the energy losses from internal friction and wave radiation into the ground. In this study, structural dampings in all modes were assumed to be five percent of critical, a value consistent with the findings of Refs. [9],[21] and [22], and only the soil structure interaction effects were assumed to affect the relative values. These interaction effects were accounted for from empirical studies performed elsewhere. The values of damping are functions of the structure's slenderness ratio, fixed base to compliant foundation frequency ratio and the level of excitation. Equations for the values of equivalent interaction damping were fit from plots published in Ref. [29], and presented in Fig. 7, corresponding to strong ground motions at high strain levels.

These damping components were combined with the structure's fixed base damping according to the relationship

$$\beta_t = \beta_{soil} + \left(\frac{T}{\tilde{T}}\right)^3 \beta_{structure} \tag{113}$$

Furthermore, it was assumed that the interactive combined dampings could never be less than the fixed base values.

3.5 Energy Relations

The portion of strain energy due to shear deformtion may be approximated by combining the individual ratios of all the lateral load resisting systems in a weighted average technique. Each system alone may be considered to be a deep beam and the ratio may be calculated from the work of each action through its resulting deformation.

$$U = \int_o^L \left(\frac{M^2}{2EI} + \frac{\kappa S^2}{2GA}\right) dx \tag{114}$$

The percent of total deformation attributed to shear will be a function of the shape of the cantilever and its loading.

$$\gamma = 100 \frac{U_S}{U_T} = 100 \frac{\kappa(\frac{r}{L})^2}{Q + \kappa(\frac{r}{L})^2} \tag{115}$$

Q = .1444 Concentrated top load

Q = .0650 Uniform Load

Q = .0851 Linearly Increasing Load

The value of Q for equal loads concentrated at each story level is a function of the total number of stories in the building.

$$Q = 0.065 \left[1 + \frac{1}{N} + \frac{2}{9N^2}\right] \tag{116}$$

Each energy ratio is weighted by the relative stiffness of the structural elements and averaged to yield a composite index. The elements are considered to be connected at the top story and thereby constrained to deflect an equal amount. The weighted factor may be the proportion of base shear a particular element attracts. This value can be calculated in a manner similar to the component stiffness method by assuming the frames to take a constant shear due to an interaction force at the top. The remainder of the shear is assumed proportioned to the shear walls in relation to their moments of inertia.

In the range of practical structures, frames may be considered to be ninety percent shear beam, hence $\gamma_{frame} = 90\%$. Accordingly, the percent of total deformation attributed to shear, and hence the ratio of total stiffness to shear stiffness, is nine tenths. The portion of base shear attributed to the frame may be calculated in a manner similar to the derivations in Ref. [18] to be

$$S_F = \frac{\left(\frac{3N^2 + 2N-1}{12} + \frac{3N^2}{130}\,\kappa\left(\frac{r}{H}\right)^2\right)(N+1)}{\left(2 + \frac{18}{130}\,\kappa\left(\frac{r}{H}\right)^2\right)\frac{N^3}{3} + \left(\frac{N\ \Sigma EI_w}{5.4\ \Sigma EI_c}\right)} \tag{117}$$

For values of $(r/H)^2 < 0.01$

$$S_F = \frac{\left(\frac{3N^2 + 2N-1}{8}\right)\left(\frac{N+1}{N^3}\right)}{1 + \frac{3\ \Sigma EI_w}{10.8\ N^2\ \Sigma EI_c}} \qquad (118)$$

The resulting weighted average of shear deformation may be expressed as:

$$\overline{\gamma} = S_F(\gamma_F) + (1-S_F) \sum_{i=1}^{N^*} \left(\gamma_{wi} \frac{(EI_w)_i}{\Sigma EI_w}\right) \qquad (119)$$

where N^* is the number of walls in the structure, ΣEI_w is the sum of the (EI) of all N^* walls at a level and ΣEI_c is the sum of all the (EI) of all the columns in the frames at a level.

CHAPTER 4. PARAMETERS

To specify the behavior of the cantilevered Timoshenko Beam used to model the different types of structures on the various foundations, several of the parameters were varied. The principal concern of this study was to model the lateral load resisting behavior, the distribution of setbacks along the height, the fundamental frequency relative to the knee in the response spectra and the foundation compliance. To effect these conditions the slenderness of the beam, the structural stiffness, the relative masses and the stiffness along the height and the shear wave velocity of the supporting medium were varied. Furthermore, basic to the analyses several parameters were assumed and held constant throughout. These constants reflect either a most typical value or an insensitive parameter whose variation would cause little significant effect. These assumptions pertain to the secondary effects of P-Δ and soil structure interaction and are described in greater detail in the next section.

4.1 Fixed Parameters

The Poisson's ratio of the elastic halfspace was assumed to be 0.45 representing a realistic value for a foundation material. The Poisson's ratio is involved in determining the impedance and damping properties of the halfspace and its effect has been investigated in Refs. [29] and [30]. The equations for the equivalent spring stiffness and frequency dependence factors are functions of the Poisson's ratio and substituting the assumed value yields the following expressions:

$$K_\psi = 4.85\ \alpha_\psi\ GR^3 \tag{120}$$

$$K_x = 5.16\ \alpha_x\ GR \tag{121}$$

In previous studies the values of α_ψ and α_x, the frequency dependence factors, have been calculated for several values of Poisson's ratio. The value of α_x for the assumed Poisson's ratio was found nearly constant and equal to unity whereas the value of α_ψ diminished with diminishing wave parameter and slenderness ratio as described earlier. A polynomial fit to the curves in Ref. [30] yielded an expression for the relationship between α_ψ and the dimensionless frequency parameter a_o.

$$\begin{aligned}\alpha_\psi = {} & 0.000677\ a_o^5 - 0.01164\ a_o^4 + 0.06828\ a_o^3 \\ & - 0.15\ a_o^2 - 0.0902\ a_o + 0.954\end{aligned} \tag{122}$$

where

$$a_o = \frac{\omega R}{C_s} = \frac{2\pi}{\sigma}\ (\frac{R}{H}) \tag{123}$$

It has been observed in Refs. [19],[29] and [30] and verified in the course of this study that although α_ψ is frequency dependent and ought to be determined in an iterative scheme, the fixed base frequency gives an adequate approximation. Little change was observed from successive refinements of the interactive fundamental frequency.

The damping characteristics of the halfspace were determined for the assumed value of the Poisson's ratio and the level of hysteretic energy dissipation corresponding to strong ground motion. A family of polynomial fits to the plots in Ref. [29] provided relations between radiation damping and the ratio of interactive to fixed base fundamental frequencies for various slendernesses of structures. These damping were expressed as percents of critical and were combined with the assumed value of fixed base structural damping as described previously. Furthermore, it was assumed that the interactive damping values could never be less than the fixed base values.

The fixed base value of structural damping was assumed to be five percent of critical for all modes of vibration. This assumption, considered typical of elastic structural response, corresponds to the bilinear response spectrum used in the modal analysis. Since it is only the relative levels of modal damping that affect the values of spectral acceleration and it is only the foundation compliance that affects the relative levels of modal damping, the overall analysis is fairly insensitive to changes in the fixed base value.

The relative mass density for the structure and supporting medium was assumed to be 0.15. This value is representative for buildings and variations lead to small changes in foundation damping and interactive fundamental frequency.

Lastly, the ratio of total weight to dead weight divided by story height, expressed in feet, was assigned the value of 0.125. This factor is representative of buildings in which the live load is one quarter the weight of the structure and the story heights are ten feet. This value is used in determining the secondary effects of P-Δ moments. Once again slight deviation from the assumed value has little effect on the distribution of shears and overturning moments along the height of the structure.

4.2 Variables

A parameter study of modal analyses of structures subjected to strong ground motions is comprised of two fundamental phases of investigation. First, the structural behavior and configuration needs to be established to determine the dynamic nature of the system. Secondly, the mode shapes need to be combined to reflect the effect of ground motion on the structure. The parameters are therefore either of the type which determines the mode shapes and relative spacing of the frequencies or those which determine the weighting by which the modes are combined. These two types of parameters are described in the following articles and are outlined in Table 1.

4.2.1 Mode of Deformation

The single most significant parameter in modeling the behavior of a cantilever Timoshenko beam is its slenderness ratio. This property determines the deformation characteristics of the model and thus the dynamic properties. By increasing the slenderness of a beam we may represent flexural behavior with its widely separated natural frequencies and corresponding mode shapes. Conversely, by decreasing the slenderness ratio we may accentuate the shear deformation behavior and the resulting modal analysis will correspond to that of a shear beam.

In choosing the values of slenderness ratio to represent the two extreme conditions and four intermediate combinations, the elastic strain energy of deformation due to a concentrated load at the free end was considered. Values of 0, 20, 40, 60, 80 and 100 percent shear deformation were chosen and the corresponding slendernesses were back calculated to evaluate the beam's dimensions.

4.2.2 Setbacks

The structural discontinuities investigated in this study were modeled as towers setback from a unit base. A tower of plan dimension thirty percent that of the base was considered a representative configuration likely to exhibit the effects of discontinuities on shear and overturning moment distributions. The relative heights of the tower and base were varied to determine the effect the location of discontinuties had on structural response to strong ground motion. Structures were assumed, at first uniform over the height, and successively setback in twenty percent intervals till the tower comprised eighty percent of the height. The thirty percent plan area setback represents a tower with thrity percent of the mass and stiffness of the base portion. The degrees of setback studied are illustrated in Fig. 2.

4.2.3 Heights and Fundamental Frequencies

Four heights of structures were investigated representing five, ten, twenty and forty story buildings. For each representation lumped masses were assigned to each floor level separated by unit story heights. The resulting natural frequencies were then scaled to a realistic value based on the height of structure and degree of setback. Structures were assigned a fixed base fundamental frequency inversely proportional to the number of stories, raised to the 3/4 power and directly proportional to a setback factor. The values of fundamental frequency were assigned relative to the frequency at which the knee in the response spectra occurs. All higher frequencies were scaled to preserve the relative spacing and hence the relative modal contribution. Two fundamental frequencies were calculated for each height of building, percent shear deformation and degree of setback. One frequency was intended to represent a stiff structure and the second a more flexible design. The corresponding constants of proportionality, based on a response spectra knee frequency of 2.5 Hz., were assumed to be 7.113 and 5.0808 respectively. These values are in agreement with the expressions for determining fundamental frequencies of structures, assuming a ten foot story height, proposed in Ref. [24].

The setback factor is the ratio of the actual fundamental frequency of a model with the base properties uniform over the height. The setback factor for uniform buildings is therefore equal to unity whereas for other configurations the factor reflects the effect of structural discontinuities on the fundamental frequency. In preserving the relative fundamental frequencies structures of the same height and percent of shear deformation may be compared directly with each other to determine the effect of the setback on the response.

An approximation, yielding greater economy of calculations, would have been to analyze a ten degree of freedom system regardless of the actual number of stories. This would have been accomplished by multiplying the masses and story heights and dividing the stiffnesses all by one tenth the actual number of stories in the structure. Unfortunately, such approximations would have made the top story shears impossible to calculate and the desired accuracy would have been lost.

4.2.4 Soil Structure Interaction Parameters

The seismic velocity and the slenderness ratios were chosen to represent the degree of soil structure interaction of the superstructure founded on a massless disk on an elastic halfspace. The slenderness ratio represents the height of the modal centroid to the radius of the foundation's base. For noncircular foundations the radius is an equivalent value related to the length of the side of the foundation in the direction of the strong ground motion. Equations for equivalent radii are given in Ref. [24]. The slenderness ratio is a significant parameter in determining the relative effects of foundation translation and rotation. Dividing the seismic velocity by the fundamental frequency of the fixed base structure and the associated height of the modal centroid yields a dimensionless wave parameter. This wave parameter is a measure of the relative stiffness of the foundation and the structure. Since the fundamental frequency is approximately inversely proportional to the height of the structure, the wave parameter is primarily a function of the shear wave velocity of the supporting soil. The seismic velocity may be interpreted as a stiffness factor ranging from several hundered feet per second for soft soils to several thousand feet per second for hard rock. Both the wave parameter and the slenderness are therefore the primary variables determining the ratio of interactive to fixed base frequencies and equivalent structural dampings of the interactive system.

In this study, the seismic velocity was assigned four values to represent different degrees of interaction as well as four slendernesses to represent different configurations of structures. The seismic velocities assumed were 250 feet per second (soft), 500 feet per second (intermediate), 1000 feet per second (hard) and infinity (fixed base). These values are intended to represent the effective seismic velocity at strain levels consistent with strong ground motion and they are substantially less than those values measured at small amplitude strain levels. The slendernesses assumed corresponded to the available data on equivalent structural dampings and the ratios were 1,1.5,2 and 5 ranging from squat to slender structures.

CHAPTER 5. RESPONSE DATA

The square root of the sum of the squares combination of the modal values of shear and overturning moments at each floor level represent the most probable distributions of seismic structural response. The distributions need to be normalized to compare the differences resulting from the parametric variations. The response data was considered to be composed of two distinct parts, the base value representing the total base shear and base overturning moments and the distribution of accelerations over the height. Treated separately, design distributions and design base factors may be applied to a uniform fixed base model, for which fundamental frequencies and hence response accelerations may be easily estimated, to determine the actual response.

5.1 Normalization of Base Shears

The most probable base shears and base overturning moments may be normalized with respect to the fixed base base shear for the uniform structure adjusted to the total weight of the setback structure. An equivalent base shear factor, representing the difference between the base and the first story normalized overturning moments divided by the story height, may be evaluated. These normalized base shear values reflect the effects of structural discontinuities, soil structure interaction and P-Δ effects, and they may be considered to be story shear and overturning moment factors. It is intended that the factor corresponding to a structural configuration and founded on a compliant footing will convert the base shear and base overturning moment, calculated for a fixed base and uniform structure, to the corresponding values for which the factors were obtained. In this fashion, one need only work with a uniform structure on a fixed base foundation and modify the resulting shears and overturning moments with the factor pertaining to the actual configuration and foundation. In many cases of preliminary design, accurate knowledge of natural frequencies and structural stiffness is limited. This method of analysis affords the designer an approach consistent with the information at hand.

5.2 Normalization of Distributions

The story shears and overturning moments may be decomposed into story force distributions which may be further decomposed into acceleration distributions along the height of the structure. The resulting distributions represent the equivalent lateral response accelerations at each floor level for calculating either story shears or overturning moments. The response distributions may be reconstructed from the story accelerations assuming unit masses and unit story heights at each level. The resulting distrtibutions may be normalized to produce unit base shears as previously described.

The story shears and overturning moments may be reconstructed using the following transformations:

$$\{\tilde{M}\} = [A_m][M]^{-1}[A_m]^{-1}\{M\} \qquad (124)$$

$$\{\tilde{S}\} = [A_s][M]^{-1}[A_s]^{-1}\{S\} \qquad (125)$$

Where $[A_s]$, $[A_s]^{-1}$, $[A_m]$ and $[A_m]^{-1}$ are defined in chapter 2.

The polynomial expressions derrived for the response distributions can be simplified for the reconstructed data. Since all the masses are equal to unity the distribution coefficients (see equation 86) simplify to the following form:

$$Z_\lambda = (N^\lambda - (j-1)^\lambda) \qquad (126)$$

5.3 Combination of Distributions

The normalized distributions may be expressed in polynomial form by means of a least squares regression technique. It was observed that for a given height of structure, percent of shear deformation and soil shear wave velocity all the distributions for the investigated combinations of fundamental frequency and structural discontinuity could be included in the same least squares routine. The resulting cubic polynomial expressions represent the best curve fit for all distributions as a function of the number of stories, deformation characteristics and soil shear wave velocity. Two sets of acceleration distributions were calculated in this fashion, one for computing story shears and the other for computing overturning moments.

It was further observed that the top story shear and overturning values, for distributions normalized according to the preceding section, were equal to the top story acceleration. A weighting, proportional to the number of stories in the structure, was assigned to this top story value to increase the least squares' sensitivity and thereby force the resulting acceleration distributions to more nearly approximate this point. In this fashion, the polynomial distributions better reflect the top story values.

CHAPTER 6. RESULTS

The data generated by means of the models discussed in Chapter 3, for the parametric variations outlined in Chapter 4 and normalized according to the procedures established in Chapter 5, are presented in this chapter. The story shear and overturning moment response to strong ground motion are separated into two components, the base value and the distribution over the height of the structure. Each component will be discussed with respect to the parameters varied.

In the course of the parameter study, several combinations of seismic velocity, slenderness ratio and fundamental period exceeded the limits of applicability of the mathematical models incorporated into this study. In particular, the upper limit of the range of applicability of damping values for the median horizontal ground motion response spectrum amplification factors, obtained from Ref. [8] and plotted in Fig. 4, is twenty percent of critical. However, for squat structures on soft soil for which the radiation damping component may be sizable (see Fig. 7) the combination of structural and radiation damping often exceeds this limit. Furthermore, the results obtained by the replacement oscillator model of the soil-structure interaction may be significantly in error for cases where the dimensionless wave parameter is less than three. It has been observed, and reported in Ref. [30], that this may be particularly true for slender high rise structures founded on very soft soils. This requirement is not too restrictive and generally overlaps the limitation imposed on the effective damping of the system. The parametric combinations which violate these limitations are indicated in the Tables of results with an asterisk, denoting that the applicability of the analysis may be questionable in the cases so identified.

6.1 Base Values

The current procedure for calculating the base shears and the base overturning moments is to multiply the total weight of the structure by the following: (1) a site effect factor; (2) a seismicity factor; (3) an occupancy factor; and (4) a base shear coefficient. This last coefficient is defined in Ref. [25] as the ratio of the maximum base shear to the weight of the structure of a uniform multidegree of freedom system. The multidegree of freedom system is assumed to have a linear fundamental mode shape and the effect of all vibrational modes is included. The plot of the base shear coefficient as a function of period is, in effect, an influence line for the base shear. However, an error in estimating the fundamental period of the structure or a variation in the spacing of the first several frequencies results in an erroneous base value. To overcome this source of error the base values presented in this chapter will account for the effects of building discontinuities and soil-structure interaction. These factors modify the base shears and base overturning moments of a uniform and rigidly founded structure, calculated by current methods, to reflect the amplification or reduction due to nonuniformities and foundation compliances. Factors accounting for the effects of the percent of shear deformation, as a deviation from the linear fundamental mode shape assumed in Ref. [25], are also presented.

6.1.1 Mode of Deformation

The effects of varying the proportion of shear deformation on the base shears and overturning moments is presented in Table 2. The values are calculated to be the base shears for a uniform rigidly founded structure of varying degree of shear deformation and number of stories, normalized with respect to the shear beam base shears. These factors account for the altered relative spacing of natural frequencies and mode shapes with increasing presence of flexural deformation and may be considered to be an expression of the effective weight of the structure. The relative spacing of the first three natural frequencies of a uniform rigidly founded shear beam increases from (1.0, 3.0, 5.0) to (1.0, 6.27, 17.55) for the corresponding flexural beam. Similarly, the relative modal base shear participation factors increase from (1.0, 0.108, 0.036) to (1.0, 0.306, 0.105).

For a given structure, as the number of stories increases the fundamental frequency decreases. The higher mode influences will vary depending on the location of the fundamental period relative to the knee in the response spectrum. When all natural frequencies exceed the frequency at which the knee in the response spectrum occurs, the relative influence of all modes are the same as the modal base shear participation factors. When the fundamental frequency is less than the frequency at which the knee occurs, the relative influence of the higher modes increases. It is apparent, from Table 2, that for a five story flexure beam, the effect of the more uniform participation of the first three modes, when combined in a square root of the sum of the squares fashion, yields a smaller effective weight than that of a shear beam. However, as the number of stories increases, and the frequencies are scaled accordingly, the larger spacing of the natural frequencies causes the higher modes to dominate. The resulting flexural beam effective weight is greater than that of a shear beam.

6.1.2 Setbacks and Soil-Structure Interaction

The effects of soil-structure interaction and setbacks on the base shears for the variations in height and fundamental period of structures with eighty percent shear deformation are presented in Tables 3 through 6. The corresponding effects on the base overturning moments for the same variation in parameters are presented in Tables 7 through 10. The base values for eighty percent shear deformation were chosen as representative, although the complete set of tabulated results are summarized in Tables 11 through 14.

The values in Tables 3 through 10 represent normalized base shears for calculating both story shears and overturning moments. The base story shear and the difference between the first two stories' overturning moments divided by the first story height for each variation of the setback and soil-structure interaction parameters were normalized with respect to the base story shear of a uniform and rigidly founded structure having the same percent of shear deformation, height and fundamental frequency. The values therefore isolate the effects of foundation compliance and structural discontinuity. Moreover, Tables 7 through 10 reflect the additional effect of base overturning moments reduced from those calculated from the story shear distributions. This reduction has, in the past, been expressed as a J coefficient which varied along the height. Since this study has treated the distributions and base values separately, the analagous J coefficient need only be expressed as a base reduction. These reductions are apparent when Tables 3 through 6 and 7 through 10 are compared.

The effect of setbacks on the models generated was: (1) to increase the fundamental frequency; (2) to decrease the ratio of second to first natural frequency; and (3) to reduce the base shear participation factor of the fundamental mode from those of a uniform building having the dimensions of the lower portion of the actual structure. The influence of the fundamental mode relative to the higher modes is heightened by the first two effects and diminished by the third. The entries in Tables 3 through 10, corresponding to infinite seismic velocity, show the influence of setbacks on a rigidly founded structure. As the height of the setback increases relative to the base portion, the setback factor increases to a maximum and then decreases. For low rise structures the peak value occurs when the setback height is roughly thirty percent of the height of the structure. For high rise structures the peak value occurs when the setback height is eighty percent of the height of the structure. When the structure is setback over its full height the model is once again uniform, though reduced in plan, and the setback factor equals the values for a uniform structure. These relationships are due entirely to the location of the fundamental frequency relative to the knee in the response spectrum. As the height of the structure increases and hence the fundamental frequency decreases, the relative influences of the three dynamical effects of structural setbacks favors the higher modes, yielding a greater amplification.

The fixed base entries for each degree of setback and each height of structure have been averaged over the six degrees of shear deformation investigated, ranging from flexure beam to shear beam. The condensed results are presented in Tables 11 and 12, where the numbers appearing in parentheses are standard deviations indicating the degree of scatter in the averaged values. Since the setback factors were determined for masses and stiffnesses reduced to thirty percent of the base values, to determine the factors for a structure with proportions differing from those studied, an extrapolation or interpolation is required. The values in Table 12, for calculating the effect of setbacks on base overturning moments, are smaller than the corresponding values in Table 11, which are for calculating the base shears. The difference between the two represents the base moment reduction factor for fixed base structures.

The effect of soil-structure interaction on the models generated was to decrease the fundamental frequency, holding the remaining natural frequencies constant, and to increase the apparent damping of the fundamental mode. The influence of both effects is to diminish the spectral acceleration of the fundamental mode while the remaining modal responses stay the same. Looking once again at Tables 3 through 10, it is apparent that the seismic velocity is the primary parameter in reducing the base response. Furthermore, for a given percent of shear deformation and height of structure, a more flexible structure, represented by a higher fundamental period, is less affected by a compliant foundation. Lastly, the slenderness of the structure has contrary influences on the base response. Equation 110 indicates that the ratio of interactive period to fixed base period increases as the slenderness ratio increases. This causes a decrease in the fundamental mode spectral acceleration. Fig. 7 shows that as the period ratio increases the apparent damping for a given slenderness increases. However, as the slenderness increases the apparent damping for a given period ratio decreases and the response spectral acceleration is amplified. It is the relative increases and decreases of the spectral acceleration that determine the modal contributions and the resulting base value factors.

The base values for the flexibly founded models for each degree of shear deformation, height of structure, fundamental period and percent setback were normalized with respect to the base values for the fixed base case. The normalized values for each seismic velocity and slenderness ratio were averaged over the six degrees of shear deformation, the four heights of structures, the two fundamental periods per height of structure and the five degrees of setback investigated. The effects of varying the seismic velocity and the slenderness ratio are summarized in Tables 13 and 14 along with the associated standard deviations. The values in Table 14, for calculating the effects of soil-structure interaction on the base overturning moments, are smaller than the corresponding values in Table 13, which are for calculating the base shears. The difference between the two is the additional base moment reduction for flexibly founded structures which augments the fixed base reductions presented earlier.

6.2 Distributions

The current procedure for calculating the base shear and overturning moment distributions over the height of a structure is to assume a linear distribution of story accelerations. Summing the products of the story acceleration and story mass, starting from the top story proceeding downwards, and normalizing with respect to the base summation yields the story shear distribution. The overturning moments are calculated from these shears as they would be calculated for a static cantilever beam subjected to a transverse loading. A provision to account for the amplified higher mode effects due to the skewed relative modal contributions in high rise, large fundamental period, structures is to provide a concentrated force at the top story not to exceed one quarter of the total base shear of the building. This procedure recognizes that the higher mode effects on shears and overturning moments are confined to the top portion of the structure due to the reversals in story accelerations in the remainder of the structure. Recently, a refinement in Ref. [24] recommended a distribution of story accelerations ranging from linear to quadratic, depending on the fundamental period. This refinement is intended to replace the linear distribution and a concentrated top story force with a single expression. The dynamic effects of setbacks on structures subjected to strong ground motion is the subject of a 1958 report of the Structural Engineers Association Of California Setback Sub-Committee and is presented in Appendix C of Ref. [25].

The distributions of accelerations for calculating story shears and overturning moments presented in this study are intended to provide the designer greater accuracy and flexibility. The accelerations for calculating story shears and overturning moments have been determined independently to represent the most probable distributions along the structure. Furthermore, the effect the type of structural lateral load resisting system has on the response distributions is presented in this chapter along with the effects of setbacks and soil structure interaction. The story acceleration distributions generated in this study are in the form of a polynomial expansion truncated after the cubic term and constrained to be zero at the base. The two constants, B_1 and B_2, specifying the contribution of the higher order terms are the coefficients of the cubic and quadratic terms, B_1^* and B_2^*, of Equation 79 divided by the coefficient of the linear term, B_3^*.

$$A_c(X) = B_1X^3 + B_2X^2 + X \qquad (127)$$

The values of B_1 and B_2 are presented in Tables 15 through 34 and illustrated in Figs. 8 through 11. The linear term coefficient has been normalized to unity for all conditions. When combined with the higher order terms the linearity of the acceleration distributions is altered in different regions along the height of the structure. The cubic term coefficient, B_1, is positive and represents a concentration at the upper stories. The quadratic term coefficient, B_2, is negative and it represents a reduction which, when coupled with the linear and cubic terms, is largely confined to the mid-region of the structure. The relative magnitudes of the coefficients will determine the shape of the acceleration distribution. The acceleration distributions must be normalized with respect to the sum of the products of each story acceleration by its corresponding story mass to be used to calculate the story shears and overturning moments.

6.2.1 Mode of Deformation

The most probable distributions of story shears and overturning moments along the height of a structure have been calculated as the square root of the sum of the squares of the modal contributions. To determine the effect of the percent of shear deformation of a structure on the distributions of story shears and overturning moments it is first necessary to consider the modal distributions and their relative influence. The fundamental mode shape for a uniform cantilevered flexural beam increases monotonically, concave downward, with the greatest curvature at the fixed end. The fundamental mode shape for a uniform cantilevered shear beam increases monotonically, concave upward, with the greatest curvature at the free end. The fundamental mode shear distributions for both beams increases monotonically, concave downward, from a free end value of zero to their fixed end values. However, flexure beams attract over fifty percent more of the base shear near the free end than do shear beams. The fundamental mode overturning moment distributions for the two types of cantilever beams increases monotonically, concave upward, from zero at their free end to their base value. The concentration of the base overturning moments near the free end is only one third greater in flexure beams than in shear beams.

The higher mode shapes do not increase monotonically and the number of sign changes equals the mode number less one. Although the higher mode shapes of the two types of beams are similar, small differences between the two are amplified in the shear and overturning moment distributions. The absolute values of the higher mode story shears and overturning moments approach a uniform distribution due to the increasing number of sign changes in their mode shapes.

Since the portion of the total weight considered effective in each mode is more uniformly distributed in flexure beam structures than in shear beam structures, the combined influence of the higher mode shapes is more pronounced with decreasing percents of shear deformation. This greater higher mode participation has the effect of amplifying the shears in the upper and lower quarters of the building from the fundamental mode values. These effects are even more pronounced for the overturning moment distributions. Furthermore, since the natural frequencies of flexure beams are more widely spaced than those of shear beams, the higher mode effects are more amplified in a high rise flexure beam structure than in a corresponding shear beam structure.

The shear distributions for a structure with significant higher mode participation increases from zero at the free end to a region of near constant shear and then flares out towards the fixed base. The location and extent of the constant region is determined by the position of the fundamental frequency relative to the knee in the response spectra as well as the percent of shear deformation in the structure. The resulting acceleration distribution, decomposed from the story shears, are 'S' shaped and the reduced values in the mid-height region produces the near uniform shears.

The acceleration distribution regression coefficients for calculating the story shears of fixed base structures are presented in Tables 15 through 18. The first column of results, corresponding to a uniform structure of a given height, indicates an increasing negative influence in the mid-height region with decreasing percents of shear deformation. This relationship is most extreme for low rise structures where the spectral accelerations for all modes are nearly equal.

When the most probable overturning moment distributions are compared with those of the fundamental mode it is apparent that the effect of the higher modes is to amplify the upper values while reducing the lower values relative to the base. These deviations from the fundamental mode overturning moments are more pronounced than the deviations observed between the most probable story shears and the fundamental mode values. The story accelerations obtained from the most probable overturning moment distributions are therefore reduced in the mid-height region to a greater extent than those from the shear distributions. The polynomial regression coefficients for calculating the overturning moment acceleration distributions of fixed based structures are presented in Tables 23 through 26. As was the case with the story shear acceleration distributions, the higher mode effects are most pronounced in high rise flexure beam structures.

6.2.2 Setbacks and Soil-Structure Interaction

The effect of setbacks on the distribution of story shears and overturning moments is primarily to alter the relative contribution of each mode to the most probable distributions. Although the mode shapes of a setback structure are different from those of a uniform structure, the difference in shape is a secondary effect and it is overshadowed by the more significant change in the spacing of the natural frequencies. The story shear regression coefficients for fixed based structures are presented in Tables 15 through 18 and the corresponding coefficients for calculating overturning moments are presented in Tables 23 through 26. These tables reflect the increased effect of higher mode participation for structures with setbacks equal to thirty percent of the area of the base. For a given height of structure and percent of shear deformation, the coefficients exhibit no specific trend over the range of setbacks. A more general set of polynomial regression coefficients were calculated for each height of structure and percent of shear deformation by grouping the five variations in setbacks into a single least squares analysis. The values for calculating story shears are presented in Table 31 and the values for calculating overturning moments are presented in Table 33. These tables have been presented in Figs. 8 and 10 where it is obvious that the greatest variation in the acceleration coefficients is in the range of low rise structures. The effect of increasing the number of stories, thereby reducing the fundamental frequency with respect to the knee in the response spectrum, is to increase the higher mode influences. However, the coefficients for a given type of structure approach uniform values as the number of stories increases. The acceleration distributions for calculating story shears of fixed base structures are illustrated directly above the corresponding distributions for calculating overturning moments on the left hand side of Figs. 12 through 17. These diagrams are normalized to a unit value at the top story and the higher mode contributions are seen to increase with increasing story height and decreasing percent of shear deformation.

The indexes of correlation for the individual distributions presented in Tables 15 through 18 and Tables 23 through 26 were closer to unity than those of the grouped acceleration distributions presented in Tables 31 through 34. This is due to the disparity between the distributions for the various values of setback. However, for preliminary design purposes the errors introduced by generalizing the distribution coefficients do not impair their usefulness.

Polynomial regression coefficients were calculated for structures on compliant foundations to determine the effects of soil-structure interaction. The distributions for structures founded on a halfspace with an effective seismic velocity of five hundred feet per second were chosen to represent these effects. The story shear and overturning moment distributions were found to be very similar over the range of structural slendernesses investigated, H/R equal to 1.0, 1.5, 2.0 and 5.0. The regression coefficients were therefore calculated for each percent of shear deformation, height of structure and percent setback while the four slendernesses were grouped into a single least squares analysis. The coefficients for calculating story shears are presented in Tables 19 through 22 and the corresponding coefficients for calculating overturning moments are presented in Tables 27 through 30. When these tables are compared with those for fixed base structures it is obvious that the single most significant effect of soil-structure interaction is to increase the higher mode participation in the most probable distributions calculated. The trends observed for the fixed base structures were also observed when soil-structure interaction was considered and the distributions for setback structures were combined in a single best fit expression for each height and percent of shear deformation. These acceleration coefficients for calculating story shears are presented in Table 32 and the corresponding coefficients for calculating overturning moments are presented in Table 34. These tables have also been plotted in Figs. 9 and 11 and the results are similar to those for fixed base structures. The acceleration distributions for calculating story shears of structures founded on a halfspace with an effective seismic velocity of five hundred feet per second are illustrated in Figs. 12 through 17 directly above the corresponding distributions for calculating overturning moments and to the right of the corresponding distributions for fixed base structures. To determine the coefficients for calculating the acceleration distributions for structures founded on compliant halfspaces with effective seismic velocities other than five hundred feet per second it is necessary to extrapolate or interpolate from the tabulated data.

CHAPTER 7. CONCLUSIONS

A procedure for determining design story shears and overturning moments to resist the effects of strong ground motions is presented. These distributions over the height of a structure are the result of a parameter study in which the type of structure, the height of structure, the vertical configuration and the foundation interactions were varied. For each model a modal analysis was performed and the square root of the sum of the squares of the responses were generated. The base magnitudes were reduced to base factors, accounting for the effects of the parameters varied. Polynomial regression analyses were performed on the normalized distributions and the coefficients were determined to account for the effects of the parameters varied.

7.1 Design Procedure

The procedure for calculating the seismic shears and overturning moments presented in this study is compatible with current code practices. The base factors and the acceleration distribution coefficients discussed in Chapter 6 may be used to calculate design shears and moments without the need of a rigorous modal analysis. Once the lateral load resisting system has been chosen, in the most preliminary stages of design, the mode of deformation of the proposed structure may be determined from the general proportions of the primary structural elements. This value may be calculated by Equations 115 through 119. With this information and the height of the structure a mode of deformation factor may be determined from Table 2. With further information regarding the uniformity of the structure over its height and the soil on which it will be founded, setback factors and soil-structure interaction factors may be determined from Tables 11 through 14. Two sets of these factors must be determined, one set for calculating the story shears and the other for calculating the overturning moments. These factors are to be multiplied by the total weight of the structure, the spectral acceleration and whatever other site effect, occupancy and seismicity factors present codes may require. The two resulting base shears will be used for calculating the story shears and the overturning moments over the height of the building. The distributions may be calculated with Equation 127 using the polynomial regression factors tabulated in Tables 31 through 34 or illustrated in Figs. 9 through 12. Once again two sets of acceleration distributions must be determined, one for calculating the story shears and the other for calculating the overturning moments. The two distributions need to be determined and normalized with respect to the sum of the products of each story acceleration by its corresponding story mass. The resulting normalized distributions must be multiplied by the base values and story masses to yield the static story forces. These two static story force distributions are to be used to calculate the probable elastic story shears and overturning moments due to a strong ground motion.

7.2 Further Study

In this study damping was assumed to be five percent of critical for the first several modes of vibration. Further investigations of existing structures are needed to determine the actual damping, both structural and radiational, at various levels of excitation. The effects of soil-structure interaction have been presented for structures supported at the surface of a homogeneous halfspace. Modifications to the effective seismic velocity and slenderness ratios need to be developed to generalize the results of this paper to structures embedded in a layered media. Furthermore, the effects of isolated spread footings and pile foundations need to be adapted to the parameters investigated. Lastly, the case where a structure temporarily lifts off part of its foundation needs to be studied and presented as a reduction to the design distributions.

REFERENCES

1) Ang, A. H.-S. and Tang, W.H., PROBABILITY CONCEPTS IN ENGINEERING PLANNING AND DESIGN, VOLUME 1 - BASIC PRINCIPLES, J. Wiley and Sons, N.Y., 1975

2) Clough, R.W. and Penzien, J., DYNAMICS OF STRUCTURES, McGraw Hill, N.J., 1975

3) Ezekiel, M. and Fox, K.A., METHODS OF CORRELATION AND REGRESSION ANALYSIS, LINEAR AND CURVILINEAR, J. Wiley and Sons, N.Y., 1959

4) Fenves, S.J., and Newmark, N.M., SEISMIC FORCES AND OVERTURNING MOMENTS IN BUILDINGS, TOWERS AND CHIMINIES, Proceedings Fourth World Conference on Earthquake Engineering, Vol. III, Santiago Chile, Pg. B5-1 to B5-12, 1969

5) Goel, S.C., P-Δ AND AXIAL COLUMN DEFORMATION IN ASEISMIC FRAMES, Journal of the Structural Division, A. S. C. E., Vol. 95, No. ST 8, Pg. 1693 - 1710, 1969

6) Garbow, B.S. and Dongarra, J.J., PATH CHART AND DOCUMENTATION FOR THE EISPACK PACKAGE OF MATRIX EIGENSYSTEM ROUTINES, Argonne National Laboratories, Applied Math Division, 1975

7) Hadjian, A.H., A. S. C. E. MANUAL OF STANDARD PRACTICE FOR STRUCTURAL DESIGN OF NUCLEAR POWER PLANTS SOIL-STRUCTURE INTERACTION, APPENDIX B - IMPEDANCE ANALYSIS, 1976

8) Hall, W.H., Mohraz, B. and Newmark, N.M., STATISTICAL STUDIES OF VERTICAL AND HORIZONTAL EARTHQUAKE SPECTRA, Report NUREG 0003 prepared for the Division of Systems Safety, United States Nuclear Reglatory Commission, Washington

D.C., 20555, 1976

9) Hart, G.C. and Vasudevan, R., EARTHQUAKE DESIGN OF BUILDINGS: DAMPING, Journal of the Structural Division, A. S. C. E., Vol. 101, No. ST 1, Pg. 11 - 30, 1975

10) Heidebrecht, A.C. and Smith, B.S., APPROXIMATE ANALYSIS OF TALL WALL-FRAME STRUCTURES, Journal of the Structural Division, A. S. C. E., Vol. 99, No. ST 2, Pg. 199 - 221, 1973

11) Heidebrecht, A.C., DYNAMIC EVALUATION OF OVERTURNING MOMENT REDUCTION FACTOR USED IN STATIC SEISMIC LOADING, Canadian Journal of Civil Engineering, Pg. 447 - 453, 1975

12) Hurty, W.C. and Rubinstein, M.F., DYNAMICS OF STRUCTURES, Prentice Hall, N.J., 1964

13) Jacobsen, L.S., NATURAL PERIODS OF UNIFORM CANTILEVER BEAMS, Transactions of the American Society of Civil Engineers, Paper No. 2025, Pg. 402 - 439

14) Jacobsen, L.S. and Ayre, R.S., ENGINEERING VIBRATIONS WITH APPLICATIONS TO STRUCTURES AND MACHINERY, McGraw Hill, N.J., 1958

15) Jennings, P.C. and Bielak, J., DYNAMICS OF BUILDING-SOIL INTERACTION, Bulletin of the Seismological Society of America, Vol. 63, No. 1, Pg. 9 - 48, 1973

16) Jolley, L.B.W., SUMMATION OF SERIES, Dover, N.Y., 1961

17) Langhaar, H.L., ENERGY METHODS IN APPLIED MECHANICS, J. Wiley and Sons, N.Y., 1962

18) Macleod, I.A., SHEAR WALL-FRAME INTERACTION, A DESIGN AID WITH COMMENTARY, Portland Cement Association

Publication, 1971

19) Meek, J.W. and Veletsos, A.S., DYNAMIC ANALYSIS AND BEHAVIOR OF STRUCTURE-FOUNDATION SYSTEMS, S.R.R. Report No. 13, Department of Civil Engineering, Rice University, Houston, Texas, 1972

20) Meirovitch, L., ELEMENTS OF VIBRATION ANALYSIS, McGraw Hill, N.J., 1975

21) Newmark, N.M. and Rosenblueth, E., FUNDAMENTALS OF EARTHQUAKE ENGINEERING, Prentice Hall, N.J., 1971

22) Raggett, A.M., ESTIMATING DAMPING OF REAL STRUCTURES, Journal of the Structural Division, A. S. C. E., Vol. 101, No. ST 9, Pg. 1822 - 1835, 1975

23) Ramsden, J.N. and Stoker, J.R., MASS CONDENSATION: A SEMI-AUTOMATIC METHOD FOR REDUCING THE SIZE OF VIBRATION PROBLEMS, International Journal for Numerical Methods in Engineering, Vol. 1, Pg. 333 - 349, 1969

24) RECOMMENDED COMPREHENSIVE SEISMIC DESIGN PROVISIONS FOR BUILDINGS, Applied Technology Council, Palo Alto, California, 1977

25) RECOMMENDED LATERAL FORCE REQUIREMENTS AND COMMENTARY, Seismology Committee Structural Engineering Association of California, 1975

26) Richart, F.E., Jr., Woods, R.D. and Hall, J.R., Jr., VIBRATIONS OF SOILS AND FOUNDATIONS, Prentice Hall, N.J., 1970

27) Teal, E.J., SEISMIC DRIFT CONTROL CRITERIA, Engineering Journal American Institute of Steel Construction, Second

Quarter, 1975

28) Timoshenko, S., Young, D.H. and Weaver, W., VIBRATION PROBLEMS IN ENGINEERING, Fourth Edition, J. Wiley and Sons, N.Y., 1974

29) Veletsos, A.S., DYNAMICS OF STRUCTURE-FOUNDATION SYSTEMS, Presented at the Symposium on Structural and Geotechnical Mechanics Honoring Dr. N.M. Newmark, 1975

30) Veletsos, A.S. and Meek, J.W., DYNAMIC BEHAVIOR OF BUILDING-FOUNDATION SYSTEMS, Int. Journal of Earthquake Engineering and Structural Dynamics, Vol. 3, No. 2, Pg. 121 - 138, 1974

31) Veletsos, A.S. and Nair, V.V.D., SEISMIC INTERACTION OF STRUCTURES ON HYSTERETIC FOUNDATIONS, Journal of the Structural Division, A. S. C. E., Vol. 101, No. ST 1, Pg. 109 - 129, 1975

32) Veletsos, A.S. and Verbic, B., VIBRATION OF VISCOELASTIC FOUNDATIONS, Int. Journal of Earthquake Engineering and Structural Dynamics, Vol. 3, No. 2, Pg. 87 - 102, 1973

33) Veletsos, A.S. and Verbic, B., BASIC RESPONSE FUNCTIONS FOR ELASTIC FOUNDATIONS, Journal of the Engineering Mechanics Division, A. S. C. E., Vol. 100, No. EM 2, Pg. 189 - 202, 1974

34) Wood, B.R., Beaulieu, D. and Adams, P.F., COLUMN DESIGN BY THE P DELTA METHOD, Journal of the Structural Division, A. S. C. E., Vol. 102, No. ST 2, Pg. 411 - 427, 1976

TABLE 1

Parameter Combinations

Percent Shear Deformation	Number of Stories	Percent Setback	Fundamental Period	Seismic Velocity (Ft./Sec.)	H/R*
0		0			
20	5	20	$.025H^{3/4}$	Infinite**	1
40	10	40		1000	1.5
60	20	60	$.035H^{3/4}$	500	2
80	40	80		250	5
100					

(*) H/R = effective modal height/radius of foundation

(**) Fixed base foundation obviates a soil-structure interaction analysis

TABLE 2

Mode of Deformation Factor

Number Of Stories	Percent Shear Deformation 0	20	40	60	80	100
5	0.83	0.87	0.90	0.93	0.96	1.00
10	0.92	0.97	0.98	0.98	0.98	1.00
20	1.14	1.13	1.13	1.05	1.00	1.00
40	1.49	1.37	1.18	1.06	1.01	1.00

TABLE 3

Base Shear Factors (5 Stories, 80% Shear Deformation)

Fundamental Period = $0.025H^{3/4}$

Seismic Velocity (Ft./Sec.)	H/R	Setback				
		0%	20%	40%	60%	80%
Infinite	All	1.000	1.173	1.117	0.968	0.898
1000	1.0	0.948	1.107	1.072	0.931	0.846
1000	1.5	0.959	1.121	1.091	0.947	0.857
1000	2.0	0.963	1.127	1.104	0.958	0.862
1000	5.0	0.946	1.104	1.118	0.969	0.845
500	1.0	0.786	0.900	0.907	0.801	0.695
500	1.5	0.837	0.966	0.998	0.865	0.743
500	2.0	0.862	0.998	1.044	0.893	0.765
500	5.0	0.815	0.940	0.979	0.848	0.729
250	1.0	0.421	0.457	0.465	*	*
250	1.5	0.528	0.585	0.591	0.603	0.530
250	2.0	0.578	0.646	0.656	0.640	0.560
250	5.0	0.554	0.622	0.640	0.641	0.558

Fundamental Period = $0.035H^{3/4}$

Seismic Velocity (Ft./Sec.)	H/R	Setback				
		0%	20%	40%	60%	80%
Infinite	All	1.000	1.164	1.249	1.135	0.965
1000	1.0	0.974	1.131	1.210	1.104	0.941
1000	1.5	0.981	1.140	1.219	1.111	0.947
1000	2.0	0.980	1.139	1.220	1.113	0.947
1000	5.0	0.972	1.129	1.206	1.102	0.940
500	1.0	0.895	1.029	1.085	1.010	0.869
500	1.5	0.918	1.059	1.122	1.038	0.891
500	2.0	0.931	1.075	1.142	1.054	0.902
500	5.0	0.902	1.039	1.101	1.024	0.880
250	1.0	0.621	0.682	0.697	0.775	0.682
250	1.5	0.710	0.795	0.821	0.843	0.737
250	2.0	0.749	0.844	0.875	0.874	0.762
250	5.0	0.704	0.790	0.822	0.851	0.742

(*) Analysis does not apply to this case.

TABLE 4

Base Shear Factors (10 Stories, 80% Shear Deformation)

Fundamental Period = $0.025H^{3/4}$

Seismic Velocity (Ft./Sec.)	H/R	Setback 0%	20%	40%	60%	80%
Infinite	All	1.000	1.163	1.257	1.198	1.004
1000	1.0	0.938	1.081	1.156	1.126	0.949
1000	1.5	0.951	1.099	1.178	1.141	0.961
1000	2.0	0.957	1.107	1.189	1.150	0.967
1000	5.0	0.937	1.081	1.158	1.129	0.951
500	1.0	0.751	0.838	0.868	0.951	0.811
500	1.5	0.811	0.916	0.961	1.004	0.853
500	2.0	0.840	0.953	1.003	1.029	0.873
500	5.0	0.794	0.895	0.942	0.998	0.848
250	1.0	*	*	*	*	*
250	1.5	0.523	0.550	0.578	0.836	0.713
250	2.0	0.567	0.607	0.636	0.857	0.731
250	5.0	0.562	0.606	0.655	0.882	0.751

Fundamental Period = $0.035H^{3/4}$

Seismic Velocity (Ft./Sec.)	H/R	Setback 0%	20%	40%	60%	80%
Infinite	All	1.000	1.140	1.241	1.350	1.134
1000	1.0	0.971	1.102	1.195	1.321	1.112
1000	1.5	0.978	1.111	1.206	1.327	1.117
1000	2.0	0.979	1.112	1.208	1.329	1.118
1000	5.0	0.970	1.100	1.193	1.320	1.111
500	1.0	0.883	0.983	1.050	1.236	1.047
500	1.5	0.909	1.019	1.095	1.261	1.067
500	2.0	0.924	1.038	1.118	1.275	1.077
500	5.0	0.896	1.001	1.075	1.252	1.059
250	1.0	0.628	0.648	0.693	1.089	0.926
250	1.5	0.707	0.752	0.799	1.125	0.957
250	2.0	0.743	0.798	0.848	1.145	0.973
250	5.0	0.715	0.764	0.819	1.138	0.967

(*) Analysis does not apply to this case.

TABLE 5

Base Shear Factors (20 Stories, 80% Shear Deformation)

Fundamental Period = $0.025H^{3/4}$

Seismic Velocity (Ft./Sec.)	H/R	Setback 0%	20%	40%	60%	80%
Infinite	All	1.000	1.145	1.235	1.385	1.218
1000	1.0	0.928	1.047	1.112	1.313	1.166
1000	1.5	0.943	1.068	1.139	1.329	1.177
1000	2.0	0.952	1.080	1.154	1.338	1.184
1000	5.0	0.931	1.052	1.121	1.321	1.171
500	1.0	0.734	0.791	0.815	1.181	1.066
500	1.5	0.796	0.873	0.908	1.218	1.094
500	2.0	0.824	0.910	0.950	1.236	1.108
500	5.0	0.788	0.864	0.904	1.221	1.096
250	1.0	*	*	*	*	*
250	1.5	*	*	*	*	*
250	2.0	*	*	*	*	*
250	5.0	*	*	*	*	*

Fundamental Period = $0.035H^{3/4}$

Seismic Velocity (Ft./Sec.)	H/R	Setback 0%	20%	40%	60%	80%
Infinite	All	1.000	1.145	1.242	1.375	1.386
1000	1.0	0.965	1.098	1.184	1.339	1.364
1000	1.5	0.973	1.109	1.197	1.347	1.369
1000	2.0	0.975	1.112	1.202	1.351	1.371
1000	5.0	0.964	1.097	1.183	1.340	1.364
500	1.0	0.856	0.953	1.007	1.244	1.304
500	1.5	0.890	0.999	1.063	1.273	1.323
500	2.0	0.909	1.023	1.092	1.288	1.332
500	5.0	0.880	0.984	1.047	1.268	1.319
250	1.0	0.617	0.645	0.693	*	*
250	1.5	0.686	0.732	0.776	1.157	1.246
250	2.0	0.720	0.776	0.821	1.173	1.257
250	5.0	0.711	0.765	0.815	1.177	1.260

(*) Analysis does not apply to this case.

TABLE 6

Base Shear Factors (40 Stories, 80% Shear Deformation)

Fundamental Period = $0.025H^{3/4}$

Seismic Velocity (Ft./Sec.)	H/R	Setback				
		0%	20%	40%	60%	80%
Infinite	All	1.000	1.145	1.258	1.382	1.488
1000	1.0	0.904	1.017	1.100	1.289	1.434
1000	1.5	0.926	1.046	1.136	1.310	1.446
1000	2.0	0.938	1.062	1.155	1.321	1.453
1000	5.0	0.915	1.031	1.119	1.302	1.442
500	1.0	0.690	0.736	0.799	1.166	1.359
500	1.5	0.757	0.822	0.887	1.197	1.378
500	2.0	0.787	0.862	0.928	1.213	1.388
500	5.0	0.761	0.829	0.900	1.207	1.384
250	1.0	*	*	*	*	*
250	1.5	*	*	*	*	*
250	2.0	*	*	*	*	*
250	5.0	*	*	*	*	*

Fundamental Period = $0.035H^{3/4}$

Seismic Velocity (Ft./Sec.)	H/R	Setback				
		0%	20%	40%	60%	80%
Infinite	All	1.000	1.143	1.248	1.387	1.473
1000	1.0	0.953	1.080	1.170	1.341	1.446
1000	1.5	0.964	1.094	1.187	1.351	1.452
1000	2.0	0.969	1.101	1.196	1.357	1.455
1000	5.0	0.956	1.083	1.174	1.345	1.449
500	1.0	0.816	0.897	0.955	1.234	1.383
500	1.5	0.861	0.957	1.025	1.267	1.402
500	2.0	0.884	0.987	1.058	1.283	1.412
500	5.0	0.857	0.949	1.018	1.269	1.404
250	1.0	*	*	*	*	*
250	1.5	0.658	0.695	0.758	1.171	1.342
250	2.0	0.693	0.739	0.800	1.185	1.352
250	5.0	0.710	0.756	0.830	1.214	1.371

(*) Analysis does not apply to this case.

TABLE 7

Base Overturning Moment Factors (5 Stories, 80% Shear Deformation)

Fundamental Period = $0.025H^{3/4}$

Seismic Velocity (Ft./Sec.)	H/R	Setback 0%	20%	40%	60%	80%
Infinite	All	0.974	1.155	1.091	0.865	0.800
1000	1.0	0.921	1.087	1.045	0.823	0.742
1000	1.5	0.932	1.102	1.064	0.841	0.754
1000	2.0	0.936	1.107	1.077	0.853	0.760
1000	5.0	0.918	1.084	1.092	0.866	0.741
500	1.0	0.752	0.876	0.874	0.673	0.564
500	1.5	0.805	0.943	0.968	0.747	0.621
500	2.0	0.832	0.976	1.016	0.780	0.648
500	5.0	0.783	0.916	0.949	0.728	0.605
250	1.0	0.356	0.408	0.398	*	*
250	1.5	0.477	0.547	0.540	0.418	0.340
250	2.0	0.531	0.612	0.610	0.470	0.385
250	5.0	0.506	0.586	0.593	0.471	0.382

Fundamental Period = $0.035H^{3/4}$

Seismic Velocity (Ft./Sec.)	H/R	Setback 0%	20%	40%	60%	80%
Infinite	All	0.950	1.128	1.204	0.965	0.786
1000	1.0	0.923	1.094	1.163	0.928	0.757
1000	1.5	0.930	1.103	1.173	0.937	0.764
1000	2.0	0.929	1.103	1.174	0.938	0.765
1000	5.0	0.921	1.092	1.160	0.926	0.756
500	1.0	0.839	0.989	1.033	0.815	0.666
500	1.5	0.863	1.020	1.072	0.849	0.694
500	2.0	0.877	1.036	1.093	0.868	0.709
500	5.0	0.846	0.999	1.049	0.831	0.679
250	1.0	0.537	0.620	0.613	0.495	0.391
250	1.5	0.638	0.742	0.751	0.595	0.480
250	2.0	0.681	0.794	0.809	0.639	0.518
250	5.0	0.631	0.737	0.753	0.605	0.488

(*) Analysis does not apply to this case.

TABLE 8

Base Overturning Moment Factors (10 Stories, 80% Shear Deformation)

Fundamental Period = $0.025H^{3/4}$

Seismic Velocity (Ft./Sec.)	H/R	Setback 0%	20%	40%	60%	80%
Infinite	All	0.929	1.109	1.195	0.984	0.796
1000	1.0	0.862	1.024	1.088	0.895	0.726
1000	1.5	0.876	1.042	1.111	0.914	0.741
1000	2.0	0.883	1.051	1.123	0.925	0.749
1000	5.0	0.861	1.023	1.090	0.900	0.729
500	1.0	0.655	0.762	0.775	0.666	0.534
500	1.5	0.722	0.848	0.878	0.738	0.596
500	2.0	0.754	0.887	0.924	0.771	0.624
500	5.0	0.703	0.825	0.857	0.731	0.588
250	1.0	*	*	*	*	*
250	1.5	0.372	0.428	0.427	0.512	0.377
250	2.0	0.431	0.498	0.502	0.538	0.408
250	5.0	0.425	0.496	0.526	0.572	0.440

Fundamental Period = $0.035H^{3/4}$

Seismic Velocity (Ft./Sec.)	H/R	Setback 0%	20%	40%	60%	80%
Infinite	All	0.871	1.041	1.127	1.001	0.791
1000	1.0	0.838	0.999	1.076	0.962	0.760
1000	1.5	0.846	1.010	1.088	0.971	0.767
1000	2.0	0.846	1.011	1.090	0.974	0.769
1000	5.0	0.836	0.997	1.073	0.961	0.759
500	1.0	0.733	0.867	0.913	0.846	0.663
500	1.5	0.765	0.907	0.963	0.882	0.693
500	2.0	0.782	0.929	0.990	0.900	0.709
500	5.0	0.749	0.887	0.940	0.869	0.682
250	1.0	0.395	0.457	0.461	0.659	0.467
250	1.5	0.510	0.594	0.607	0.696	0.517
250	2.0	0.558	0.651	0.670	0.721	0.545
250	5.0	0.520	0.608	0.632	0.714	0.536

(*) Analysis does not apply to this case.

TABLE 9

Base Overturning Moment Factors (20 Stories, 80% Shear Deformation)

Fundamental Period = $0.025H^{3/4}$

Seismic Velocity (Ft./Sec.)	H/R	Setback 0%	20%	40%	60%	80%
Infinite	All	0.848	1.010	1.107	1.028	0.831
1000	1.0	0.762	0.898	0.969	0.935	0.757
1000	1.5	0.781	0.923	1.000	0.955	0.773
1000	2.0	0.791	0.936	1.016	0.967	0.782
1000	5.0	0.766	0.904	0.980	0.945	0.764
500	1.0	0.511	0.581	0.605	0.781	0.618
500	1.5	0.595	0.688	0.726	0.816	0.654
500	2.0	0.633	0.734	0.777	0.837	0.673
500	5.0	0.584	0.676	0.721	0.821	0.657
250	1.0	*	*	*	*	*
250	1.5	*	*	*	*	*
250	2.0	*	*	*	*	*
250	5.0	*	*	*	*	*

Fundamental Period = $0.035H^{3/4}$

Seismic Velocity (Ft./Sec.)	H/R	Setback 0%	20%	40%	60%	80%
Infinite	All	0.841	0.995	1.086	1.006	0.899
1000	1.0	0.799	0.940	1.018	0.960	0.868
1000	1.5	0.809	0.953	1.033	0.970	0.875
1000	2.0	0.812	0.957	1.039	0.975	0.878
1000	5.0	0.798	0.939	1.018	0.961	0.869
500	1.0	0.664	0.766	0.806	0.834	0.790
500	1.5	0.708	0.822	0.875	0.873	0.813
500	2.0	0.730	0.851	0.909	0.892	0.825
500	5.0	0.693	0.803	0.855	0.867	0.810
250	1.0	0.303	0.322	0.345	*	*
250	1.5	0.424	0.468	0.488	0.751	0.761
250	2.0	0.477	0.532	0.556	0.760	0.758
250	5.0	0.460	0.513	0.545	0.767	0.765

(*) Analysis does not apply to this case.

TABLE 10

Base Overturning Moment Factors (40 Stories, 80% Shear Deformation)

Fundamental Period = $0.025H^{3/4}$

Seismic Velocity (Ft./Sec.)	H/R	Setback 0%	20%	40%	60%	80%
Infinite	All	0.838	0.991	1.081	1.014	0.978
1000	1.0	0.722	0.839	0.891	0.894	0.916
1000	1.5	0.749	0.874	0.936	0.921	0.929
1000	2.0	0.763	0.893	0.959	0.935	0.936
1000	5.0	0.735	0.856	0.915	0.911	0.925
500	1.0	0.425	0.464	0.473	0.778	0.921
500	1.5	0.525	0.590	0.610	0.791	0.893
500	2.0	0.568	0.643	0.668	0.806	0.891
500	5.0	0.531	0.599	0.629	0.802	0.895
250	1.0	*	*	*	*	*
250	1.5	*	*	*	*	*
250	2.0	*	*	*	*	*
250	5.0	*	*	*	*	*

Fundamental Period = $0.035H^{3/4}$

Seismic Velocity (Ft./Sec.)	H/R	Setback 0%	20%	40%	60%	80%
Infinite	All	0.832	0.981	1.067	0.984	0.958
1000	1.0	0.776	0.908	0.975	0.922	0.924
1000	1.5	0.788	0.924	0.995	0.936	0.932
1000	2.0	0.794	0.932	1.006	0.943	0.936
1000	5.0	0.778	0.910	0.980	0.928	0.929
500	1.0	0.599	0.680	0.701	0.781	0.871
500	1.5	0.659	0.757	0.794	0.823	0.882
500	2.0	0.688	0.794	0.837	0.844	0.891
500	5.0	0.651	0.746	0.785	0.826	0.887
250	1.0	*	*	*	*	*
250	1.5	0.355	0.378	0.394	0.746	0.936
250	2.0	0.414	0.450	0.468	0.746	0.908
250	5.0	0.430	0.469	0.508	0.769	0.903

(*) Analysis does not apply to this case.

TABLE 11

Base Shear Setback Factor

Setback	Number of Stories			
	5	10	20	40
0%	1.000 (0.0)	1.000 (0.0)	1.000 (0.0)	1.000 (0.0)
20%	1.170 (0.024)	1.156 (0.022)	1.124 (0.023)	1.138 (0.026)
40%	1.186 (0.100)	1.258 (0.024)	1.227 (0.012)	1.240 (0.023)
60%	1.077 (0.115)	1.289 (0.082)	1.417 (0.095)	1.454 (0.107)
80%	0.954 (0.061)	1.082 (0.067)	1.252 (0.105)	1.456 (0.153)

Note: Numbers within parentheses are standard deviations

TABLE 12

Base Overturning Moment Setback Factor

Setback	Number of Stories			
	5	10	20	40
0%	0.947 (0.024)	0.882 (0.042)	0.815 (0.048)	0.798 (0.053)
20%	1.131 (0.016)	1.061 (0.047)	0.955 (0.058)	0.933 (0.058)
40%	1.136 (0.089)	1.151 (0.044)	1.052 (0.053)	1.020 (0.055)
60%	0.930 (0.082)	1.033 (0.055)	1.100 (0.099)	1.125 (0.138)
80%	0.801 (0.023)	0.819 (0.033)	0.882 (0.049)	1.024 (0.100)

Note: Numbers within parentheses are standard deviations

TABLE 13

Base Shear Soil-Structure Interaction Factor

Fundamental Period = $0.25H^{3/4}$

Seismic Velocity (Ft./Sec.)	Slenderness Ratio 1	1.5	2	5
1000	0.936 (0.024)	0.952 (0.020)	0.960 (0.018)	0.947 (0.029)
500	0.788 (0.079)	0.837 (0.061)	0.860 (0.056)	0.834 (0.064)
250	0.452 (0.070)	0.586 (0.095)	0.621 (0.083)	0.636 (0.087)

Fundamental Period = $0.35H^{3/4}$

Seismic Velocity (Ft./Sec.)	Slenderness Ratio 1	1.5	2	5
1000	0.970 (0.012)	0.977 (0.009)	0.979 (0.008)	0.970 (0.012)
500	0.887 (0.047)	0.912 (0.036)	0.926 (0.030)	0.905 (0.039)
250	0.672 (0.102)	0.764 (0.102)	0.788 (0.089)	0.780 (0.098)

Note: Numbers within parentheses are standard deviations

TABLE 14

Base Overturning Moment Soil-Structure Interaction Factor

Fundamental Period = $0.25H^{3/4}$

Seismic Velocity (Ft./Sec.)	Slenderness Ratio 1	1.5	2	5
1000	0.917 (0.039)	0.937 (0.031)	0.948 (0.028)	0.930 (0.041)
500	0.733 (0.143)	0.792 (0.106)	0.821 (0.093)	0.788 (0.105)
250	0.384 (0.047)	0.456 (0.124)	0.506 (0.106)	0.529 (0.092)

Fundamental Period = $0.35H^{3/4}$

Seismic Velocity (Ft./Sec.)	Slenderness Ratio 1	1.5	2	5
1000	0.960 (0.020)	0.969 (0.015)	0.972 (0.013)	0.960 (0.019)
500	0.850 (0.087)	0.883 (0.063)	0.901 (0.052)	0.873 (0.067)
250	0.546 (0.136)	0.685 (0.183)	0.718 (0.158)	0.703 (0.157)

Note: Numbers within parentheses are standard deviations

TABLE 15

Story Shear Acceleration Distribution Coefficients

5 Stories   Seismic Velocity = Infinite

Coefficient B_1

Percent Shear Deformation	Setback				
	0%	20%	40%	60%	80%
0	1.727	2.059	2.003	2.045	1.952
20	1.562	1.749	1.709	1.844	1.804
40	1.364	1.467	1.397	1.645	1.684
60	1.094	1.199	1.098	1.384	1.524
80	0.771	0.971	0.844	1.026	1.306
100	0.477	0.805	0.656	0.557	1.033

Coefficient B_2

Percent Shear Deformation	Setback				
	0%	20%	40%	60%	80%
0	-1.921	-1.812	-1.727	-2.283	-2.292
20	-1.887	-1.739	-1.589	-2.151	-2.194
40	-1.681	-1.542	-1.318	-1.907	-2.042
60	-1.400	-1.378	-1.099	-1.558	-1.836
80	-1.109	-1.277	-0.965	-1.090	-1.577
100	-0.903	-1.241	-0.913	-0.505	-1.274

Index of Correlation

Percent Shear Deformation	Setback				
	0%	20%	40%	60%	80%
0	0.999	1.000	1.000	1.000	0.999
20	0.999	1.000	1.000	1.000	0.999
40	1.000	1.000	1.000	1.000	0.999
60	1.000	1.000	1.000	0.999	0.999
80	1.000	1.000	1.000	0.999	0.999
100	1.000	1.000	1.000	0.999	1.000

TABLE 16

Story Shear Acceleration Distribution Coefficients

10 Stories   Seismic Velocity = Infinite

Coefficient B_1

Percent Shear Deformation	Setback 0%	20%	40%	60%	80%
0	2.162	2.611	2.500	2.309	2.229
20	2.006	2.337	2.236	2.134	2.100
40	1.930	2.176	2.032	2.030	2.072
60	1.817	1.991	1.801	1.923	2.054
80	1.591	1.755	1.534	1.782	2.016
100	1.255	1.502	1.247	1.564	1.942

Coefficient B_2

Percent Shear Deformation	Setback 0%	20%	40%	60%	80%
0	-2.722	-2.874	-2.700	-2.793	-2.808
20	-2.624	-2.663	-2.484	-2.679	-2.727
40	-2.523	-2.486	-2.239	-2.564	-2.685
60	-2.360	-2.291	-1.981	-2.419	-2.638
80	-2.085	-2.084	-1.734	-2.224	-2.567
100	-1.713	-1.906	-1.524	-1.928	-2.454

Index of Correlation

Percent Shear Deformation	Setback 0%	20%	40%	60%	80%
0	0.995	0.998	0.998	0.996	0.992
20	0.997	0.999	0.999	0.997	0.995
40	0.998	0.999	0.999	0.997	0.996
60	0.998	0.999	0.999	0.996	0.997
80	0.999	0.999	0.999	0.996	0.998
100	0.999	0.999	0.999	0.996	0.997

TABLE 17

Story Shear Acceleration Distribution Coefficients

20 Stories Seismic Velocity = Infinite

Coefficient B_1

Percent Shear Deformation	Setback 0%	20%	40%	60%	80%
0	2.300	2.796	2.739	2.429	2.293
20	2.193	2.594	2.555	2.325	2.216
40	2.192	2.567	2.464	2.288	2.247
60	2.181	2.521	2.328	2.250	2.292
80	2.058	2.383	2.053	2.167	2.330
100	1.780	2.157	1.738	2.029	2.351

Coefficient B_2

Percent Shear Deformation	Setback 0%	20%	40%	60%	80%
0	-2.982	-3.231	-3.171	-3.054	-2.979
20	-2.913	-3.073	-3.007	-2.989	-2.932
40	-2.874	-2.997	-2.835	-2.929	-2.946
60	-2.802	-2.878	-2.617	-2.848	-2.960
80	-2.603	-2.704	-2.309	-2.695	-2.962
100	-2.292	-2.504	-2.049	-2.478	-2.946

Index of Correlation

Percent Shear Deformation	Setback 0%	20%	40%	60%	80%
0	0.987	0.995	0.995	0.988	0.983
20	0.994	0.998	0.999	0.995	0.992
40	0.998	0.999	0.999	0.996	0.995
60	0.999	0.999	0.999	0.995	0.997
80	0.999	1.000	1.000	0.995	0.996
100	0.999	1.000	1.000	0.996	0.995

TABLE 18

Story Shear Acceleration Distribution Coefficients

40 Stories   Seismic Velocity = Infinite

Coefficient B_1

Percent Shear Deformation	Setback 0%	20%	40%	60%	80%
0	2.360	2.850	2.805	2.463	2.278
20	2.309	2.755	2.678	2.417	2.300
40	2.348	2.810	2.640	2.427	2.370
60	2.352	2.792	2.525	2.417	2.420
80	2.265	2.662	2.304	2.374	2.463
100	2.018	2.394	2.002	2.276	2.489

Coefficient B_2

Percent Shear Deformation	Setback 0%	20%	40%	60%	80%
0	-3.074	-3.353	-3.315	-3.130	-3.006
20	-3.031	-3.267	-3.181	-3.092	-3.031
40	-3.019	-3.241	-3.060	-3.065	-3.073
60	-2.955	-3.143	-2.860	-3.006	-3.092
80	-2.807	-2.976	-2.611	-2.905	-3.103
100	-2.543	-2.738	-2.351	-2.746	-3.092

Index of Correlation

Percent Shear Deformation	Setback 0%	20%	40%	60%	80%
0	0.989	0.993	0.993	0.984	0.982
20	0.999	0.999	0.999	0.998	0.995
40	0.999	0.999	0.999	0.999	0.991
60	0.999	0.999	0.999	0.998	0.990
80	0.999	0.999	0.999	0.998	0.990
100	0.999	0.999	0.999	0.998	0.993

TABLE 19

Story Shear Acceleration Distribution Coefficients

5 Stories Seismic Velocity = 500 Ft./Sec.

Coefficient B_1

Percent Shear Deformation	Setback 0%	20%	40%	60%	80%
0	1.836	2.235	2.171	2.076	1.975
20	1.695	1.964	1.914	1.928	1.886
40	1.539	1.717	1.626	1.784	1.832
60	1.302	1.448	1.310	1.589	1.750
80	0.971	1.184	1.010	1.306	1.615
100	0.621	0.962	0.775	0.916	1.404

Coefficient B_2

Percent Shear Deformation	Setback 0%	20%	40%	60%	80%
0	-2.228	-2.278	-2.228	-2.555	-2.536
20	-2.166	-2.139	-2.016	-2.432	-2.465
40	-1.980	-1.914	-1.692	-2.234	-2.376
60	-1.701	-1.693	-1.387	-1.951	-2.245
80	-1.360	-1.516	-1.161	-1.556	-2.056
100	-1.065	-1.402	-1.038	-1.044	-1.792

Index of Correlation

Percent Shear Deformation	Setback 0%	20%	40%	60%	80%
0	0.999	1.000	1.000	0.999	0.998
20	1.000	1.000	1.000	1.000	0.999
40	1.000	1.000	1.000	0.999	0.999
60	1.000	1.000	1.000	0.999	1.000
80	1.000	1.000	1.000	0.999	1.000
100	1.000	1.000	1.000	0.999	1.000

TABLE 20

Story Shear Acceleration Distribution Coefficients

10 Stories   Seismic Velocity = 500 Ft./Sec.

Coefficient B_1

Percent Shear Deformation	Setback 0%	20%	40%	60%	80%
0	2.198	2.677	2.614	2.340	2.222
20	2.066	2.459	2.413	2.217	2.134
40	2.028	2.370	2.290	2.156	2.144
60	1.972	2.253	2.126	2.094	2.169
80	1.815	2.048	1.876	2.004	2.182
100	1.477	1.773	1.544	1.853	2.163

Coefficient B_2

Percent Shear Deformation	Setback 0%	20%	40%	60%	80%
0	-2.850	-3.101	-3.058	-2.999	-2.927
20	-2.759	-2.913	-2.853	-2.900	-2.862
40	-2.694	-2.781	-2.653	-2.819	-2.853
60	-2.584	-2.614	-2.408	-2.715	-2.846
80	-2.360	-2.395	-2.114	-2.568	-2.818
100	-1.984	-2.164	-1.815	-2.336	-2.751

Index of Correlation

Percent Shear Deformation	Setback 0%	20%	40%	60%	80%
0	0.995	0.997	0.997	0.993	0.989
20	0.998	1.000	0.999	0.998	0.996
40	0.998	1.000	0.999	0.996	0.998
60	0.999	0.999	0.999	0.995	0.998
80	0.999	1.000	0.999	0.994	0.998
100	0.999	0.999	0.999	0.994	0.997

TABLE 21

Story Shear Acceleration Distribution Coefficients

20 Stories Seismic Velocity = 500 Ft./Sec.

Coefficient B_1

Percent Shear Deformation	Setback				
	0%	20%	40%	60%	80%
0	2.318	2.797	2.770	2.478	2.293
20	2.225	2.635	2.628	2.371	2.247
40	2.248	2.666	2.621	2.333	2.301
60	2.292	2.720	2.604	2.325	2.376
80	2.278	2.696	2.451	2.318	2.452
100	2.111	2.531	2.152	2.275	2.523

Coefficient B_2

Percent Shear Deformation	Setback				
	0%	20%	40%	60%	80%
0	-3.042	-3.324	-3.320	-3.171	-3.037
20	-2.978	-3.192	-3.177	-3.084	-3.004
40	-2.976	-3.172	-3.098	-3.035	-3.039
60	-2.967	-3.137	-2.981	-2.996	-3.084
80	-2.874	-3.033	-2.743	-2.935	-3.124
100	-2.640	-2.845	-2.446	-2.822	-3.150

Index of Correlation

Percent Shear Deformation	Setback				
	0%	20%	40%	60%	80%
0	0.989	0.994	0.992	0.984	0.981
20	0.997	0.999	0.998	0.996	0.996
40	0.997	0.998	0.998	0.994	0.998
60	0.995	0.999	0.998	0.991	0.997
80	0.997	0.999	0.998	0.990	0.993
100	0.998	0.999	0.999	0.991	0.987

TABLE 22

Story Shear Acceleration Distribution Coefficients

40 Stories Seismic Velocity = 500 Ft./Sec.

Coefficient B_1

Percent Shear Deformation	Setback 0%	20%	40%	60%	80%
0	2.390	2.869	2.811	2.534	2.311
20	2.348	2.784	2.723	2.458	2.344
40	2.406	2.886	2.769	2.475	2.440
60	2.476	2.983	2.802	2.496	2.527
80	2.516	3.011	2.733	2.524	2.615
100	2.422	2.862	2.504	2.527	2.691

Coefficient B_2

Percent Shear Deformation	Setback 0%	20%	40%	60%	80%
0	-3.115	-3.407	-3.377	-3.217	-3.055
20	-3.089	-3.340	-3.291	-3.162	-3.089
40	-3.118	-3.382	-3.276	-3.164	-3.161
60	-3.137	-3.396	-3.220	-3.154	-3.220
80	-3.111	-3.344	-3.079	-3.139	-3.275
100	-2.963	-3.167	-2.835	-3.090	-3.313

Index of Correlation

Percent Shear Deformation	Setback 0%	20%	40%	60%	80%
0	0.990	0.994	0.992	0.983	0.984
20	0.998	0.999	0.999	0.997	0.997
40	0.996	0.998	0.997	0.997	0.992
60	0.994	0.998	0.996	0.995	0.986
80	0.994	0.997	0.996	0.994	0.977
100	0.995	0.996	0.996	0.993	0.976

TABLE 23

Story Overturning Moment Acceleration Distribution Coefficients

5 Stories   Seismic Velocity = Infinite

Coefficient B_1

Percent Shear Deformation	Setback 0%	20%	40%	60%	80%
0	2.014	2.175	2.179	2.458	2.297
20	1.860	1.920	1.941	2.346	2.235
40	1.595	1.609	1.612	2.127	2.136
60	1.217	1.313	1.264	1.650	1.948
80	0.803	1.073	0.961	0.621	1.646
100	0.478	0.905	0.736	-1.461	1.200

Coefficient B_2

Percent Shear Deformation	Setback 0%	20%	40%	60%	80%
0	-2.319	-2.154	-2.216	-2.647	-2.660
20	-2.111	-1.939	-1.912	-2.366	-2.523
40	-1.766	-1.686	-1.540	-1.809	-2.311
60	-1.370	-1.507	-1.243	-1.794	-2.004
80	-1.031	-1.409	-1.058	-1.084	-1.580
100	-0.850	-1.377	-0.977	4.444	-0.979

Index of Correlation

Percent Shear Deformation	Setback 0%	20%	40%	60%	80%
0	1.000	1.000	1.000	1.000	1.000
20	1.000	1.000	1.000	1.000	1.000
40	1.000	1.000	1.000	1.000	1.000
60	1.000	1.000	1.000	1.000	1.000
80	1.000	1.000	1.000	1.000	1.000
100	1.000	1.000	1.000	1.000	1.000

TABLE 24

Story Overturning Moment Acceleration Distribution Coefficients

10 Stories   Seismic Velocity = Infinite

Coefficient B_1

Percent Shear Deformation	Setback				
	0%	20%	40%	60%	80%
0	2.352	2.610	2.544	2.610	2.390
20	2.384	2.587	2.508	2.664	2.449
40	2.392	2.469	2.383	2.742	2.540
60	2.287	2.232	2.156	2.824	2.632
80	1.947	1.909	1.848	2.877	2.711
100	1.396	1.590	1.505	2.642	2.788

Coefficient B_2

Percent Shear Deformation	Setback				
	0%	20%	40%	60%	80%
0	-2.974	-2.983	-2.906	-3.110	-3.022
20	-2.960	-2.874	-2.787	-3.098	-3.057
40	-2.874	-2.681	-2.561	-3.019	-3.084
60	-2.658	-2.432	-2.286	-2.839	-3.093
80	-2.248	-2.176	-2.011	-2.424	-3.067
100	-1.745	-1.976	-1.775	-1.283	-2.992

Index of Correlation

Percent Shear Deformation	Setback				
	0%	20%	40%	60%	80%
0	1.000	1.000	1.000	1.000	1.000
20	1.000	1.000	1.000	1.000	1.000
40	1.000	1.000	1.000	1.000	1.000
60	1.000	1.000	1.000	1.000	1.000
80	1.000	1.000	1.000	1.000	0.999
100	1.000	1.000	1.000	1.000	0.999

TABLE 25

Story Overturning Moment Acceleration Distribution Coefficients

20 Stories Seismic Velocity = Infinite

Coefficient B_1

Percent Shear Deformation	Setback				
	0%	20%	40%	60%	80%
0	2.525	2.873	2.806	2.739	2.451
20	2.642	3.009	2.895	2.851	2.576
40	2.772	3.134	2.915	3.006	2.749
60	2.843	3.064	2.794	3.207	2.905
80	2.626	2.779	2.445	3.348	3.040
100	2.150	2.385	2.051	3.290	3.163

Coefficient B_2

Percent Shear Deformation	Setback				
	0%	20%	40%	60%	80%
0	-3.251	-3.374	-3.341	-3.389	-3.188
20	-3.331	-3.431	-3.364	-3.467	-3.293
40	-3.364	-3.421	-3.260	-3.511	-3.410
60	-3.316	-3.250	-3.052	-3.534	-3.497
80	-3.012	-2.967	-2.705	-3.396	-3.563
100	-2.562	-2.670	-2.397	-2.995	-3.618

Index of Correlation

Percent Shear Deformation	Setback				
	0%	20%	40%	60%	80%
0	0.999	1.000	1.000	0.999	0.999
20	0.999	1.000	1.000	0.999	0.999
40	1.000	1.000	1.000	0.999	0.999
60	1.000	1.000	1.000	1.000	0.999
80	1.000	1.000	1.000	1.000	1.000
100	1.000	1.000	1.000	1.000	1.000

TABLE 26

Story Overturning Moment Acceleration Distribution Coefficients

40 Stories   Seismic Velocity = Infinite

Coefficient B_1

Percent Shear Deformation	Setback 0%	20%	40%	60%	80%
0	2.600	2.980	2.914	2.805	2.475
20	2.724	3.176	3.029	2.907	2.628
40	2.841	3.303	3.070	3.055	2.768
60	2.860	3.234	2.926	3.212	2.874
80	2.674	2.956	2.628	3.299	2.938
100	2.290	2.570	2.260	3.230	3.001

Coefficient B_2

Percent Shear Deformation	Setback 0%	20%	40%	60%	80%
0	-3.355	-3.547	-3.514	-3.502	-3.258
20	-3.421	-3.636	-3.537	-3.552	-3.372
40	-3.453	-3.634	-3.467	-3.599	-3.461
60	-3.380	-3.481	-3.250	-3.604	-3.518
80	-3.146	-3.214	-2.963	-3.503	-3.541
100	-2.783	-2.901	-2.666	-3.223	-3.554

Index of Correlation

Percent Shear Deformation	Setback 0%	20%	40%	60%	80%
0	0.999	1.000	1.000	0.999	0.999
20	1.000	1.000	1.000	1.000	1.000
40	1.000	1.000	1.000	1.000	1.000
60	1.000	1.000	1.000	1.000	1.000
80	1.000	1.000	1.000	1.000	1.000
100	1.000	1.000	1.000	1.000	1.000

TABLE 27

Story Overturning Moment Acceleration Distribution Coefficients

5 Stories   Seismic Velocity = 500 Ft./Sec.

Coefficient B_1

Percent Shear Deformation	Setback 0%	20%	40%	60%	80%
0	2.107	2.331	2.316	2.463	2.295
20	2.016	2.148	2.148	2.435	2.314
40	1.826	1.880	1.865	2.354	2.325
60	1.490	1.575	1.507	2.107	2.276
80	1.042	1.292	1.156	1.451	2.129
100	0.633	1.067	0.880	-0.156	1.829

Coefficient B_2

Percent Shear Deformation	Setback 0%	20%	40%	60%	80%
0	-2.580	-2.537	-2.601	-2.932	-2.883
20	-2.423	-2.334	-2.320	-2.763	-2.833
40	-2.132	-2.064	-1.934	-2.411	-2.738
60	-1.730	-1.823	-1.561	-1.716	-2.564
80	-1.305	-1.650	-1.283	-0.295	-2.267
100	-1.009	-1.544	-1.129	2.649	-1.749

Index of Correlation

Percent Shear Deformation	Setback 0%	20%	40%	60%	80%
0	1.000	1.000	1.000	1.000	1.000
20	1.000	1.000	1.000	1.000	1.000
40	1.000	1.000	1.000	1.000	1.000
60	1.000	1.000	1.000	1.000	1.000
80	1.000	1.000	1.000	1.000	1.000
100	1.000	1.000	1.000	1.000	1.000

TABLE 28

Story Overturning Moment Acceleration Distribution Coefficients

10 Stories   Seismic Velocity = 500 Ft./Sec.

Coefficient B_1

Percent Shear Deformation	Setback 0%	20%	40%	60%	80%
0	2.394	2.711	2.665	2.629	2.382
20	2.467	2.782	2.724	2.735	2.491
40	2.558	2.786	2.727	2.901	2.655
60	2.579	2.635	2.595	3.152	2.853
80	2.355	2.305	2.290	3.550	3.080
100	1.778	1.908	1.864	4.132	3.389

Coefficient B_2

Percent Shear Deformation	Setback 0%	20%	40%	60%	80%
0	-3.093	-3.212	-3.218	-3.313	-3.135
20	-3.120	-3.182	-3.171	-3.356	-3.210
40	-3.116	-3.073	-3.035	-3.395	-3.308
60	-3.008	-2.853	-2.789	-3.417	-3.412
80	-2.667	-2.547	-2.455	-3.361	-3.512
100	-2.094	-2.259	-2.112	-2.865	-3.617

Index of Correlation

Percent Shear Deformation	Setback 0%	20%	40%	60%	80%
0	1.000	1.000	1.000	1.000	1.000
20	1.000	1.000	1.000	1.000	1.000
40	1.000	1.000	1.000	1.000	1.000
60	1.000	1.000	1.000	1.000	1.000
80	1.000	1.000	1.000	1.000	0.999
100	1.000	1.000	1.000	1.000	0.999

TABLE 29

Story Overturning Moment Acceleration Distribution Coefficients

20 Stories Seismic Velocity = 500 Ft./Sec.

Coefficient B_1

Percent Shear Deformation	Setback 0%	20%	40%	60%	80%
0	2.539	2.910	2.849	2.762	2.429
20	2.685	3.134	3.012	2.884	2.591
40	2.910	3.462	3.216	3.087	2.835
60	3.180	3.654	3.305	3.424	3.117
80	3.191	3.494	3.032	3.883	3.422
100	2.762	3.008	3.562	4.394	3.751

Coefficient B_2

Percent Shear Deformation	Setback 0%	20%	40%	60%	80%
0	-3.305	-3.494	-3.486	-3.498	-3.232
20	-3.413	-3.623	-3.568	-3.581	-3.363
40	-3.546	-3.777	-3.627	-3.699	-3.547
60	-3.676	-3.787	-3.569	-3.882	-3.747
80	-3.549	-3.553	-3.252	-4.065	-3.954
100	-3.103	-3.157	-2.857	-4.133	-4.167

Index of Correlation

Percent Shear Deformation	Setback 0%	20%	40%	60%	80%
0	0.999	1.000	1.000	0.997	0.999
20	0.998	1.000	1.000	0.996	0.999
40	0.999	1.000	1.000	0.997	0.998
60	0.999	1.000	1.000	0.998	0.997
80	0.999	1.000	1.000	0.999	0.996
100	1.000	1.000	1.000	0.999	0.996

TABLE 30

Story Overturning Moment Acceleration Distribution Coefficients

40 Stories Seismic Velocity = 500 Ft./Sec.

Coefficient B_1

Percent Shear Deformation	Setback 0%	20%	40%	60%	80%
0	2.606	2.984	2.943	2.810	2.493
20	2.765	3.291	3.144	2.960	2.729
40	2.995	3.669	3.401	3.166	2.887
60	3.221	3.901	3.520	3.465	3.093
80	3.249	3.744	3.326	3.849	3.246
100	2.959	3.315	2.898	4.256	3.453

Coefficient B_2

Percent Shear Deformation	Setback 0%	20%	40%	60%	80%
0	-3.385	-3.601	-3.594	-3.551	-3.301
20	-3.497	-3.793	-3.711	-3.656	-3.488
40	-3.645	-4.000	-3.838	-3.787	-3.607
60	-3.761	-4.068	-3.829	-3.962	-3.757
80	-3.701	-3.867	-3.604	-4.156	-3.860
100	-3.394	-3.497	-3.241	-4.285	-3.993

Index of Correlation

Percent Shear Deformation	Setback 0%	20%	40%	60%	80%
0	0.994	0.999	0.999	0.997	0.988
20	0.993	0.999	0.999	0.992	0.968
40	0.995	0.999	0.999	0.999	0.979
60	0.996	0.999	0.999	0.996	0.977
80	0.997	0.999	0.999	0.997	0.984
100	0.998	0.999	0.999	0.998	0.989

TABLE 31

Story Shear Acceleration Distribution Coefficients

Seismic Velocity = Infinite

Coefficient B_1

Number of Stories	Percent Shear Deformation					
	0%	20%	40%	60%	80%	100%
5	1.950	1.738	1.527	1.274	0.990	0.714
10	2.328	2.138	2.040	1.930	1.769	1.538
20	2.469	2.338	2.317	2.295	2.214	2.065
40	2.512	2.454	2.479	2.472	2.415	2.276

Coefficient B_2

Number of Stories	Percent Shear Deformation					
	0%	20%	40%	60%	80%	100%
5	-2.063	-1.961	-1.743	-1.483	-1.221	-1.005
10	-2.780	-2.650	-2.534	-2.389	-2.199	-1.961
20	-3.064	-2.971	-2.919	-2.846	-2.712	-2.536
40	-3.153	-3.103	-3.082	-3.022	-2.921	-2.762

Index of Correlation

Number of Stories	percent Shear Deformation					
	0%	20%	40%	60%	80%	100%
5	0.999	0.999	0.999	0.999	0.999	0.998
10	0.992	0.992	0.994	0.996	0.997	0.997
20	0.972	0.975	0.980	0.986	0.991	0.993
40	0.955	0.965	0.970	0.978	0.985	0.991

TABLE 32

Story Shear Acceleration Distribution Coefficients

Seismic Velocity = 500 Ft./Sec.

Coefficient B_1

Number of Stories	Percent Shear Deformation					
	0%	20%	40%	60%	80%	100%
5	2.035	1.872	1.715	1.510	1.247	0.954
10	2.370	2.223	2.172	2.117	2.011	1.820
20	2.500	2.385	2.392	2.421	2.420	2.349
40	2.552	2.499	2.554	2.610	2.643	2.604

Coefficient B_2

Number of Stories	Percent Shear Deformation					
	0%	20%	40%	60%	80%	100%
5	-2.403	-2.288	-2.098	-1.854	-1.575	-1.303
10	-2.973	-2.855	-2.775	-2.674	-2.519	-2.294
20	-3.159	-3.070	-3.051	-3.032	-2.973	-2.853
40	-3.215	-3.176	-3.201	-3.212	-3.196	-3.116

Index of Correlation

Number of Stories	Percent Shear Deformation					
	0%	20%	40%	60%	80%	100%
5	0.997	0.998	0.999	0.999	0.999	0.999
10	0.982	0.985	0.988	0.991	0.994	0.995
20	0.958	0.966	0.967	0.971	0.979	0.984
40	0.950	0.958	0.954	0.957	0.964	0.974

TABLE 33

Story Overturning Moment Acceleration Distribution Coefficients

Seismic Velocity = Infinite

Coefficient B_1

Number of Stories	Percent Shear Deformation					
	0%	20%	40%	60%	80%	100%
5	2.229	2.068	1.814	1.463	1.064	0.696
10	2.476	2.500	2.508	2.445	2.253	1.906
20	2.626	2.735	2.866	2.949	2.876	2.652
40	2.682	2.807	2.926	2.973	2.896	2.706

Coefficient B_2

Number of Stories	Percent Shear Deformation					
	0%	20%	40%	60%	80%	100%
5	-2.433	-2.200	-1.851	-1.458	-1.095	-0.824
10	-3.005	-2.980	-2.892	-2.726	-2.455	-2.091
20	-3.289	-3.363	-3.403	-3.379	-3.222	-2.977
40	-3.396	-3.465	-3.504	-3.468	-3.341	-3.131

Index of Correlation

Number of Stories	Percent Shear Deformation					
	0%	20%	40%	60%	80%	100%
5	1.000	1.000	1.000	1.000	1.000	1.000
10	1.000	1.000	1.000	0.999	0.999	0.999
20	0.998	0.998	0.999	0.999	0.999	0.998
40	0.995	0.998	0.998	0.998	0.998	0.998

TABLE 34

Story Overturning Moment Acceleration Distribution Coefficients

Seismic Velocity = 500 Ft./Sec.

Coefficient B_1

Number of Stories	Percent Shear Deformation					
	0%	20%	40%	60%	80%	100%
5	2.302	2.226	2.071	1.798	1.414	0.992
10	2.521	2.603	2.710	2.785	2.737	2.464
20	2.635	2.773	2.996	3.257	3.413	3.350
40	2.688	2.873	3.068	3.284	3.389	3.372

Coefficient B_2

Number of Stories	Percent Shear Deformation					
	0%	20%	40%	60%	80%	100%
5	-2.743	-2.580	-2.307	-1.940	-1.527	-1.148
10	-3.189	-3.216	-3.223	-3.170	-2.989	-2.629
20	-3.373	-3.471	-3.607	-3.746	-3.770	-3.621
40	-3.440	-3.574	-3.701	-3.826	-3.851	-3.768

Index of Correlation

Number of Stories	Percent Shear Deformation					
	0%	20%	40%	60%	80%	100%
5	1.000	1.000	1.000	1.000	1.000	1.000
10	0.999	0.999	0.999	0.999	0.999	0.998
20	0.992	0.994	0.995	0.994	0.993	0.992
40	0.974	0.978	0.982	0.983	0.985	0.986

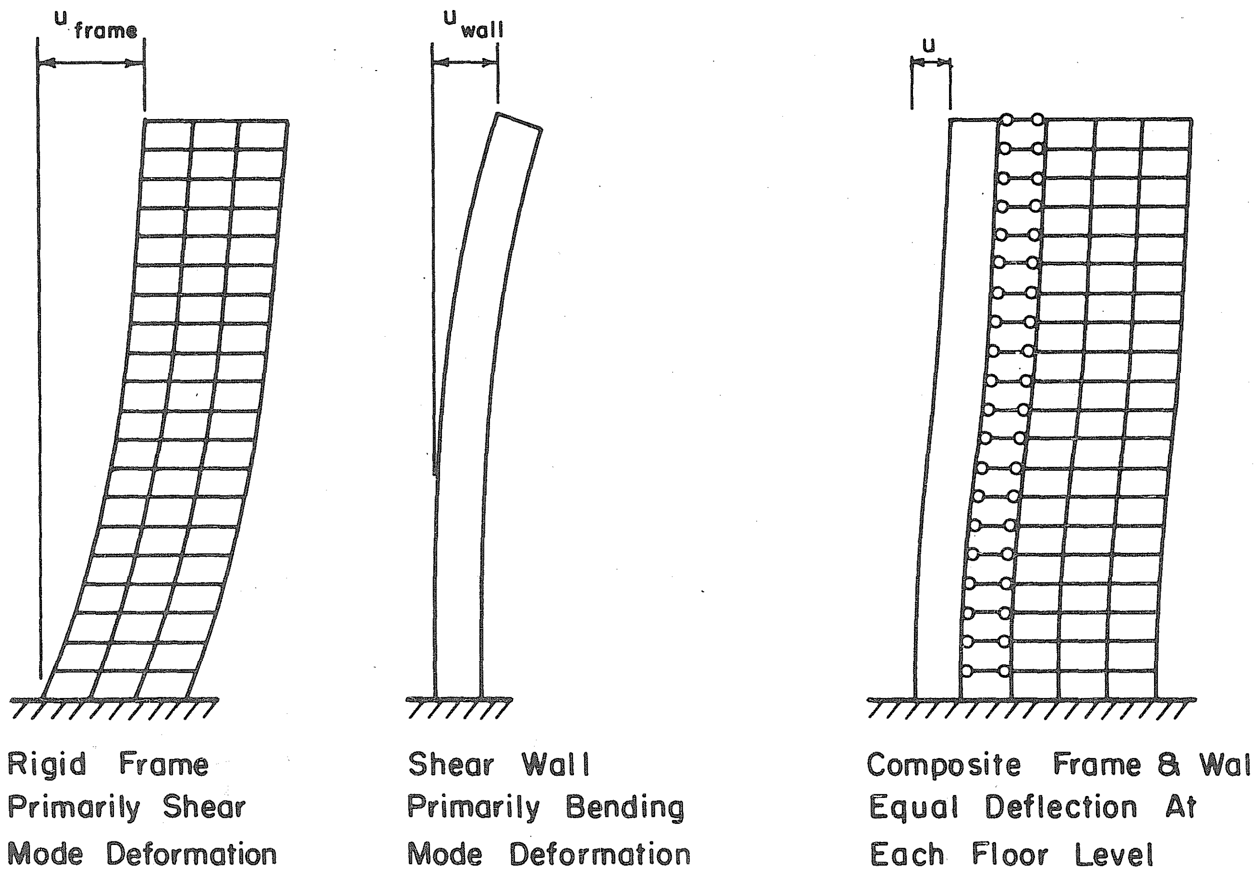

FIG. 1 DEFORMATION MODES OF FRAME-WALL STRUCTURES

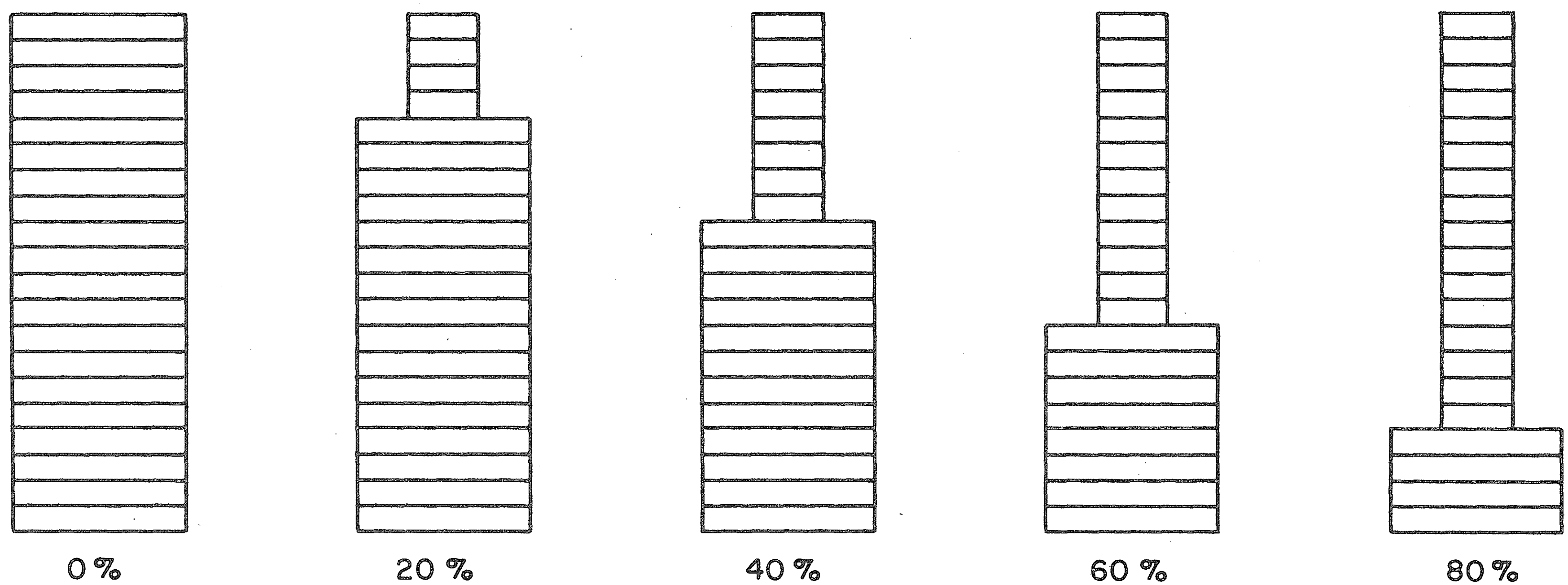

FIG. 2 DEGREES OF SETBACK STUDIED, Setback Stiffness and Mass = 30% of Base Value

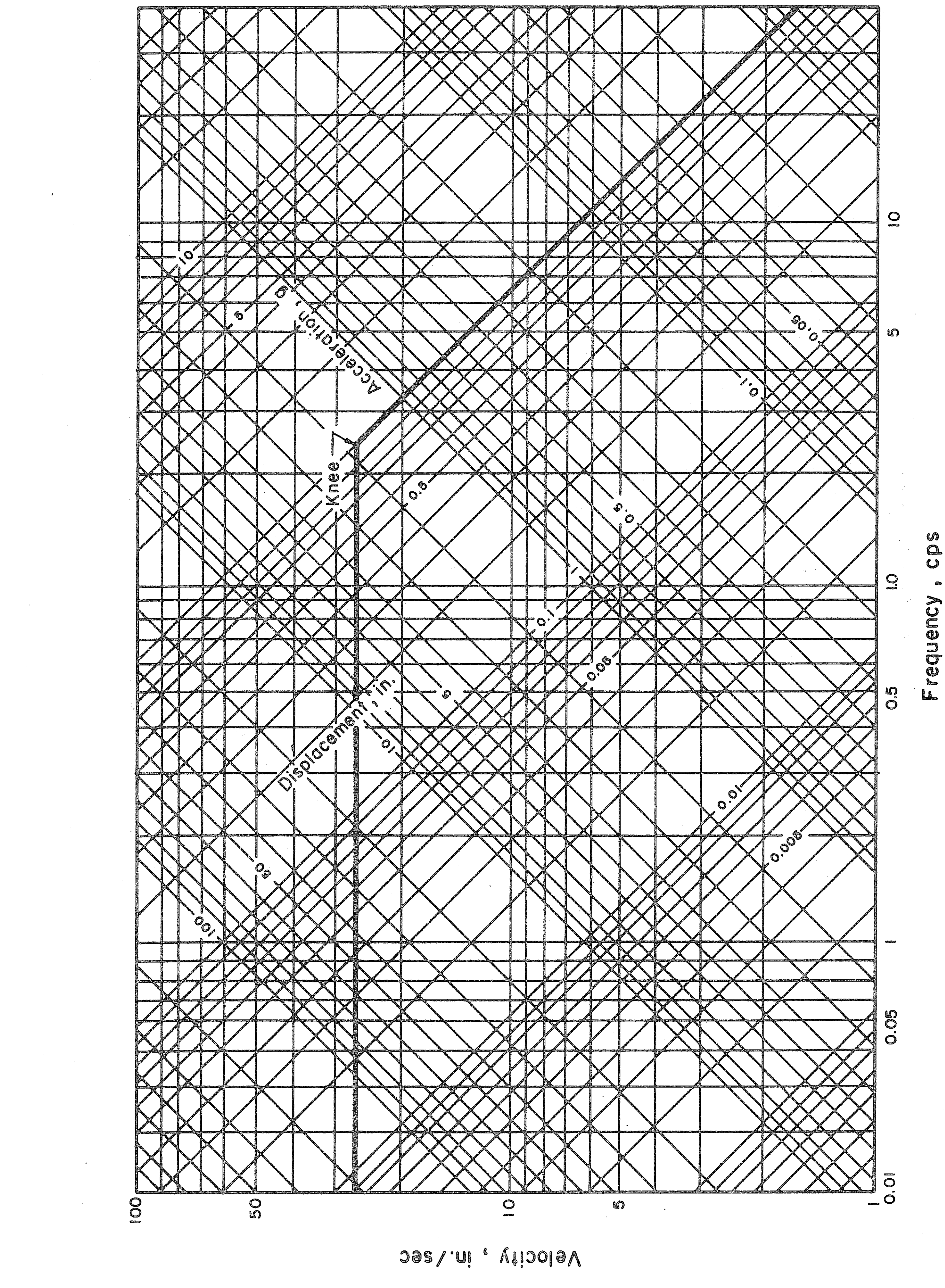

FIG. 3 RESPONSE SPECTRUM

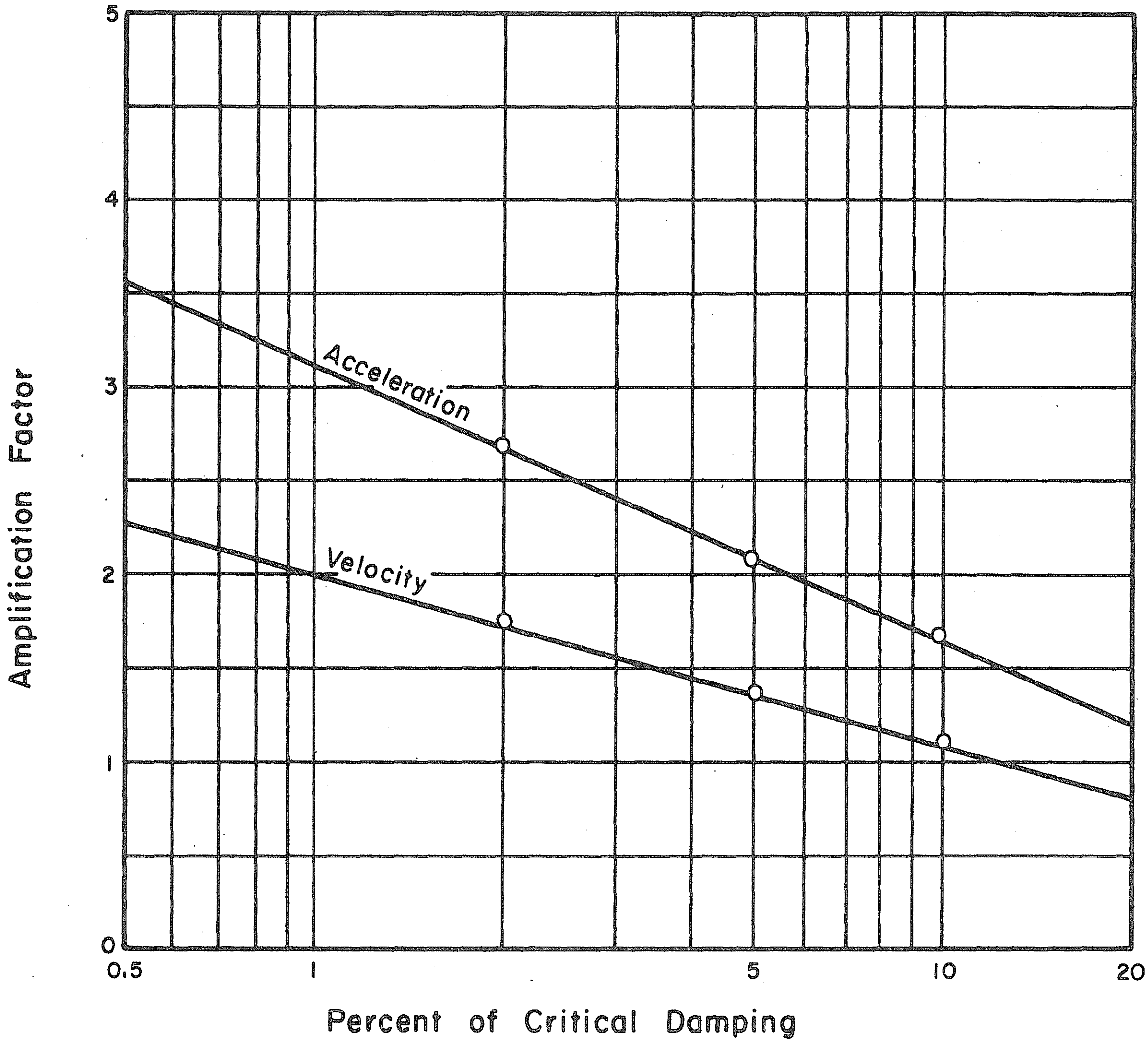

FIG. 4 MEDIAN HORIZONTAL GROUND MOTION RESPONSE SPECTRUM AMPLIFICATION FACTOR

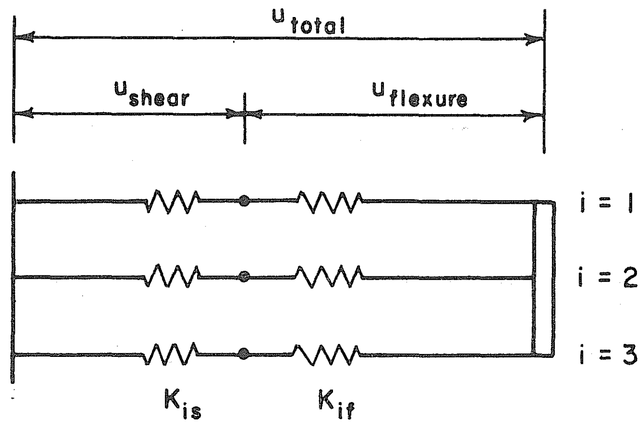

FIG. 5a SERIES AND PARALLEL REPRESENTATION OF LATERAL RESISTING ELEMENTS IN A STRUCTURE

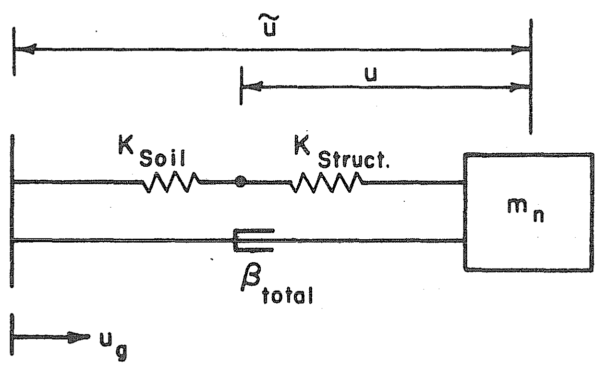

FIG. 5b REPLACEMENT OSCILLATOR

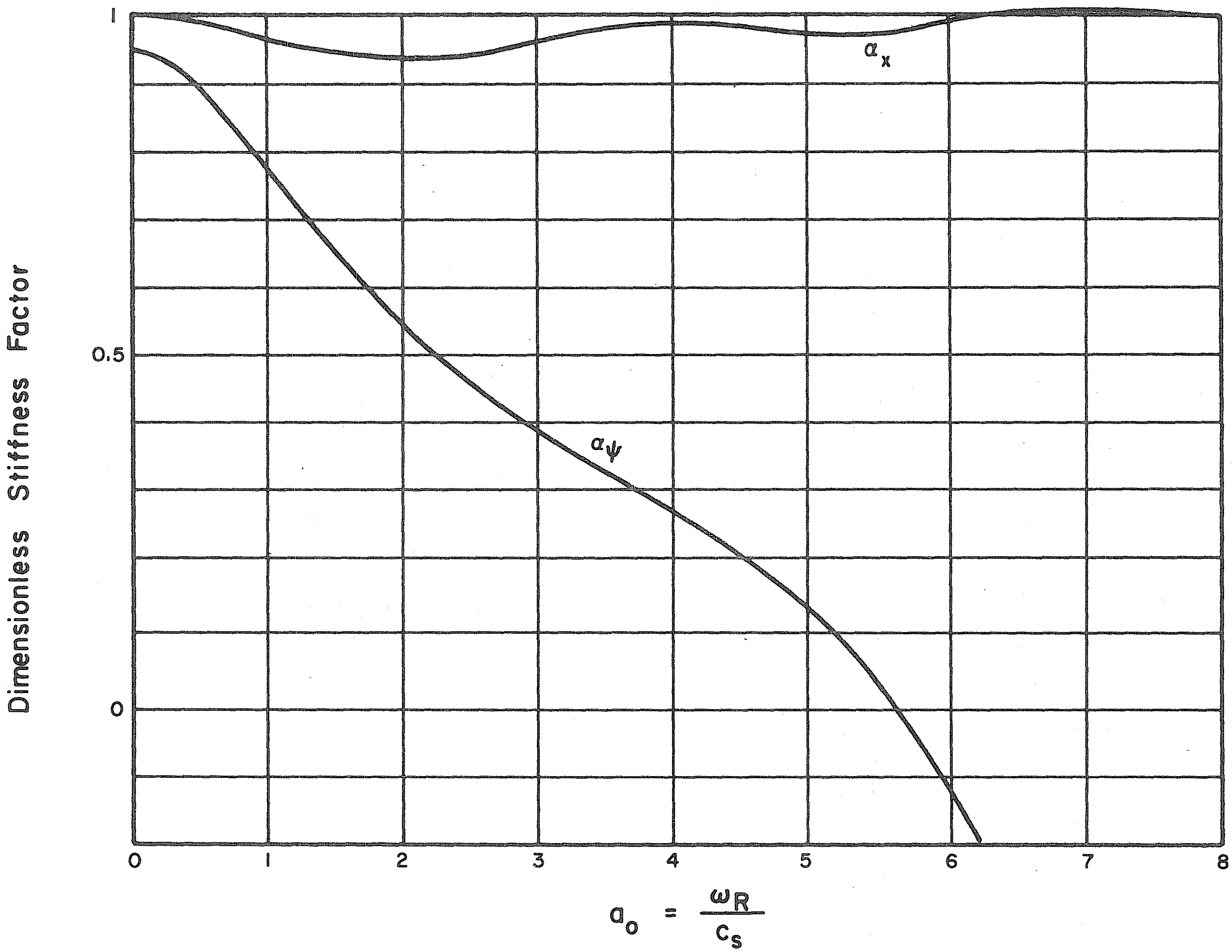

FIG. 6 DIMENSIONLESS STIFFNESS FACTOR FOR FREQUENCY DEPENDENT INTERACTION

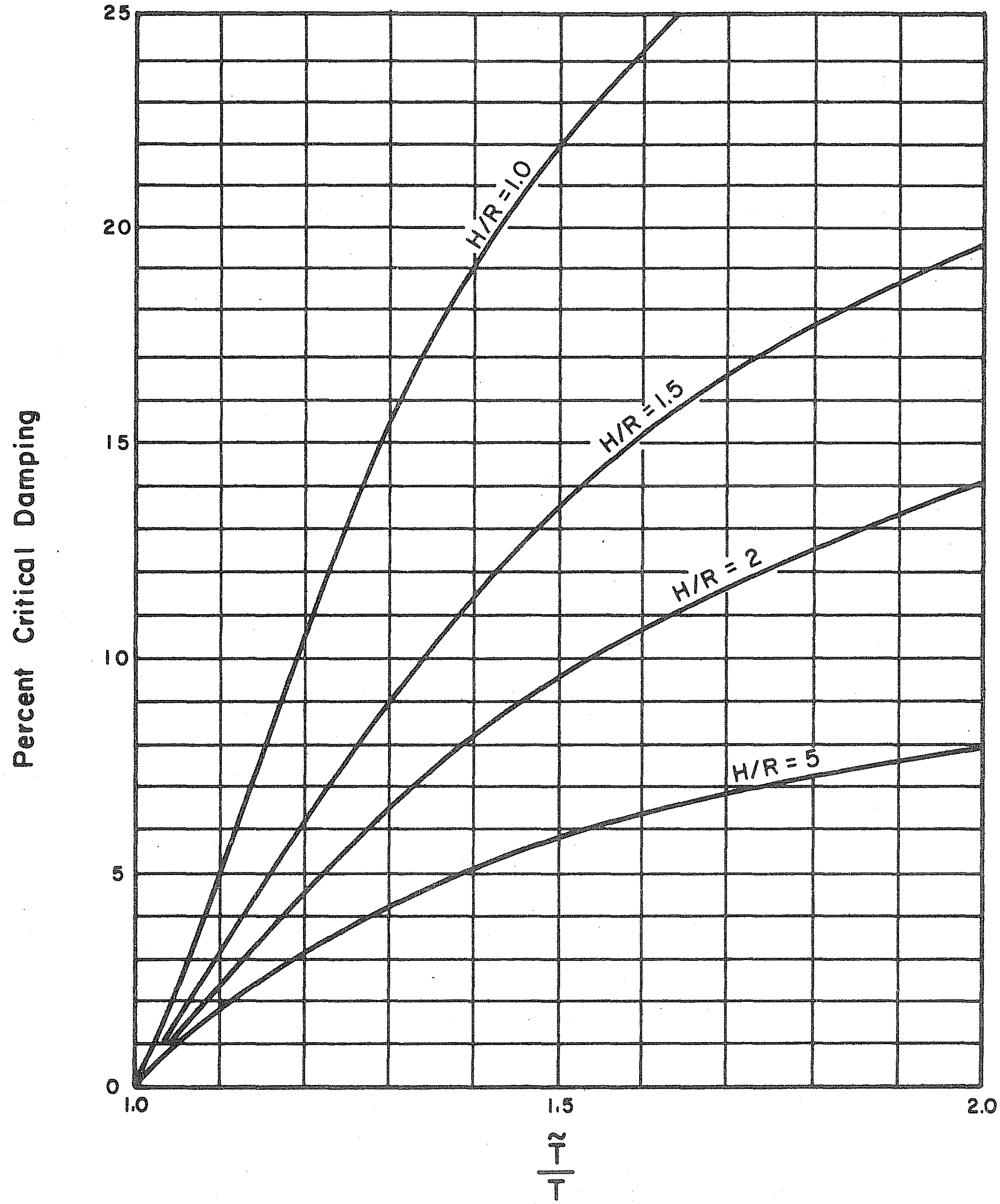

FIG. 7 RADIATION DAMPING DUE TO FOUNDATION INTERACTION

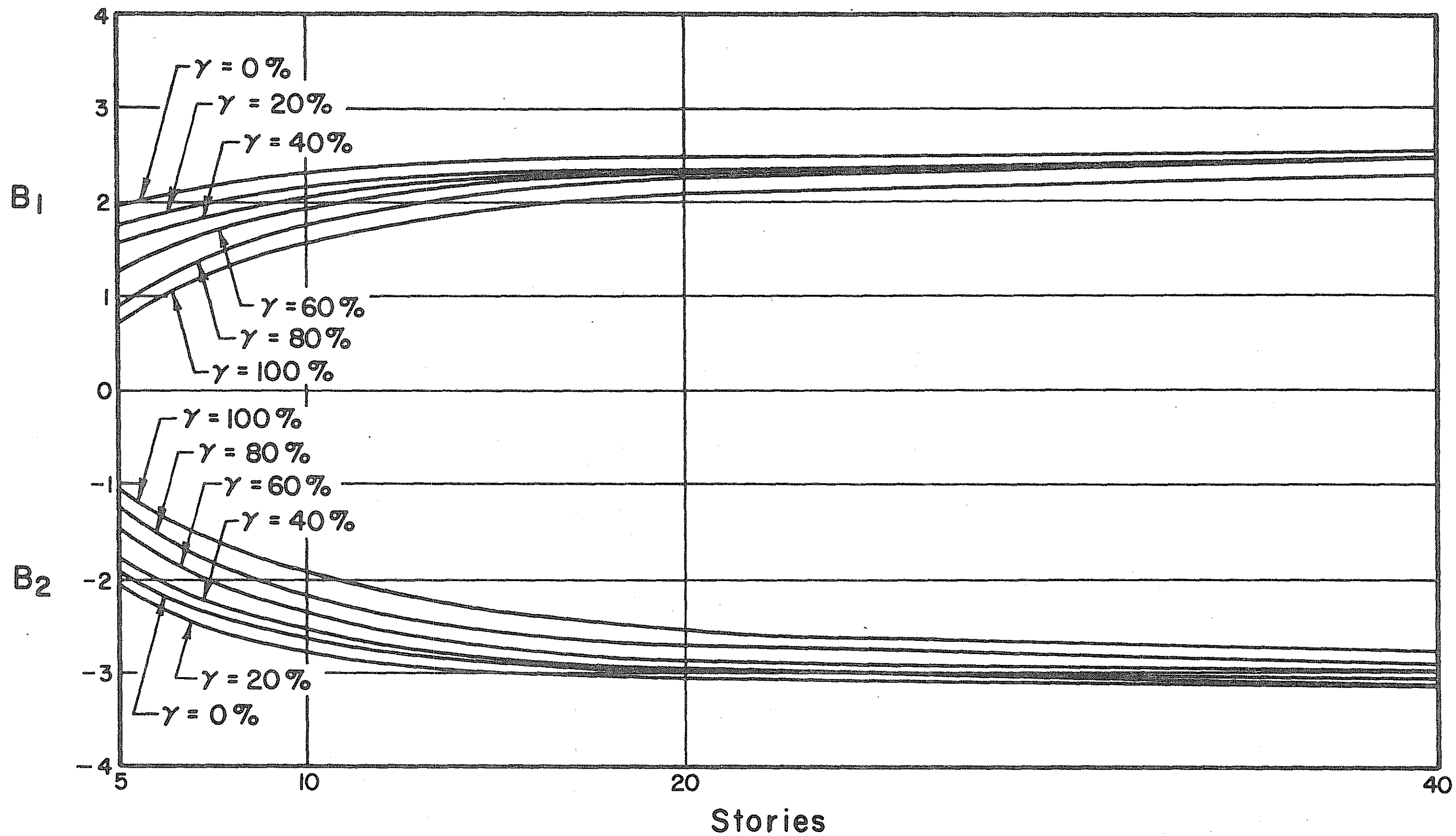

FIG. 8 STORY SHEAR ACCELERATION DISTRIBUTION COEFFICIENTS, Seismic Velocity = Infinite

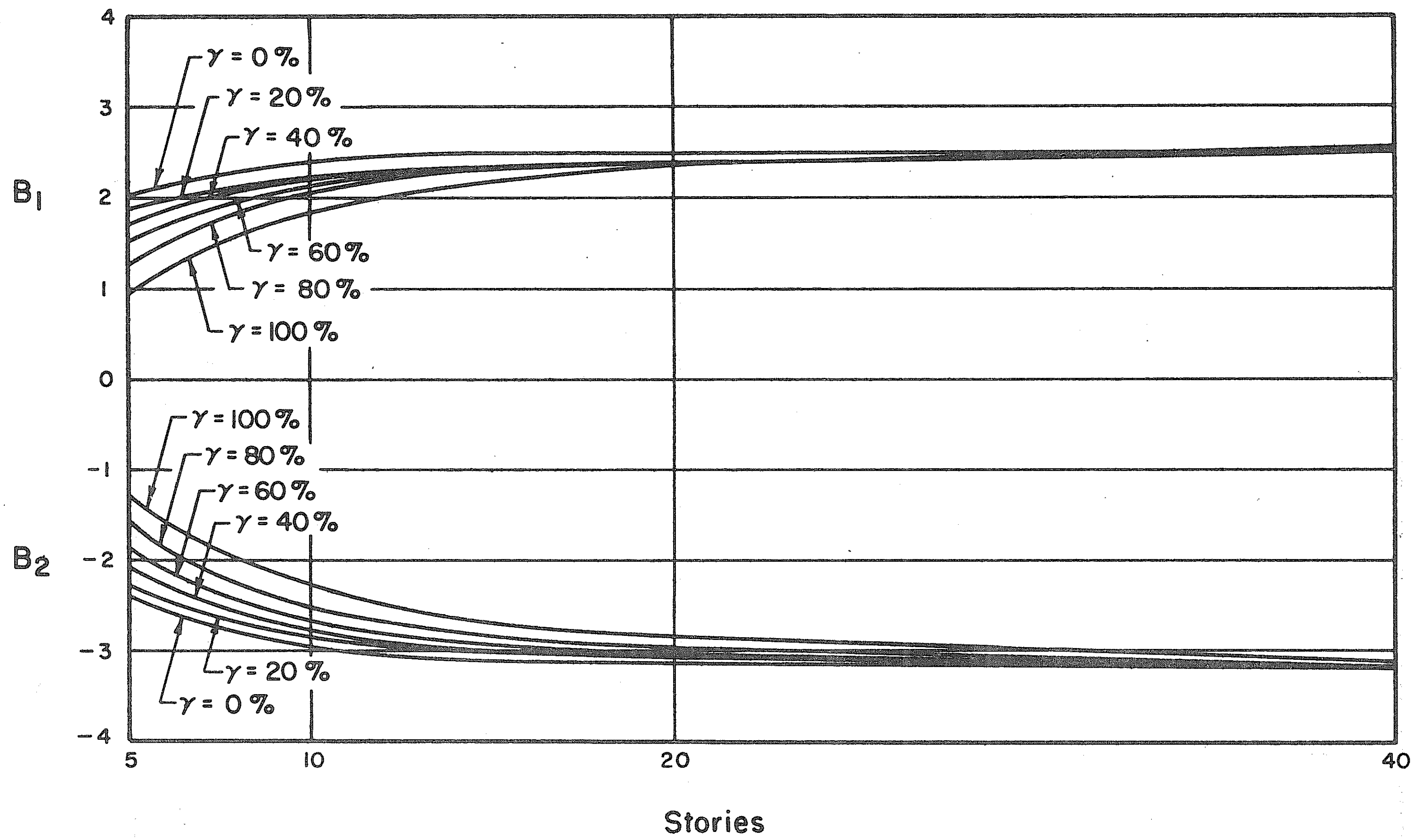

FIG. 9 STORY SHEAR ACCELERATION DISTRIBUTION COEFFICIENTS, Seismic Velocity = 500 Ft./Sec.

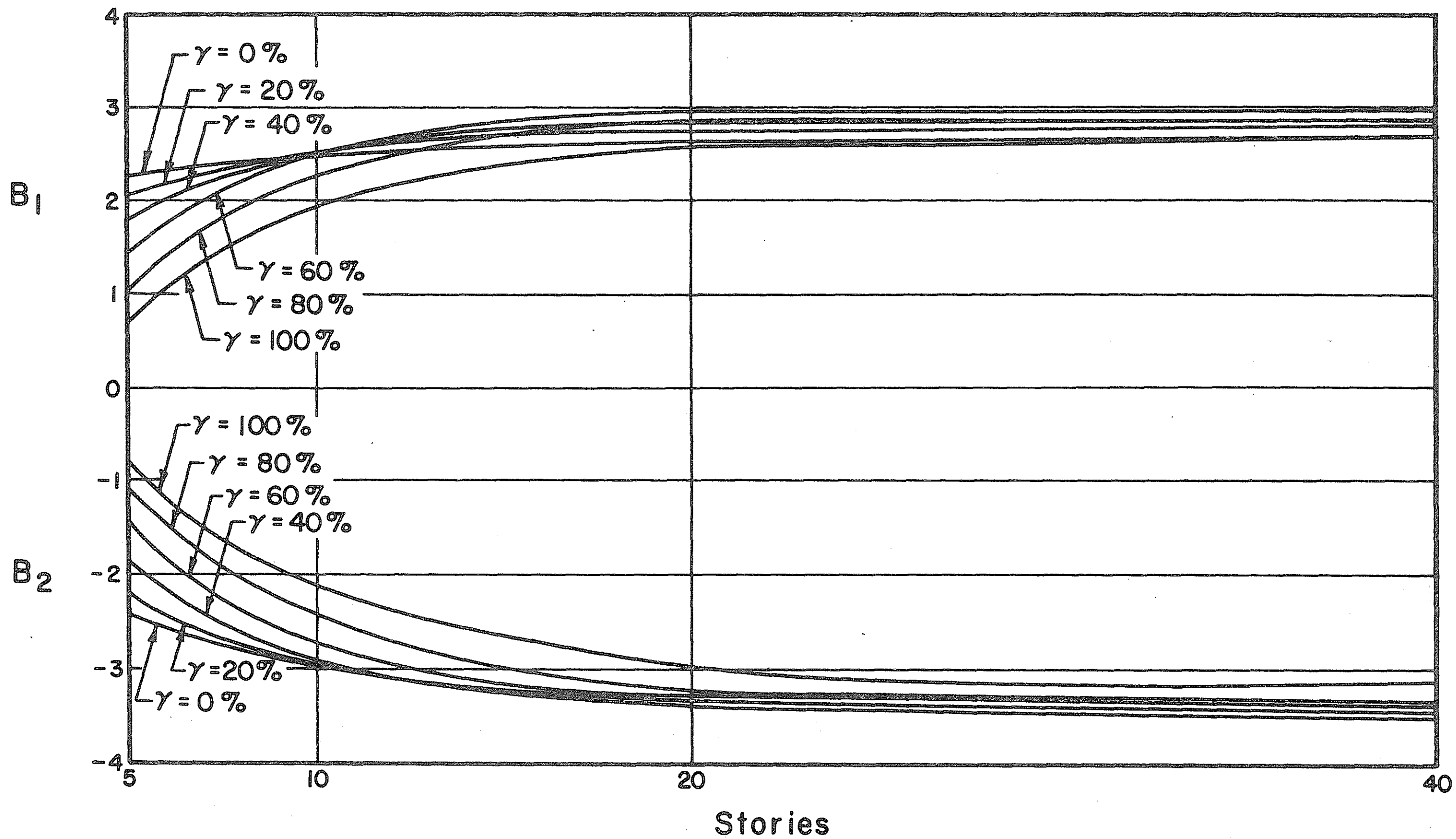

FIG. 10 STORY OVERTURNING MOMENT ACCELERATION COEFFICIENTS, Seismic Velocity = Infinite

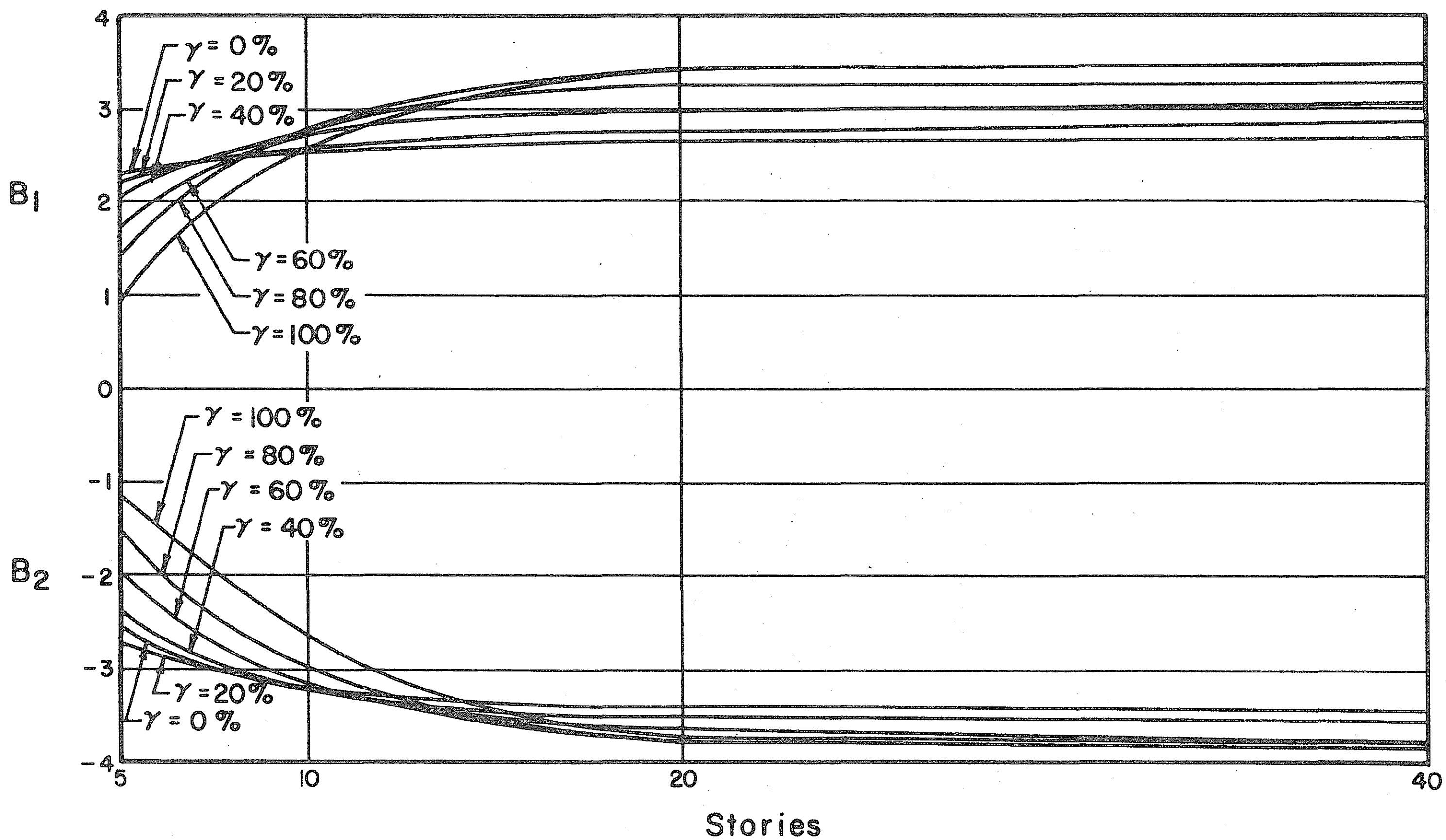

FIG. 11 STORY OVERTURNING MOMENT ACCELERATION DISTRIBUTION COEFFICIENTS, Seismic Velocity = 500 Ft./Sec.

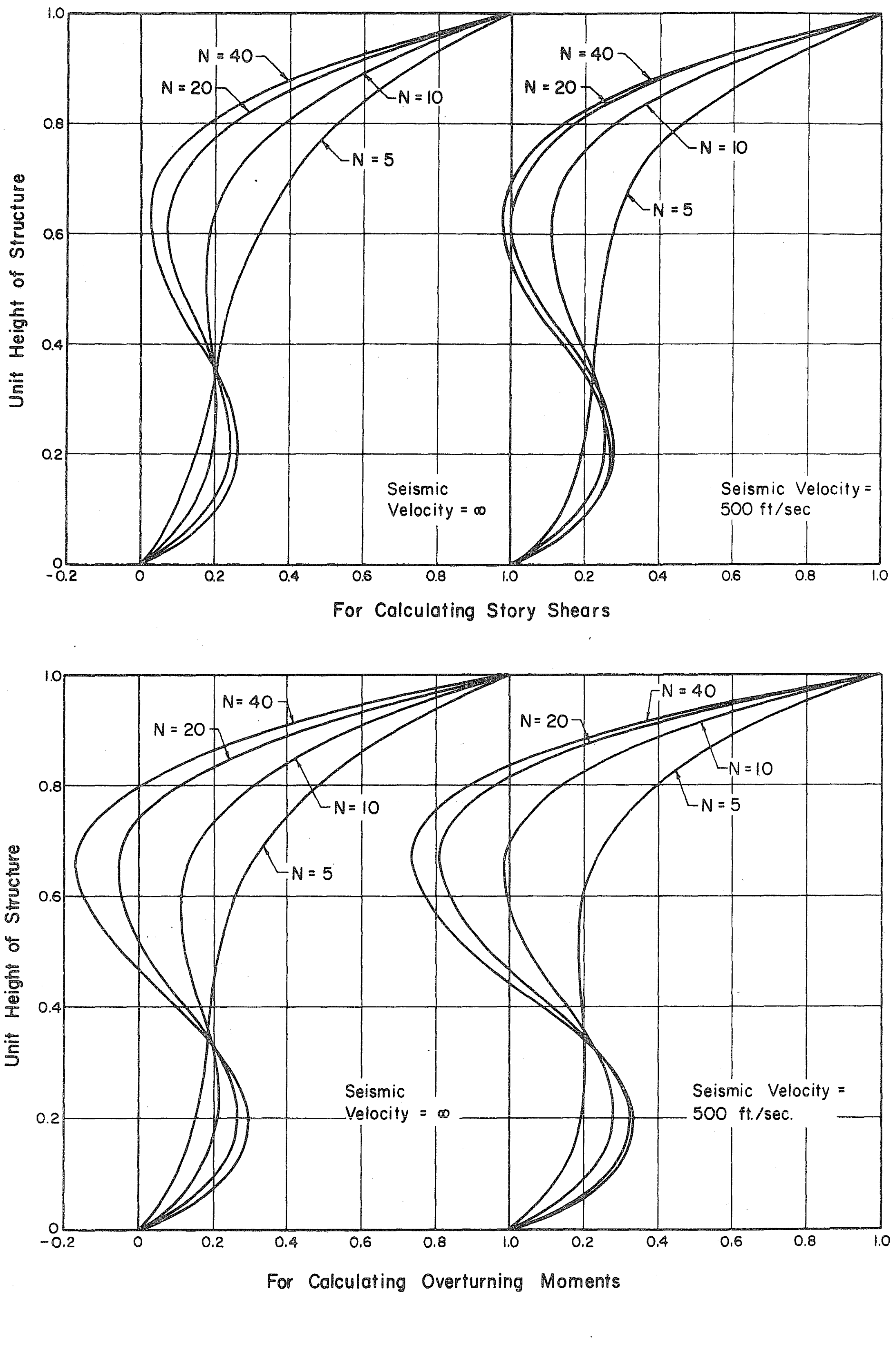

FIG. 12 ACCELERATION DISTRIBUTIONS OVER THE HEIGHT OF THE STRUCTURE, 0% Shear Deformation

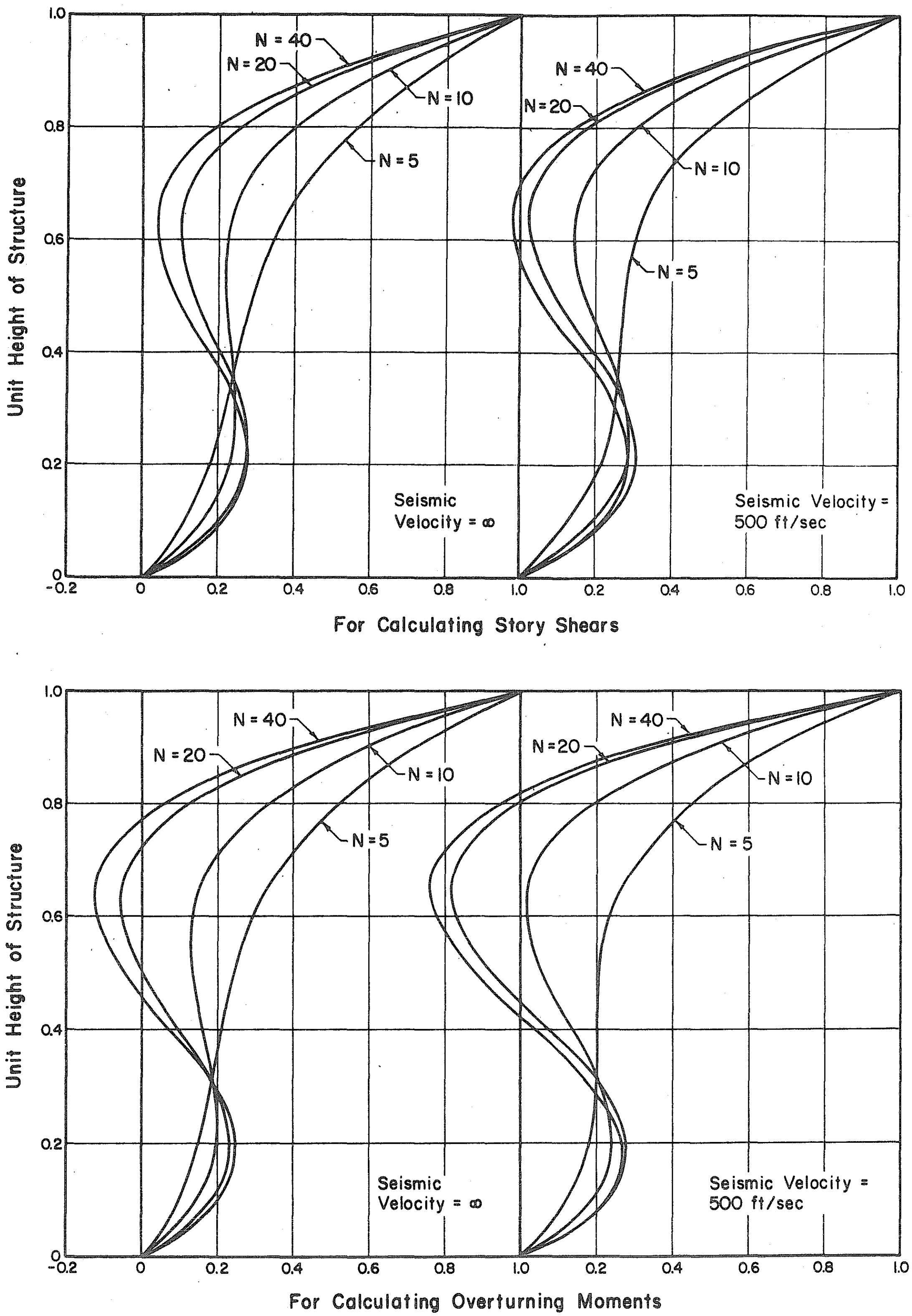

FIG. 13 ACCELERATION DISTRIBUTIONS OVER THE HEIGHT OF THE STRUCTURE, 20% Shear Deformation

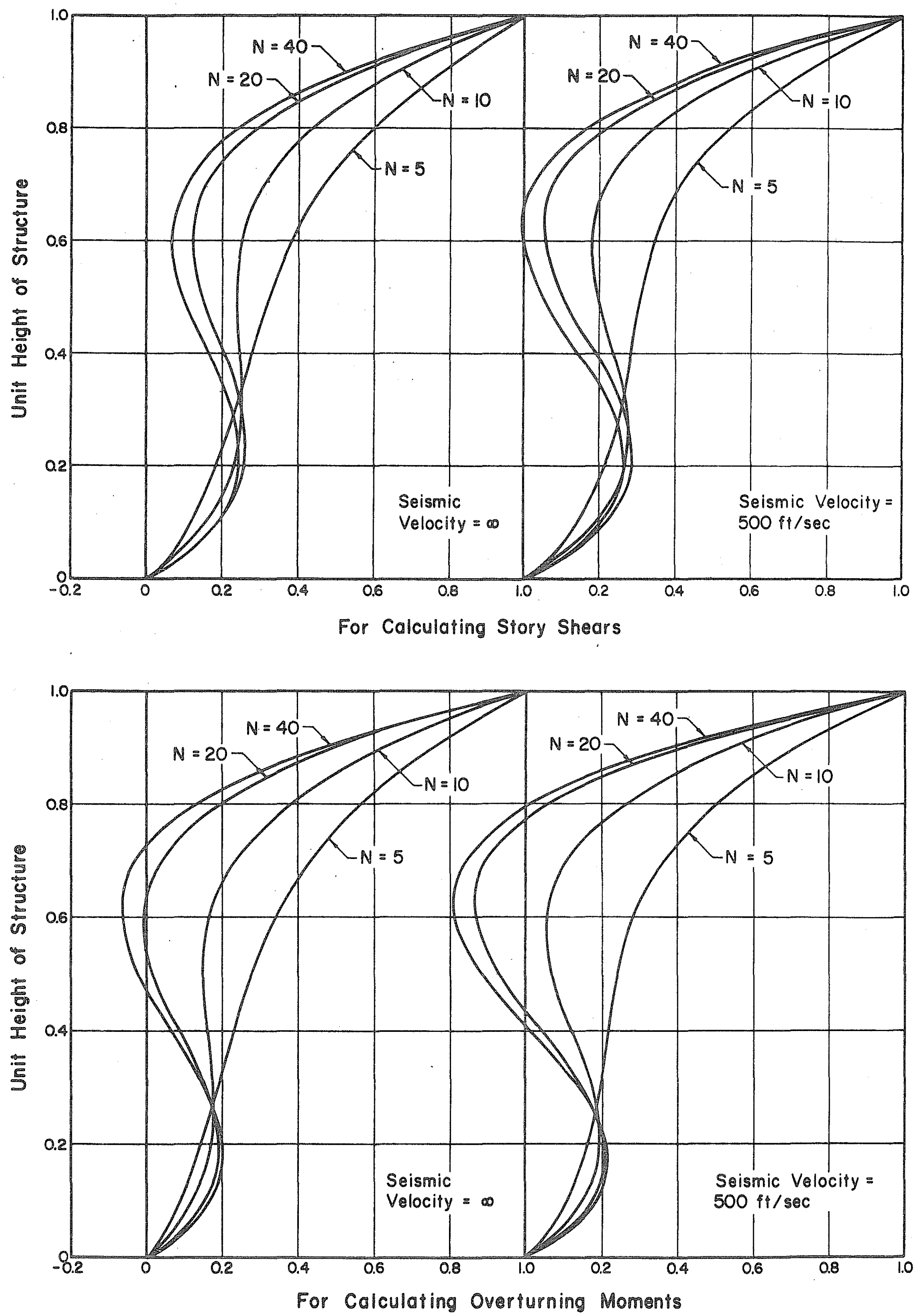

FIG. 14 ACCELERATION DISTRIBUTIONS OVER THE HEIGHT OF THE STRUCTURE, 40% Shear Deformation

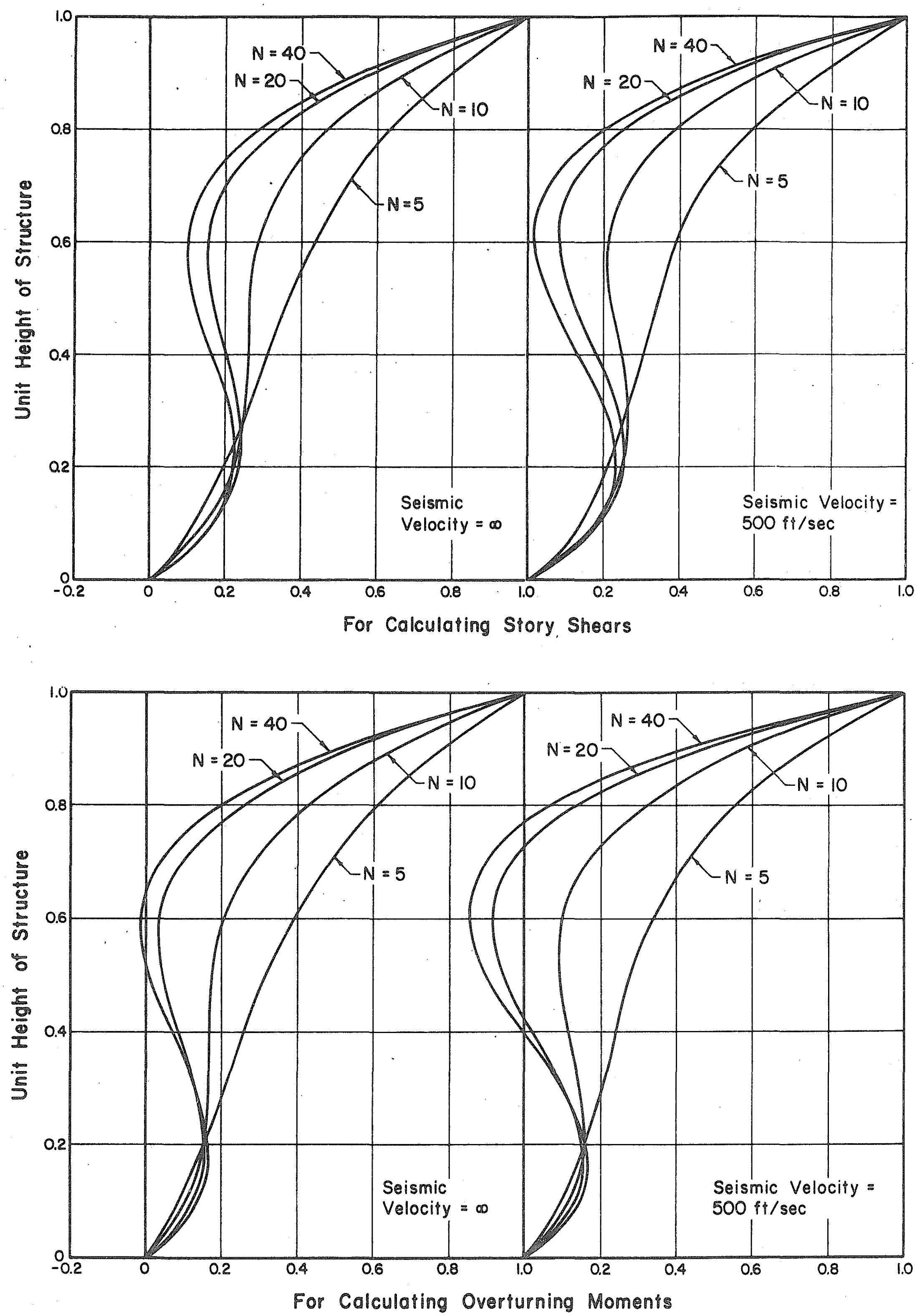

FIG. 15 ACCELERATION DISTRIBUTIONS OVER THE HEIGHT OF THE STRUCTURE, 60% Shear Deformation

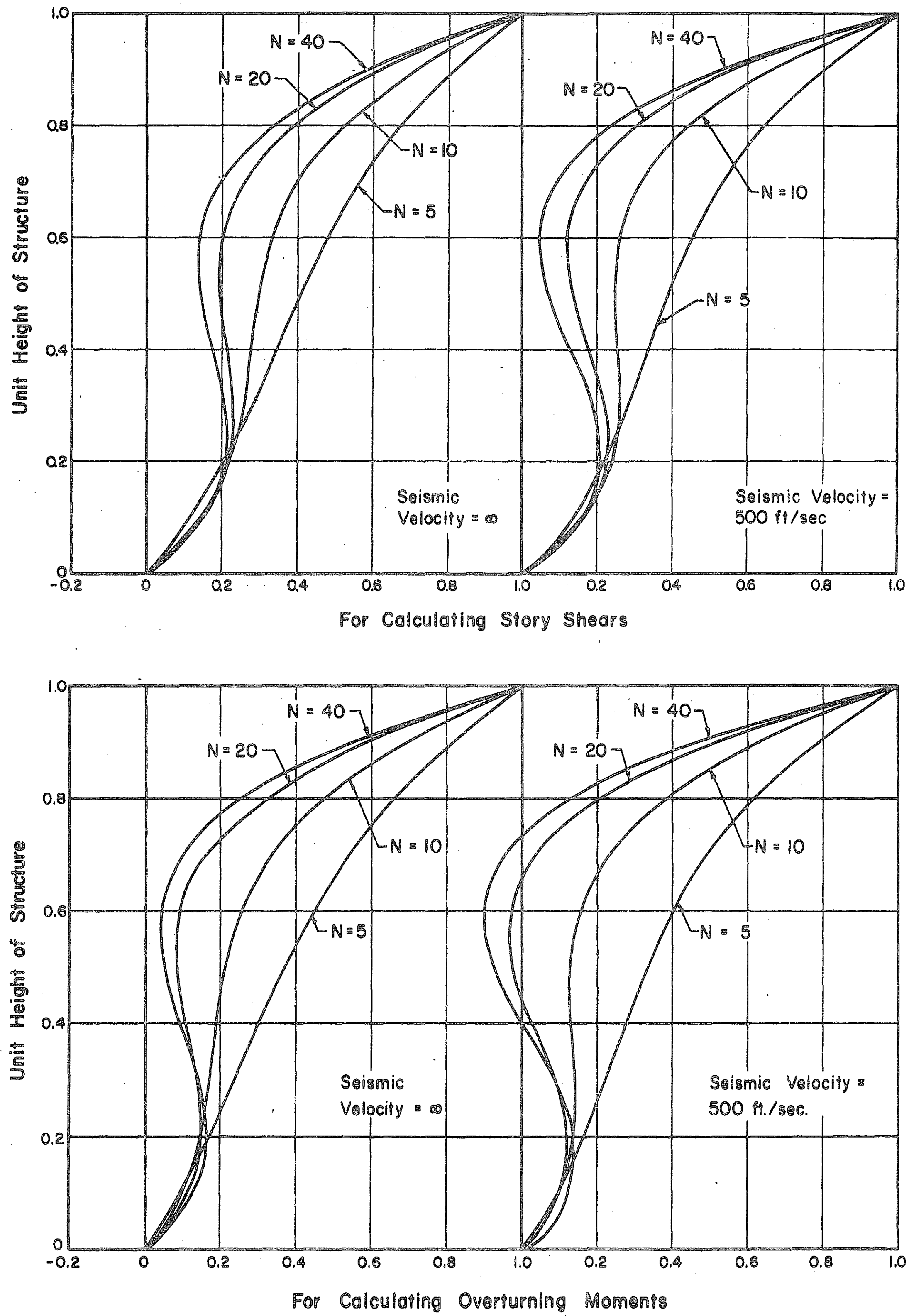

FIG. 16 ACCELERATION DISTRIBUTIONS OVER THE HEIGHT OF THE STRUCTURE, 80% Shear Deformation

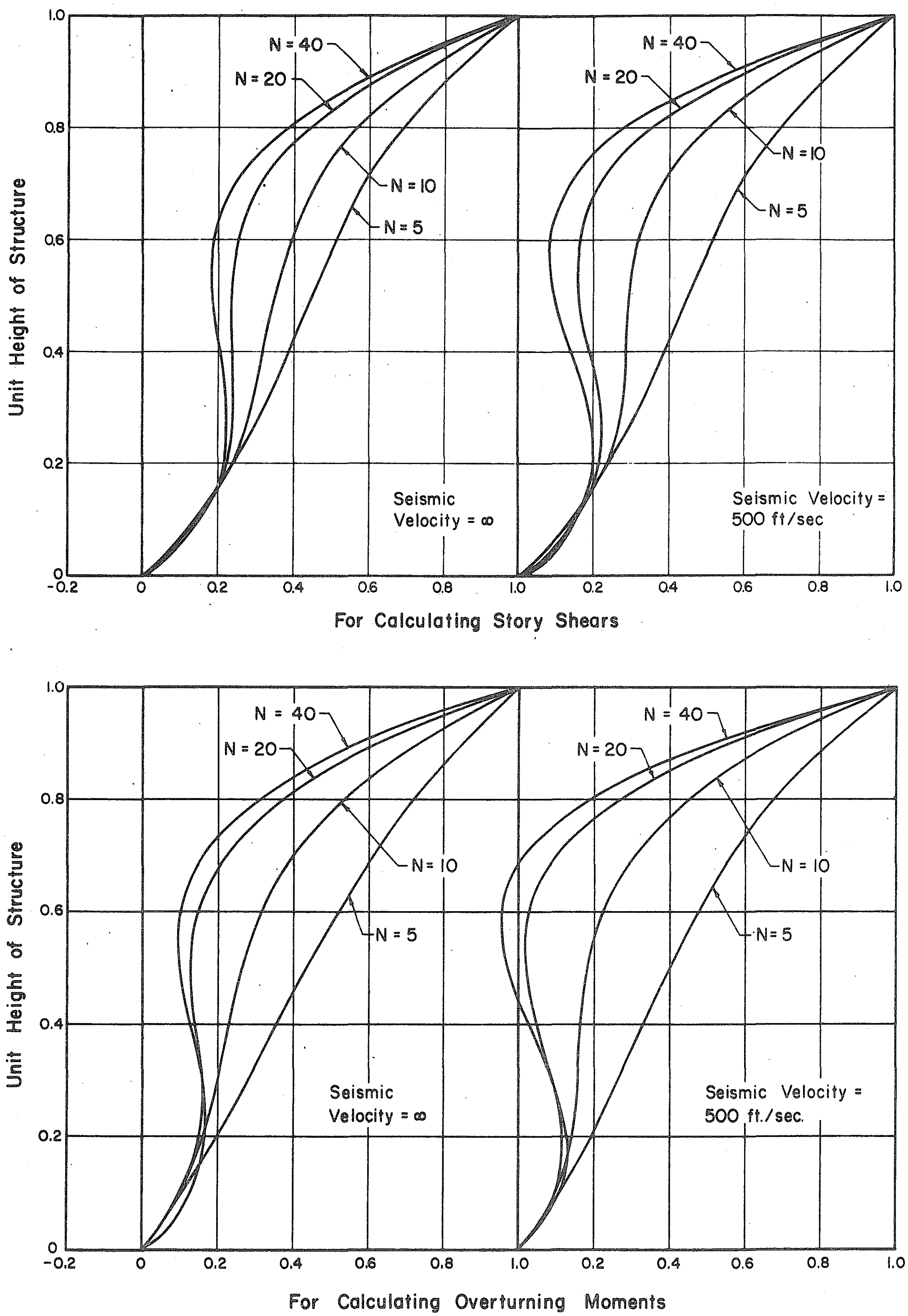

FIG. 17 ACCELERATION DISTRIBUTIONS OVER THE HEIGHT OF THE STRUCTURE, 100% Shear Deformation